TAMPEREEN TEKNILLINEN YLIOPISTO
TAMPERE UNIVERSITY OF TECHNOLOGY

VOITTO KÄNKÄNEN

OPTIMIZATION OF SILICONE ELASTOMER FORMULATIONS FOR TWO CONTROLLED RELEASE DRUG DELIVERY PRODUCTS

Master of Science Thesis

Examiner: Professor Jyrki Vuorinen

Examiner and topic approved in the Technical Sciences Faculty Council meeting on June 3, 2015

ABSTRACT

TAMPERE UNIVERSITY OF TECHNOLOGY
Master's Degree Programme in Materials Science
KÄNKÄNEN, VOITTO: Optimization of Silicone Elastomer Formulations for Two Controlled Release Drug Delivery Products
Master of Science Thesis, 92 pages, 8 appendix pages
August 2015
Major: Technical Polymer Materials
Examiner: Professor Jyrki Vuorinen
Keywords: Silicone, Silica, Diffusion, Controlled Release Drug Delivery

The goal of controlled release (CR) is to improve the spatial and temporal presentation of an active pharmaceutical ingredient (API) in the body. It can, for example, reduce the systemic side effects of a drug, facilitate its absorption to the body and improve patient compliance and convenience.

Polymers play an essential role in CR technology. Silicone polymers have been used as biomaterials for decades thanks to their biocompatibility and biostability and they have also found their place in controlled release applications. Elastomer materials are usually compounded with large amounts of fillers to improve their properties. The most common filler for silicone elastomers is amorphous silica (silicon dioxide), which is mainly used to improve the mechanical properties of the material.

In this work, the effect of silica concentration of a silicone elastomer on the drug release rate from two diffusion-controlled drug delivery devices is studied. The elastomer material acts as a diffusion-controlling membrane in these two products. The goals of this thesis work were, firstly, to find a material composition that could be used for the two products and, secondly, to create a simple empirical model that could be used to predict drug release rates from the products. The performance of this material was also compared with materials that were currently in use.

The specimen manufacturing process consisted of typical elastomer processing, such as mixing, extrusion and heat vulcanization as well as product-specific assembly methods. Through material and specimen characterization and *in vitro* release rate analysis, suitable material compositions were found and successful statistical models created, explaining up to 97% of variance in drug release rate, depending on the studied time point and API. For one of the two active ingredients studied, it was found that the storage time between manufacturing and use must be controlled due to different diffusional properties of the API. This thesis acted as a step towards the introduction of these materials into product manufacturing.

TIIVISTELMÄ

TAMPEREEN TEKNILLINEN YLIOPISTO
Materiaalitekniikan koulutusohjelma
KÄNKÄNEN, VOITTO: Silikonielastomeerin koostumuksen optimointi kahdessa kontrolloidun lääkeannostelun sovelluksessa
Diplomityö, 92 sivua, 8 liitesivua
Elokuu 2015
Pääaine: Tekniset polymeerimateriaalit
Tarkastaja: professori Jyrki Vuorinen
Avainsanat: silikoni, silika, diffuusio, kontrolloitu lääkeannostelu

Kontrolloidulla lääkeannostelulla (Controlled Release Drug Delivery) pyritään lääkeaineen annostelupaikan, -ajan ja -nopeuden optimointiin. Sen avulla voidaan muun muassa vähentää lääkkeen systeemisiä sivuvaikutuksia, parantaa lääkkeen imeytymistä elimistöön ja edistää potilaiden hoitomyöntyvyyttä.

Polymeerit ovat hyvin keskeisessä osassa kontrolloidun lääkeannostelun tekniikassa. Silikonipolymeerejä on käytetty laajalti biomateriaaleina jo kymmeniä vuosia niiden biokompatibiliteetin ja biostabiilisuuden ansiosta ja niitä on hyödynnetty myös kontrolloidun lääkeannostelun sovelluksissa. Kuten elastomeerimateriaaleihin yleisesti, myös silikonielastomeereihin sekoitetaan merkittäviä määriä täyteaineita materiaalin ominaisuuksien parantamiseksi. Silikonielastomeereilla yleisin käytetty täyteaine on amorfinen silika (piidioksidi), jota käytetään pääasiassa materiaalin mekaanisten ominaisuuksien parantamiseksi.

Tässä työssä tutkittiin silikonielastomeerin silikapitoisuuden vaikutusta lääkeaineen vapautumisnopeuteen kahdesta eri tuotteesta, joissa materiaali toimii diffuusiota kontrolloivana membraanina. Lisäksi materiaalia verrattiin jo käytössä oleviin silikonielastomeereihin. Työn tavoitteena oli yhtäältä löytää materiaalikoostumus, joka mahdollistaisi materiaalin käyttämisen molemmissa valmisteissa ja toisaalta luoda yksinkertainen empiirinen malli, joka kuvaisi materiaalin täyteainepitoisuuden vaikutusta tuotespesifiseen lääkeaineen vapautumisnopeuteen.

Näytteenvalmistuksessa käytettiin tyypillisiä elastomeerien prosessointimenetelmiä, kuten sekoitusta, ekstruusiota ja lämpövulkanointia sekä tuotteille ominaisia kokoonpanomenetelmiä. Materiaalien karakterisoinnin ja tuotenäytteiden *in vitro* vapautumisnopeusanalyysien avulla löydettiin käyttökelpoinen materiaalikoostumus molemmille tuotteille. Lisäksi toisella tuotteista havaittiin, että tuotteiden varastointiaikaa ennen käyttöä on kontrolloitava kyseisen lääkeaineen diffuusio-ominaisuuksien vuoksi. Vapautumisnopeutta mallinnettiin onnistuneesti lineaarisella regressiolla täyteainepitoisuuden sekä tuotteen dimensioita kuvaavan tekijän funktiona. Mallit pystyivät käytetystä lääkeaineesta ja aikapisteestä riippuen selittämään jopa 97 % vapautumisnopeuden varianssista. Työ toimi askeleena kohti materiaalien käyttöönottoa.

FOREWORD

This thesis work was conducted between September 2014 and April 2015 at Bayer Oy, Turku, Finland. The study was a part two product development projects. The work was supervised by Dr. Mikael Stolt and Dr. Svante Holmberg from Bayer Oy and examined by Professor Jyrki Vuorinen from Tampere University of Technology.

I would like to thank my supervisors for all their help and guidance as well as the examiner of this written work for his interest and insights. I would also like to thank Dr. Pirjo Kortesuo and Dr. Joachim Moede for giving me this thesis opportunity as well as M.Sc. Harri Jukarainen for pieces of practical and theoretical advice. I extend my gratitude to all the individuals in Bayer Oy's product development that helped me during this thesis and provided a pleasant environment to work in.

MATHEMATICAL SYMBOLS

a	inner radius of a cylinder
b	outer radius of a cylinder
c	concentration
c_1	concentration, when $r = a$
c_2	concentration, when $r = b$
c_s	saturation concentration, solubility
D	diffusion coefficient, diffusivity
DF	dimension factor
f	number of factors in an experiment
H	height of a cylinder
J	diffusional flux
J_x, J_y, J_z	diffusional fluxes in x, y and z-directions
k_a	constant in rate-law
K	partition coefficient
M_t	cumulative amount of drug released at time t
M_∞	cumulative amount of drug released at infinite time
MSE	mean square error
MST	mean square total variance
MT_{min}	smallest membrane thickness in a cross-section
MT_{max}	largest membrane thickness in a cross-section
n	sample size (except in Section 2.1)
n	exponent in reaction rate-law (only in Section 2.1)
p	statistical p-value
Q_x, Q_y, Q_z	amount of substance diffusing into a volume element in unit time in x, y and z-directions
Q_t	amount of substance diffusing out of a cylinder of unit length in time t
r	radius, radial distance from the center of a cylinder
R	correlation coefficient
RR	release rate
R^2	coefficient of determination
R^2_{adj}	adjusted coefficient of determination
SSE	error sum of squares
SST	total sum of squares
S	standard distance of data points from a regression line
S'	storage modulus
TGA	thermogravimetric residue (in weight-%)
x	position in x-direction or x-coordinate (only in Section 2.1)
x	predictor variable (except in section 2.1)

x_1, x_2, x_3, x_4, x_i	predictor variables, i:th predictor variable, i:th value of the predictor variable x
X_i	i:th value of variable X
$\bar{X}$	mean value of variable X
Y_i	i:th value of variable Y
$\bar{Y}$	mean value of variable Y
y	position in y-direction or y-coordinate (only in Section 2.1)
y	response variable (except in section 2.1)
y_i	i:th value of the response variable y
α	statistical significance level
$\beta_0, \beta_1, \beta_2, \beta_3, \beta_4, \beta_i$	regression coefficients, i:th regression coefficient
$\hat{\beta}_0, \hat{\beta}_1, \hat{\beta}_2$	estimated regression coefficients
ϵ	random error term, residual error
η^*	complex viscosity
ω	angular frequency

ABBREVIATIONS

ANCOVA	Analysis of Covariance
ANOVA	Analysis of Variance
API	Active Pharmaceutical Ingredient
BME	Biomedical Engineering
CDD	Controlled Drug Delivery
CR	Controlled Release
DDS	Drug Delivery System
DoE	Design of Experiments
HPLC	High Pressure Liquid Chromatography
ID	Inner Diameter
LADME	Pharmacokinetic sequence (Liberation, Absorption, Distribution, Metabolism and Elimination)
MLR	Multiple Linear Regression
OD	Outer Diameter
PDDS	Polymeric Drug Delivery System
PLA	Poly(lactic acid)
PLGA	Poly(lactic-co-glycolic acid)
PDMS	Polydimethylsiloxane
RTV	Room Temperature Vulcanizing
RSM	Response Surface Methodology
SD	Standard Deviation
SiO_2	Silica, silicon dioxide
TGA	Thermogravimetry

1 INTRODUCTION

At the core of this thesis work are so-called *polymeric drug delivery systems* (PDDS). In a PDDS, a polymer material, in one way or another controls the release of an active pharmaceutical ingredient (API) into a specific site within the human body. This technology is central to the products of Bayer Oy and since the polymer materials are essential for product performance, a considerable amount of work has been done on polymer development within the company. The present work is intended to act as a step forward towards the deployment of new silicone elastomer materials.

One motivational aspect behind this study is the advantage of having several possible material providers. Alternative material sources help to ensure process continuity. In addition, having increased control over the polymerization and compounding processes yields, besides certainty and knowledge, also more flexibility, especially when material batch sizes are small.

This thesis work concentrates on the development of two polymeric drug delivery products and it has two main objectives regarding the new materials. Firstly, it seeks to determine, whether it is possible to find *a single polymer formulation* that could be used *for both products* in question. This would result in cost savings in the future, e.g., through increases in material batch sizes. Secondly, this work seeks to find correlations between vital process parameters and product performance and to express them via a simple *statistical model* that could be expanded and refined in further studies.

To achieve these objectives, carefully planned *designed experiments* are conducted. Important variables within the manufacturing process are chosen and the experimentation is performed by varying and controlling their levels. The product manufacturing process involves several steps: preparation and extrusion of a drug-elastomer mixture, extrusion coating, post-curing and product assembly. All stages are monitored with in-process controls. The measured response variable that represents product performance in this work is the in vitro release rate of an API from the product.

This work is divided into six chapters, including this introductory chapter. In the second chapter, basic concepts of polymeric drug delivery technology, silicone elastomers, elastomer processing, experimental design and statistical analysis methods are discussed. Both the author and the examiner of this thesis come from a materials science and engineering background and the theoretical part of this thesis is constructed accord-

ingly: rather elementary aspects of biomedical engineering, biomaterials and pharmacology are discussed, whereas a more advanced approach is taken on subjects related to materials processing and polymers.

Chapter 3, Materials and Methods, describes the developed products in question, the specimen preparation process as well as the materials and analysis methods used in this study. Chapter 4, Results and Discussion, contains the gathered data and results obtained through statistical analysis. The last chapter is reserved for conclusions and suggestions for the direction of future studies.

2 THEORETICAL BACKGROUND

2.1 Polymeric Drug Delivery

This work concentrates on two products that share a common goal – they are medicinal products designed to release active pharmaceutical ingredients (API) in a controlled, predetermined manner. The performance of such products is based on controlled drug delivery (CDD) or controlled release (CR) technology. This section seeks to explain the principles and peculiarities of this modern field of medicine and technology. It begins by giving a brief introduction to the field of biomaterials and explaining some of the related terminology.

2.1.1 Biomaterials Science and Biomedical Engineering

In this thesis, engineering tools and methods are used in the development of medicinal products, which makes this work an example of *biomedical engineering*. The discipline of biomedical engineering (BME) integrates the fields of medicine and engineering and provides tools and equipment for diagnostics, treatment and research [1, p. 2]. The modern health care system is characterized by an immense variety of machines, devices and instruments, many of which are products of BME. For the purpose of this thesis, the most interesting branch of BME is the field of biomaterials.

As discussed above, biomaterials are a branch of biomedical engineering. Quite similarly, the science of *controlled drug delivery* originates from *biomaterials science*. Briefly put, biomaterials science is a field of science that studies materials with a special emphasis on their interactions with biological environments [2, p. xxvi]. It is a multidisciplinary endeavor, requiring expertise in chemistry, physics and biology, as well as medicine and engineering [2, p. xxv].

A commonly accepted definition for a *biomaterial* is *"A nonviable material used in a medical device, intended to interact with biological systems"* (Williams (1987), as cited by Ratner et al.) [2, p. xxvi]. This broad definition also includes materials used in medical devices that are not in direct contact with the body, such as cell growing platforms in tissue engineering (where the cells are being grown outside the body) or tubings used in hemodialysis devices (which only come in contact with blood).

Biomaterials can be either synthetic or natural by origin [2, p. xxv]. All main material classes (plastics and elastomers, metals, ceramics and composites) have their representatives in the biomaterial family [2, p. xxvii]. Examples of common biomaterial applications include prostheses, artificial joints (most commonly hip, knee and shoulder joints), catheters, stents, contact lenses and intraocular lenses, bone fixation screws and plates, breast implants and contraceptive intrauterine devices. Table 1 presents some biomaterials used in various large-scale applications.

Table 1: *Examples of large-scale applications of biomaterials (modified from* [2, p. xxvii]*).*

Application	***Biomaterials used***
Implants for joint replacement	Stainless steel, titanium, polyethylene
Plates and screws for bone fixation	Metals, poly(lactic acid)
Bone cement	Poly(methyl methacrylate)
Pacemaker	Titanium, polyurethane
Hemodialysis	Polysulfone, silicone
Stent	Stainless steel, other metals, poly(lactic acid)
Catheter	Teflon, silicone, polyurethane
Contact lenses	Acrylate/methacrylate/silicone polymers
Sutures	Poly(lactic acid), polydioxanone, polypropylene, stainless steel
Breast implants	Silicone
Intrauterine devices	Silicone, copper

The concept of *biocompatibility* is central to the use of biomaterials. A broadly endorsed definition for biocompatibility is *"the ability of a material to perform with an appropriate host response in a specific application"* (Williams (1987), as cited by Ratner et al.) [2, p. xxvii]. For example, in the process of implantation, tissue injury unavoidably occurs, which initiates defense systems in the body. These include inflammation, wound healing process and so-called foreign body responses. Assessing how severe and long-lasting these symptoms are plays a major part of determining an implant's biocompatibility [2, p. 503].

A complex set of factors determine the biocompatibility of a material. In addition, medical devices or implants are generally constructed from multiple materials, and the biocompatibility of such a device is not necessarily a sum of the individual material compatibilities. Instead, the biocompatibility of such a device must be studied as a whole [2, p. xxvi].

Through the years, as new inventions and applications have appeared, the definition of biocompatibility has also evolved. It can be argued that since the first biomaterial products came to market 60–70 years ago, biomaterials have experienced three generations of development regarding the host response [2, p. xxviii]. The first approach was to

choose materials that were not necessarily designed for medical applications but possessed sufficiently similar (mechanical) properties as the tissue they were used to replace and to ensure that they did not elicit a deleterious response in the body. In other words, the goal was *bioinertness*, to have minimum interaction with the living tissue.

Shortly after, the second generation of biomaterial development began. In contrast to the first generation materials, the goal of these materials was to have controlled interactions with the host tissues [2, p. xxviii]. Termed *bioactive*, these materials were specifically designed to be used in biomedical applications. Examples of bioactive materials include those used in controlled drug delivery applications as well as *bioresorbable* and *biodegradable* materials that experience controlled degradation within the body, resulting in a safe, non-surgical removal of the material if all the degradation products are non-toxic.

The third generation of biomaterial development is directed towards *tissue engineering* and *regenerative therapeutics*. The goal of regenerative therapeutics is to generate functional tissue from patient's own cells to compensate for the loss of organs or tissue caused by disease or trauma [2, p. xxix]. This strategy removes two issues encountered with transplants using donated organs, namely the lack of donors and possible transplant rejection due to low biocompatibility [3, p. 589].

Biomaterials play an important role in tissue engineering as they are used to manufacture *scaffolds* onto which functional tissue is grown. These scaffolds can be made of synthetic or natural, typically porous, bioresorbable polymer materials [2, p. xxix]. Differentiated or undifferentiated (stem) cells, depending on the application, are seeded on the scaffold, the tissue is matured *in vitro* and the resulting construct is implanted. Successful tissue replacements achieved thus far using tissue engineering in humans include bladders, trachea, skin and epithelium, bone and cartilage [2, p. xxix] [3, p. 589] [4].

This study focuses on two (non-degradable) products that are designed to have interactions with the body, more precisely to release a drug substance in a controlled manner. This means that they are bioactive and thus represent the second generation of biomaterial evolution. The following subsections treat the subject of drug delivery in greater detail.

2.1.2 Pharmacokinetics

Pharmacokinetics is a branch of pharmacology that studies the fate of a drug after its administration, i.e. what are the *effects of the body on the drug*. Pharmacodynamics, in contrast, studies the effects of the drug on the body. Pharmacokinetics can be thought of as a special case of chemical kinetics with the human body as the (bio)chemical environment.

There are several motivational aspects to the study of pharmacokinetics. For a drug to be effective, a sufficient amount of the active ingredient must reach the target site in the body. However, increasing dosages can prove dangerous, since excessive drug concentrations can cause undesirable systemic side effects. Furthermore, several medical conditions require uninterrupted medication for prolonged periods of time. This is why it is important to understand how the drug concentrations evolve within the body after a drug formulation has been administered. The optimum plasma concentration region is called the *therapeutic window* and it is limited by a *minimum effective level* and a *maximum desired level* of a drug. [2, pp. 1024–1025] [5, p. 16]. The ratio of the two levels is called the *therapeutic index*. The lower the therapeutic index of a drug, the more accurate dosage is required for safe and effective treatment.

Clinical study of pharmacokinetics usually involves measurements of drug concentration in the blood or other bodily fluids as the drug is administered. Concentration data can be used to determine safe and effective ranges for the drug dosage, even though the relationship between plasma concentration and a response can in fact be quite complex [6, p. 176].

What happens to an API after a drug formulation has been administered can be described by the *LADME* sequence: *Liberation* of the API from the carrier unit, *absorption* into the bloodstream, *distribution* within the body, *metabolism* by the body and *excretion* (or *elimination*) from the body [2, p. 1024] [6, p. 176]. The sequence is described below in greater detail.

With intravenous injections, practically the entire administered dose reaches the systemic circulation, whereas with oral formulations, a large part of the drug is lost due to incomplete absorption in the gastrointestinal tract (i.e. poor *bioavailability*) and so-called *first-pass metabolism* in the liver and the gastrointestinal tract [6, p. 177]. The amount that reaches the systemic circulation is then distributed in the blood throughout the body, moving in and out of tissues. Some tissues absorb the active ingredient more rapidly and to a larger extent than others, depending on different binding effects, active transport mechanisms, the extent of blood perfusion and other factors [6, p. 177] [5, pp. 8–10]. Once in the systemic circulation, a drug molecule is susceptible to metabolism (biochemical reactions that transform it into another molecule) and excretion (elimination of the substance from the plasma). Metabolism and excretion are, for the most part, accomplished by the liver and the kidneys, respectively [2, p. 1024] [6, p. 178].

The rate of absorption, drug distribution in the system, and the rates of metabolism and excretion are largely defined by the biochemical properties of an API. Liberation, however, can be controlled by modifying the drug formulation, i.e., properties of the carrier and the excipients it consists of. This is precisely what controlled release technology is

for. Various approaches to controlled drug release and designs for the drug carriers are presented in the following two subsections.

2.1.3 Controlled Release

The goal of controlled release technology is to improve the spatial and temporal presentation of a drug, i.e., to enable the introduction of an active ingredient to a desired location within the body at a certain moment in time or during a certain period of time [5, p. 19]. This can result in increased efficiency and decreased side effects as well as improved patient compliance and safety. A true controlled release system has a predictable and reproducible drug release profile that is relatively independent of environmental conditions [7, p. 2].

An obvious advantage of controlled release formulations is illustrated in Figures 1 and 2, which show simple pharmacokinetic curves for two drug formulations. Figure 1 represents a conventional multiple dose (oral or intravenous) formulation and Figure 2 a single-dose near zero-order controlled release (CR) formulation. With the multiple dose formulation, the drug concentration fluctuates constantly between potentially harmful and ineffective levels, increasing after each dose, reaching a peak value and collapsing again. With the CR formulation, the concentration stays well within the therapeutic window for the majority of the time.

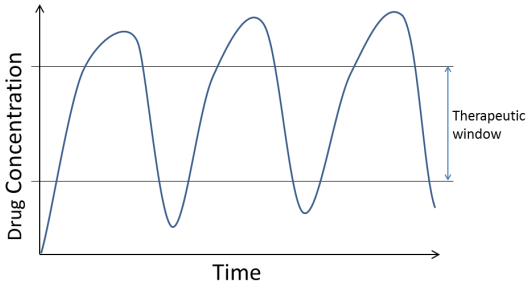

Figure 1: *A simple pharmacokinetic curve for a conventional multiple dose formulation (based on illustrations in* [2]*).*

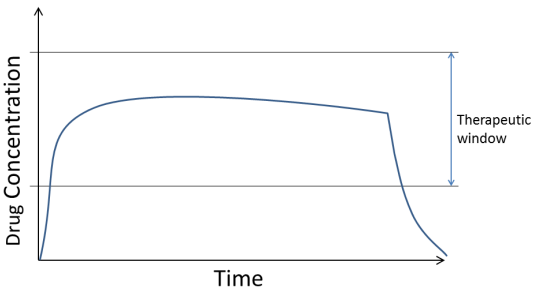

Figure 2*: A simple pharmacokinetic curve for a single-dose near zero-order CR formulation (based on illustrations in* [2]*).*

One could argue that the variations in drug concentration could be smoothed out simply by shortening the dosage intervals to provide a more steady supply of drug. However, this is not feasible due to issues with patient compliance, especially for drugs with low therapeutic indices [8, pp. 1–2]. At present, the treatment of many of the globally most common medical conditions require regular intake of pharmaceuticals and the effectiveness of the treatment depends heavily on patient compliance.

With certain drug delivery systems (DDS), such as long acting implants, dosage intervals can be extended to several years, reducing or removing problems with medical

compliance, as patients no longer have to remember to take the medication and drug abuse and misuse become very difficult. As overall drug levels in the body are minimized and a stable supply of active ingredient is achieved, controlled drug delivery can provide both safe and effective treatments that require little attention between doses.

A variety of DDS for different administration routes and active ingredients have been developed over the years. Polymers play an important role as excipients in most of these systems. Some are designed to last for hours, others for several years. In their textbook, Ratner et al. have divided the contemporary DDS into five classes: *injected nanocarriers*, *injected depot DDS*, *implants* and *inserts*, *smart DDS*, *transdermal DDS* and *oral DDS* [2, pp. 1024–1087].

Intravenously injected nanocarriers include so-called PEGylated systems (bonded to poly(ethylene glycol)), polymeric micelles, liposomes, dendrimers, polymer-drug conjugates, polymer-drug polyelectrolyte complexes and drug nanoparticles [2, p. 1027]. Besides prolonging the liberation of an API using the methods above, it is also possible to influence another pharmacokinetic parameter, namely distribution. This is achieved by attaching targeting ligands to drug nanoparticles to increase their affinities towards certain tissues [5, pp. 29, 41].

Injected depot DDS differ from injected nanocarriers by their size. The dimensions of injected depot carriers are usually in the order of micrometers. They are essentially biodegradable polymer microparticles or phase separating drug/polymer solutions. At present, PLA and PLGA (poly(lactic acid) and poly(lactic-co-glycolic acid)) copolymers are the most common materials for injected depot DDS, though various exotic material concepts have been introduced, including polymers and gels that exhibit *in situ* cross-linking, precipitation or solidification [2, pp. 1055–1060].

Non-degradable CDD implants and inserts are commonly made of silicone polymers, ethylene vinyl acetate copolymers, acrylate (co)polymers, vinylidene fluoride copolymers or urethanes [2, p. 1063]. Degradable implants are usually made of various different copolymers, featuring lactic acid and glycolic acid polymers, polyanhydrides, poly(ethylene glycols), poly(ortho esters) and poly(phosphoesters) [2, p. 1065]. The devices are, for the most part, of the monolithic type or of the reservoir type. The designs are discussed in greater detail in subsection 2.1.4.

While transdermal (through-the-skin) medication usually involves simple creams and ointments, several CDD systems have also been developed for this administration route. Typically in the form of a patch, these systems feature a rate-controlling membrane that dictates the maximum amount of drug that can enter the body through the skin, (provided that the skin has a higher permeability to the drug than the membrane does) [2, p. 1075]. Controlled release technology can also tackle problems in oral formulations,

namely poor bioavailability, stability, solubility and absorption of drugs [2, p. 1083]. For example, an orally administered DDS can be designed to delay the drug release to protect the drug from the acidic environment of the stomach.

Though constant (zero-order) release is often desirable, it is not always the optimum release profile [2, p. 1025]. Smart drug delivery devices react to changes in their environment, and alter their drug release rates accordingly, in a controlled manner. Possible stimuli include, for instance, temperature, pH, enzymes, ultrasound and electromagnetic fields [2, pp.1071–1072] [9–11]. The release rate could follow biological rhythms such as menstrual or circadian rhythms or it could increase as blood glucose levels go up [12] [13].

2.1.4 Temporal Control of Drug Release

There are several ways to classify CDD devices and formulations, such as by size, biodegradability, administration route, time of use, etc. The present work focuses specifically on drug release rates, i.e., the temporal control of drug release. Thus, the classification of devices is made according to the means by which drug release rate is controlled and the processes that govern the release. Smart DDS, reacting to external (extracorporeal) stimuli or feedback from the body are not discussed here.

The mechanisms that result in drug release from a carrier include drug *dissolution, partitioning*, *diffusion*, *osmosis*, material *swelling* and *erosion* [5, p. 30]. In addition, specific *enzymatic* or *hydrolytic reactions* can alter the release kinetics [7, p. 6]. Furthermore, distribution of drug nanoparticles within the body and thus the ultimate location of drug release can be influenced by *targeting*.

It is worth noting, that often the drug is released by more than one mechanism and different mechanisms may be involved at different stages of the process [5, p. 19]. For example, in a bioerodible system, material swelling, water penetration and drug diffusion in the swollen matrix may constitute a major part of the overall drug release, even if erosion would be the primary mechanism of release. The kinetics of each step must be evaluated and important, rate-determining steps identified if a thorough understanding of the release is to be achieved. The following subsections classify CDD systems according to their *dominant release mechanisms*. Diffusion controlled systems are discussed in greatest detail, since the present study focuses on such devices.

2.1.4.1 Diffusion Controlled Systems

Diffusion of active agents in a polymer matrix

Diffusion occurs through random collisions of particles due to the kinetic energy they possess as heat and it causes concentration gradients to smooth out over time. Macroscopically, diffusion in an isotropic material can be analyzed using Fick's first law

$$J = -D\frac{\partial c}{\partial x}\ , \tag{2.1}$$

where J is the *diffusion flux* (amount of substance passing through a unit of area in a unit of time) D is the *diffusivity* or the *diffusion coefficient*, c is the concentration of the diffusing species and x denotes the position [7, p. 11] [14, p. 505] [15, p. 2].

Diffusivity is a proportionality constant that represents a species' mobility in a diffusion medium and it may depend on concentration and various other variables [5, p. 31] [7, p. 11]. Several factors can affect the diffusion of a drug in a polymer matrix. These include composition, molecular weight distribution and morphology of the polymer, as well as concentration of the diffusing species [7, p. 15]. The last one is known to have a very significant effect on molecular diffusivity in polymers [15, p. 2].

Various different methods and theoretical models have been developed for determining and predicting diffusivities and solubilities of organic molecules in polymer materials [5, pp.143–150] [16–19]. Quantification of these two parameters is crucial if mechanistic models are to be used to predict drug release. If the diffusivity of a species in the system is known, Fick's first law can be used to calculate the rate of diffusion in a system irrespective of the actual mechanisms by which diffusion occurs [7, p. 11]. Fick's first law assumes that the driving force of diffusion is the concentration gradient of a species. Even though this is a proper approximation in many cases, the driving force is more precisely the chemical potential gradient [7, pp. 11–12].

Let us consider diffusion through a volume element that has edges of lengths $2dx$, $2dy$ and $2dz$ in a Cartesian coordinate system. At the center of this element, is point P. In point P, the diffusional flux in the x-direction is J_x. Through one of the two faces of the volume element perpendicular to the x-axis, the diffusional flux into the element is then $(J_x - \frac{\partial J_x}{\partial x})dx$ and through the opposite face it is $(J_x + \frac{\partial J_x}{\partial x})dx$. Thus, the quantity of material accumulating into the element per time unit in the x-direction, Q_x, is

$$\begin{aligned} Q_x &= dx2dy2dz\left(J_x - \frac{\partial J_x}{dx}\right) + dx2dy2dz\left(J_x + \frac{\partial J_x}{\partial x}\right) \\ &= -8dxdydz\left(\frac{\partial J_x}{\partial x}\right) \end{aligned}$$

Performing similar calculations for y- and z-directions yields

$$Q_y = -8dxdydz\left(\frac{\partial J_y}{\partial y}\right)$$
$$Q_z = -8dxdydz\left(\frac{\partial J_z}{\partial z}\right)$$

The total change in concentration in the element per time unit can be calculated by dividing the amounts of accumulated material per time unit with the total volume of the element, yielding

$$\frac{\partial c}{\partial t} = \frac{Q_x+Q_y+Q_z}{8dxdydz},$$

$$\frac{\partial c}{\partial t} = -\frac{\partial J_x}{\partial x} - \frac{\partial J_y}{\partial y} - \frac{\partial J_z}{\partial z}, \tag{2.2}$$

and finally by differentiating the diffusion fluxes according to Equation (2.1), assuming that diffusivity is independent of position (x, y, z), we arrive at the three-dimensional presentation of Fick's second law [15, pp. 3–4] [20, pp. 1–3]:

$$\frac{\partial c}{\partial t} = -D\left(\frac{\partial^2 c}{\partial x^2} + \frac{\partial^2 c}{\partial y^2} + \frac{\partial^2 c}{\partial z^2}\right). \tag{2.3}$$

Several analytical solutions for Equation (2.3) can be found in the literature for rectangular, cylindrical and spherical geometries [7] [15]. If the diffusion coefficient cannot be assumed independent of concentration, time and position, solving Fick's second law analytically becomes difficult. However, numerical techniques with certain approximations can be used to model diffusion with non-constant diffusion coefficients.

According to McGregor, as cited by Fan and Singh, depending on the porosity and pore size distribution of the polymer matrix, different models can be used to evaluate the diffusion behavior [7, p. 15]. If the pores are small with respect to the sizes of diffusing molecules, intimate molecular interactions between the polymer molecules and the diffusing species should be included in the model. This is the case for macroscopically homogeneous polymers. In contrast, if the pores are significantly larger than the mean free paths of the diffusing species, the transport process mainly occurs in the fluid within the pores and the polymer phase acts as little more than a container.

The *free volume theory* proposes that the total volume a liquid occupies consists of the actual volume of molecules and the free volume between the molecules [7, p. 16]. The actual volume is independent of temperature, whereas free volume is proportional to temperature and has a zero value at the absolute zero. This theory has been further applied to several polymer-solvent systems and can be used to model diffusion in macroscopically homogeneous polymers.

The free volume theory of diffusion views the solute and polymer molecules as having impermeable cores surrounded by microscopic voids of free volume [5, p. 33]. As the system is constantly fluctuating due to thermal energy, these voids change in size and distribution so that occasionally a diffusing particle can pass through. Due to increasing molecular mobility, the probability of obtaining a large enough void increases with temperature. The proportionality constant between free volume and temperature changes abruptly at the glass transition temperature (T_g) of a polymer as do the mechanisms of diffusion [7, pp. 15–22] [21, p. 383] [14, p. 500].

As mentioned before, changes in polymer composition through copolymerization or blending or simply by the addition of water, can cause the free volume of a polymer matrix to increase and augment the diffusivity as well [5, pp. 33–34]. Furthermore, crystallinity of a matrix can reduce the diffusion rates significantly, as crystalline regions possess significantly less free volume than amorphous regions and are virtually impenetrable to drug molecules [5, p. 34]. The effect of fillers on diffusion in silicone elastomers is discussed in subsection 2.2.4.

Diffusion controlled systems

In a true diffusion controlled system, the drug release rate is determined solely by the rate of diffusion of an active agent through one or more components of the device [7, p. 44]. Diffusion controlled drug delivery systems can be divided into two main categories: *monolithic* and *reservoir* systems. Monolithic systems consist of a homogeneous mixture of drug and polymer, whereas reservoir systems are characterized by a drug core surrounded by a *rate-controlling membrane* [7, p. 9] [5, p. 32]. Figure 3 shows a schematic illustration of drug release from the two types of diffusion controlled DDS.

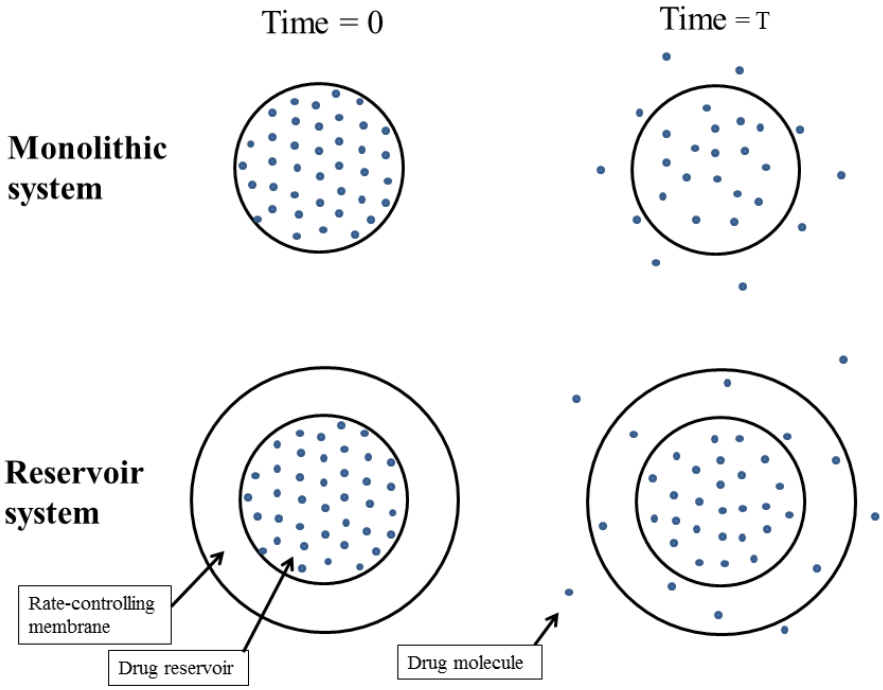

Figure 3: A schematic illustration of the drug release process from monolithic and reservoir-type controlled drug delivery devices.

When introduced *in vivo*, monolithic devices show a strong initial burst of drug release as drug is dissolved rapidly from the surface. Simultaneously, new drug diffuses to the surface from inside the device and an evolving concentration gradient is formed. If the formulation is such, that the active ingredient is dissolved in the polymer matrix, the process of drug release from a monolithic device involves [7, p. 9]

1) Diffusion to the device surface
2) Partition between the matrix and the surrounding medium at the surface
3) Transport from the device surface

If, instead, the drug is dispersed as particles in the matrix, it first needs to dissolve into the polymer matrix before it can start to diffuse to the device surface [7, p. 9]. This is the case if the matrix is saturated with drug.

As time progresses and drug concentration near the surface diminishes, the overall release rate decreases as the drug molecules have to diffuse a longer distance to reach the device surface, resulting in a non-zero-order release profile. This can be overcome with exotic geometries and coatings, but it is often unfeasible [5, p. 33]. Release from a monolithic system has been successfully described by the Higuchi model derived from Fick's second law and other models based on Higuchi's work [5, pp. 141–142] [22] [23]. Specific equations for monolithic devices are not discussed here.

If the matrix has a porous structure, the cavities may either obstruct the diffusion (if the pores are empty) or enhance the diffusion (if the pores contain the external dissolution medium), resulting in several steps of dissolution, partition and diffusion [7, pp. 9–10]. This phenomenon can also occur in the membranes of reservoir-type systems. In addition, too slow drug transport from the device surface results in non-zero API concentrations at the surface, which can affect the total rate of diffusion from the device, as can be seen from Equation 2.1. This applies for both monolithic and reservoir type devices.

Reservoir systems, in contrast to monolithic systems, can provide a zero-order release profile. These systems, also known as *membrane-controlled* systems, feature a reservoir of drug surrounded by a polymer membrane. A significant burst release can occur with these systems as well, since drug diffuses to the membrane from the reservoir during storage [7, p. 51]. After administration, the concentration gradient becomes more or less linear, as concentration near the surface approaches zero. If the reservoir core is loaded with drug in excess of its solubility, the device is said to have a *constant activity source* [5, p. 130]. As long as the core remains saturated with drug, the drug will diffuse through the membrane at a constant rate [14, p. 519] [7, p. 9].

In reservoir systems, the release process follows the following sequence [7, p. 9]:

1) Diffusion within the reservoir core
2) Dissolution to membrane or partition between core and membrane matrices
3) Diffusion through the membrane to the device surface
4) Partition between membrane and surrounding medium
5) Transport from the device surface

It is essential that the membrane is and remains intact throughout the use of the device, especially if the drug in the reservoir is not bound to any solid carrier material, since even a small crevice or puncture in the membrane could cause the drug to leak out, ruining the designed release kinetics [5, p. 33]. The carrier material must have a low enough viscosity to enable a stable, thorough contact with the membrane, but it should not be able to diffuse through the membrane [7, pp. 39–40].

Drug diffusion from a cylindrical reservoir-type device

The devices studied in this work are mainly of the reservoir type. Assuming, that diffusion through the membrane is the rate-limiting step, mathematical diffusion models can be used to predict drug release rate from such devices. Fick’s second law for a long, cylindrical reservoir device can be written as

$$\frac{\partial c}{\partial t} = \frac{1}{r}\frac{\partial}{\partial r}\left(rD\frac{\partial c}{\partial r}\right), \tag{2.5}$$

where r is the radius or the radial distance from the center of the cylinder [15, p. 69] [20, p. 3]. This equation assumes that the diffusion is completely radial, meaning that end effects are negligible.

If the diffusion coefficient is assumed to be independent of position (and thus concentration), a solution can be found for steady-state diffusion from a hollow cylinder. The steady-state condition can be expressed as

$$\frac{d}{dr}\left(r\frac{dc}{dr}\right) = 0, \quad a < r < b \tag{2.6}$$

where a and b are the inner and outer radii of the cylinder [15, p. 69]. A general solution for c is given by

$$c = A + B\ ln\ r\ , \tag{2.7}$$

where A and B are constants that correspond to boundary conditions $r = a$ and $r = b$. If the concentrations at the surfaces are kept constant, c can be expressed as

$$c = \frac{c_1 \ln(b/r) + c_2 \ln(r/a)}{\ln(b/a)}, \tag{2.8}$$

where c_1 is the concentration at $r = a$ and c_2 is the concentration at $r = b$ [15, p. 69]. The resulting concentration profile across the membrane in the case that $c_2 = 0$ is plotted in Figure 4 below.

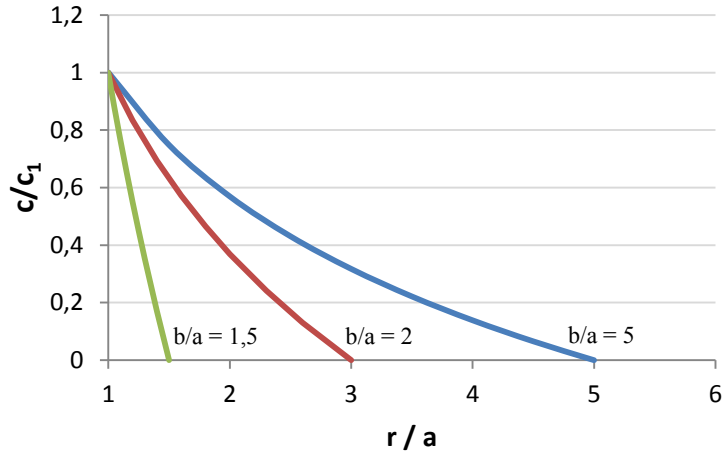

Figure 4: A graph presenting the concentration profile across the membrane for three different $\boldsymbol{b/a}$ *ratios for a cylindrical device. Zero concentration at the outer surface, constant diffusivity and steady-state diffusion are assumed.* $\boldsymbol{c}$ *is the concentration at position* $\boldsymbol{r}$*,* $\boldsymbol{a}$ *is the inner and* $\boldsymbol{b}$ *the outer radius of the membrane and* $\boldsymbol{c_1}$ *is the reservoir drug concentration.*

Furthermore, Q_t, the amount of substance diffusing in time t through unit length of the cylinder can be written as [15, p. 69]

$$Q_t = \frac{2\pi Dt(c_2 - c_1)}{\ln(b/a)}. \tag{2.9}$$

If diffusivity is assumed constant or if the concentration dependence of diffusivity is known for the polymer-API-combination, this mechanistic model could be used to predict the steady-state release rate of an active agent from a cylindrical reservoir device that fulfills the following requirements:

1) The rate of diffusion through the ends of the device must be negligible.
2) Surface concentrations must remain constant.
3) The membrane material must be homogeneous.

Equation (2.9) can also be presented in another form for devices with constant activity sources. As discussed earlier, if we assume that the reservoir is loaded with an excess of drug and drug transport from the device surface is rapid, a constant diffusional flux is achieved. In this case, the amount of drug released from a cylindrical device follows the equation

$$\frac{dM_t}{dt} = \frac{2\pi HDKc_s}{\ln(b/a)}, \tag{2.10}$$

where M_t is the cumulative amount of drug released at time t, H is the height of the cylinder, K is the partition coefficient for the drug between the reservoir and the membrane and c_s is the saturation concentration of drug in the reservoir [5, p. 135] [24].

2.1.4.2 Swelling Controlled Systems

A polymeric drug delivery system is usually classified as swelling controlled if swelling of the polymer network is a significant step in the overall drug release from the system. Overall, drug release from a swelling-controlled PDDS occurs by the following physical phenomena: water diffusion, polymer chain relaxation, polymer dissolution, drug dissolution and drug diffusion (followed by drug transport from the device surface) [5, p. 153]. Depending on the rates of these successive steps, one or many of them may determine the overall release rate from the device.

As water penetrates a polymer network in high enough concentrations, it will induce a polymer chain relaxation process. The concentration of water needed to induce this process depends on the physicochemical nature of the polymer. As the polymer chains "relax", their molecular mobility is increased significantly and the system increases in volume [5, pp. 153–154]. The kinetics of drug transport in these two states (non-swollen vs. swollen) are fundamentally different. In an ideal case, if polymer chain relaxation is the slowest step and if the surface area of the swelling front does not change with time, the overall release will follow zero-order kinetics [5, p. 158].

Since hardly any swellable device exhibits purely swelling-controlled release and none of the aforementioned steps of the release process are instantaneous, moving fronts and boundaries (see Figure 5) will form within the system [5, pp. 158–160] [7, pp. 110–113]. Let us consider a case where the system is loaded with an excess of drug, resulting in undissolved drug as particles in the matrix. At the center of the device, there will be a non-swollen, unaffected part of the system. As water penetrates the system, a moving *swelling front* is formed. The swelling front consists of incompletely swollen material containing dissolved drug molecules and, if drug dissolution is slow, also undissolved drug particles. Some undissolved drug may also be present in the swollen polymer network, creating a *diffusion front*. The dissolved drug diffuses, down its concentration gradient, in the swollen polymer network, out of the device and into the surrounding fluid. At the outer edges of the device, there may even be an *erosion front*, if the swollen polymer is susceptible to erosion.

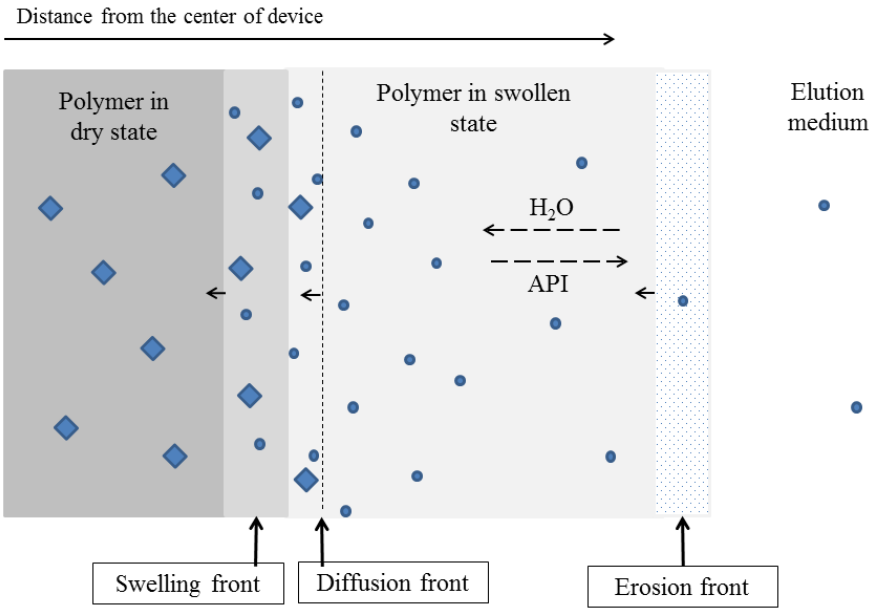

Figure 5: A schematic presentation of the drug release process from a swellable drug delivery device in one dimension. Diamonds represent undissolved drug particles and small circles represent dissolved drug molecules.

Since the diffusional behavior of a drug is fundamentally different in different regions of the partly swollen system, modelling overall release rate for a swellable system is challenging. A simple, general equation for drug release from a swellable system can be written in the form

$$\frac{M_t}{M_\infty} = k_a t^n \,, \tag{2.11}$$

where M_t is the cumulative amount of drug released at time t, M_∞ is the total amount of drug released at infinite time and k_a and n are constants dependent on the nature of interactions between the matrix polymer, the penetrating solvent and the API [7, pp. 126–127] [5, p. 158]. For example, if $n = 0.5$, drug release rate is controlled by Fickian diffusion, meaning that drug diffusion is the lowers step in the process. Additionally, if $n = 1.0$, drug release rate is controlled by the advancement of the swelling front. In this case, diffusivity of drug in the swollen region is much faster than in the non-swollen region. The rate of drug diffusion must also be much higher than the rate of solvent diffusion.

A large variety of models have been developed to study the penetration of a solvent into a polymer matrix with different sets of assumptions and varying success [7, pp. 120–124]. Furthermore, the combined effects of the various phenomena on the overall release have been studied extensively and several rather complex sets of equations for predicting the drug release rate can be found in the literature, of which only some can be analytically solved [7, pp. 130–152].

2.1.4.3 Erosion Controlled Systems

In erosion controlled systems, mass loss of the system controls, to a significant degree, the release of a drug. Thus, the polymer is an active participant in the drug release process. In an ideal erosion controlled device, the drug molecules are physically or chemically immobilized in the polymer matrix and released only by its erosion [7, p. 89]. This implies that the total release rate is directly proportional to the erosion rate. In reality, however, the overall release rate is determined by the rates of various different processes.

The term erosion refers to mass loss of the system, whereas degradation refers more specifically to polymer chain cleavage leading to small molecular weight degradation products that can be eliminated by the body [5, p. 172]. Degradation can be seen as one step of erosion. Erosion also includes water uptake, changes in the structural integrity of the material and physical removal of the material into its surroundings [5, p. 173].

Erosion controlled devices are usually monolithic systems, though reservoir-type systems exist as well [7, p. 5]. In all erosion-controlled systems, water uptake is an essential part of the process. Erosion of a polymeric device (through aqueous hydrolysis) has several steps [5, p. 180]:

1) Wetting of the device surface
2) Diffusion of water into the matrix
3) Polymer degradation and, if possible
4) Removal of degradation products through diffusion

Erosion mechanisms can be divided into two main categories: *surface erosion* and *bulk erosion* [5, p. 180] [7, p. 5]. A schematic presentation of the two processes is shown in Figure 6. In surface erosion, the water diffusion step is slower than the degradation step, leading to gradual loss of material from the surface. The average molecular weight remains relatively high for a long period of time. In bulk erosion, water penetrates the material rapidly, but polymer degradation is slow, leading to a gradual decrease in the average molecular weight with very low initial mass loss. Once a critical chain length is reached, the device disintegrates, resulting in rapid mass loss. In principle, a surface eroding system can provide a constant release rate if its surface area remains constant and drug diffusion is insignificant [7, p. 90].

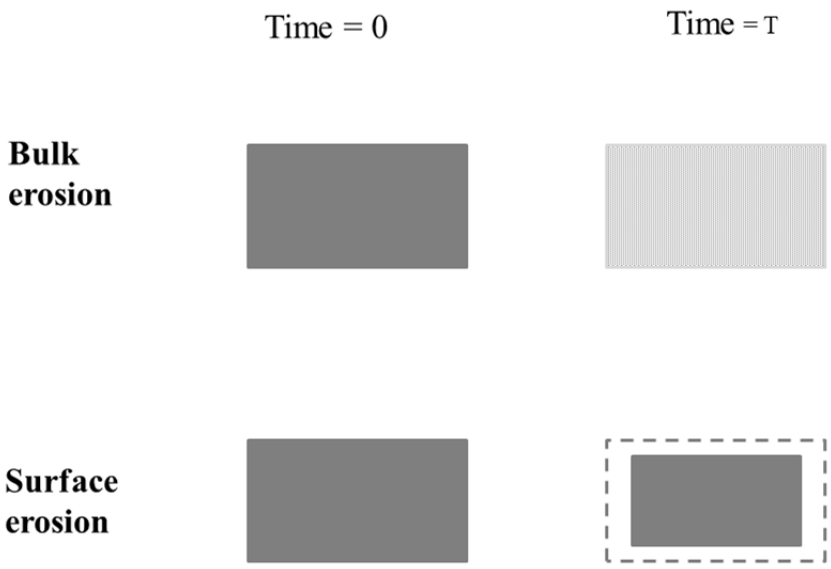

Figure 6: A schematic illustration of the difference between bulk and surface erosion. Dashed line depicts the original dimensions of the eroded body.

Due to their water-absorbing nature, hydrophilic polymers commonly exhibit bulk erosion behavior, whereas more hydrophobic polymers favor surface erosion. Chemical structure of the polymer can be designed to facilitate chain cleavage through hydrolysis or specific enzymatic reactions by incorporating labile bonds, such as carbon-nitrogen bonds in polyurethanes or carbon-oxygen bonds in polyesters [7, p. 91]. Chain cleavage can be designed to occur in side-chains, crosslinks or the polymer backbone depending on the desired erosion kinetics [5, pp. 173–174]. Besides the chemical nature of the cleavable bonds, rates of polymer hydrolysis are also affected by factors such as morphology and the nature of neighboring substituent groups [7, p. 92].

Degradation behavior of the device is not only dictated by the choice of polymer material, since the addition of any substances (excipients, active agents, etc.) into the matrix will change the degradation behavior, e.g., through catalysis or plasticization [5, p. 182]. Especially if hydrophilic molecules are incorporated in a bioerodible device, different osmotic mechanisms can play a significant role in system behavior and the resulting water uptake can cause matrix swelling, ruptures in the matrix, drug diffusion or convective mass transfer [5, p. 180]. Furthermore, variations in environmental (in vitro) and physiological (in vivo) conditions can have significant effects on erosion kinetics [5, p. 175].

The majority of degradable DDS fall under three categories: injectable microparticles, preformed implants and injectable in-situ forming implants [5, pp. 171–172]. As the categories differ in size and structure, they also exhibit different release profiles. Microparticles, generally having a diameter of 10 to 100 µm, are characterized by large surface areas compared to volume and so they often show release profiles with strong ini-

tial burst release [5, pp. 186, 189]. The burst is followed by a local release rate minimum and a shallow exponential increase and decrease. These fluctuations can be smoothed out by blending or with suitable matrix porosity [5, p. 189]. Preformed and in-situ formed implants are significantly larger in size than microparticles, so they naturally exhibit a slower release and are usually functional over a longer period of time. For in-situ forming implants, a significant amount of drug may be released during the injection and hardening of the unhardened mixture [5, pp. 205–206].

2.1.4.4 Osmosis Controlled Systems

Water penetration and osmosis play a significant role in erosion and swelling controlled DDS and so they have already been briefly discussed in previous subsections. In such systems, osmosis, the diffusion of water, is a non-dominant step - its rate does not determine drug release rate from the device to a large degree.

An example of an osmosis controlled device is the osmotic pump (see Figure 7). It consists of a tablet or capsule containing solid, water-soluble drug surrounded by a membrane that is permeable to water but the drug cannot pass through it. At one side of the membrane, a small hole is drilled and as the system is placed in an aqueous solution, an osmotic pressure gradient arises. Water begins to penetrate the system through the membrane, dissolving the drug, which results in a flow of dissolved drug through the tiny orifice. As long as drug concentration in the core remains above its solubility, a constant release of drug from the device is maintained [5, pp. 21–22].

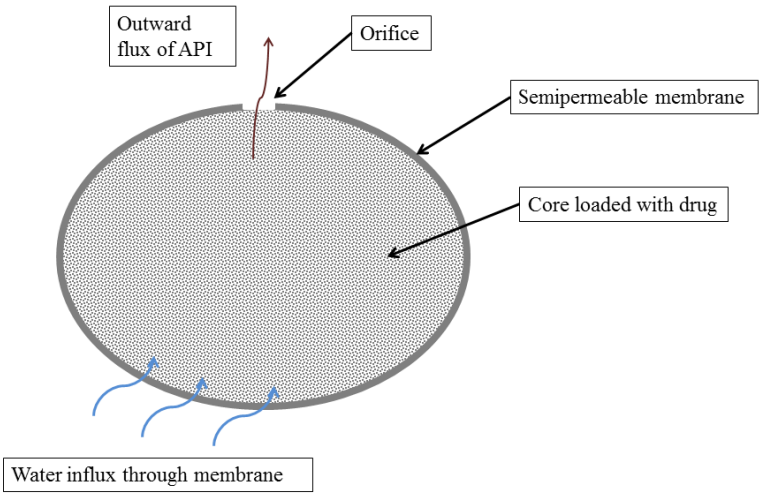

Figure 7: A schematic presentation of the structure of a simple osmotic pump.

More efficient versions of the osmotic pump feature additives that, upon introduction to water, exert a pressure to promote a more rapid flow of drug from the device [5, p. 22]. Different geometries and designs have been applied to improve the release profile by minimizing drug diffusion through the membrane, as few membranes are completely drug-impermeable [7, pp. 159–161].

Osmosis controlled monolithic devices have also been prepared and studied. The principle of this technique is embedding particulate dispersion of osmotically active drugs with low solubilities and diffusivities within a polymer matrix [7, pp. 162–163]. As the drug particles near the surface absorb water from the surroundings, a local pressure gradient arises, eventually causing matrix rupture and drug release. This differs from erosion-controlled release in the sense that ruptures are caused by osmotically induced stresses and not by polymer degradation.

2.2 Silicone Elastomers

This study focuses on the performance of silicone elastomer materials in controlled release drug delivery products. The goal of this section is to give a brief overview of the chemistry, practical applications and compounding of silicone elastomers.

2.2.1 Siloxane Polymers – Classification and Synthesis

Silicones (or *polysiloxanes, siloxane polymers)* are semi-organic polymers that have a backbone consisting of *siloxane* units [25, pp. 12–13]. Siloxane is a chemical group consisting of repeating silicon and oxygen atoms [25, p. 10]. A chemical structure of a siloxane group is presented in Figure 8. The name siloxane is a portmanteau that comes from the words silicon, oxygen and alkane. Silicon and oxygen are usually found in the nature in the form of silicate minerals. By mass, silicon and oxygen are the most abundant elements in the earth's crust [26] [25, p. 27].

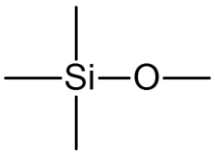

Figure 8: Structural formula of a siloxane group.

Another important bond in silicones is the carbon-silicon bond between silicon atoms in the backbone and the connected substituent groups. Compounds of carbon and silicon, so-called organosilanes (or organosilicon compounds) are not found in the nature and they were first synthesized, in the late 19th century, using a Friedel-Crafts dialkylzinc reaction [25, p. 3].

The process of silicone synthesis essentially begins with the reduction of silica (sand) into silicon at high temperatures [25, p. 367]. Elementary silicon is then reacted with an alkyl halide, most commonly methyl chloride that is first produced by reacting hydrochloric acid with methanol [25, pp. 382–384] [27]. The reaction between silicon and

methyl chloride occurs at elevated temperatures and features a copper catalyst, resulting in a mixture of silanes (Me_xSiCl_y) and byproducts. This so-called Direct Process,

$$x\,Si + y\,CH_3Cl \xrightarrow[\Delta]{cat.} Me_2SiCl_2 + MeSiCl_3 + Me_3SiCl + MeHSiCl_2 + other\ silanes\ and\ byproducts\ , \qquad (2.12)$$

developed by Rochow and Müller, is the most commercially significant route to organosilicon compounds [25, p. 383] [27]. Dimethyldichlorosilane, the species with the highest yield (over 50%), is then hydrolyzed to give a series of cyclic and linear oligomers and hydrochloric acid [27]. The hydrochloric acid can then be returned into the production process of methyl chloride.

The chosen polymerization reaction depends on the structure of the oligomers. Bifunctional silanes are polymerized by condensation (step-growth polymerization) and cyclic oligosiloxanes by ring-opening polymerization [28, p. 1]. The chemical structure of the most common polymerization end-product, polydimethylsiloxane (PDMS), is shown in Figure 9.

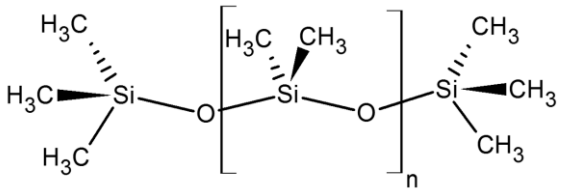

Figure 9: Structural formula of a trimethylsiloxy-terminated polydimethylsiloxane.

The simple PDMS structure can be modified by the substitution of functional groups, creating unique property combinations. Properties and applications of silicones will be discussed in section 2.2.3.

2.2.2 Vulcanization Methods

Though the siloxane backbone is highly polar, its intermolecular interactions are largely hindered by the organic side groups. As a result, linear silicone polymers are mechanically weak materials. To create strong and elastic materials, rubbers, they must be crosslinked. The crosslinking reactions are made possible by tri- or tetrafunctional silanes containing groups that react under ionic conditions to form $Si-O$ crosslinks or by using organic parts of the polymer (vinyl or methyl groups and the hydrogen atom) to form organic crosslinks [25, p. 282].

In practice, silicones are usually crosslinked using one of three methods: heat-sensitive radical cure, moisture cure at ambient temperature or transition metal catalyzed cure by hydrosilylation. [25, p. 282] [28, pp. 567–615]. Other more or less significant methods

include radiation cure, crosslinking via organic side chains and direct cure by a catalyzed reaction of hydrosilane with a silanol [25, pp. 282–291] [28, p. 569].

Heat-sensitive radical cure methods usually involve the use of peroxides that undergo thermal dissociation, resulting in radicals that act as crosslinking initiators. The radicals attack the carbon-hydrogen bonds in the side groups to form macroradicals that react between one another and create $C - C$ crosslinks [25, pp. 287–288] [28, p. 569]. An example of such a reaction series with dibenzoyl peroxide is shown in equations

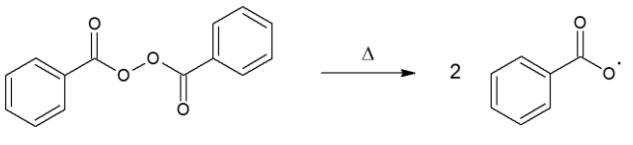

(2.13),

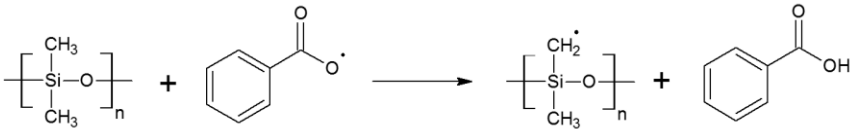

(2.14)

and

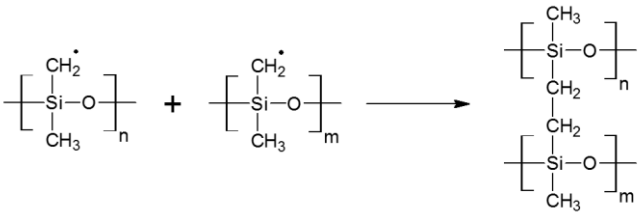

(2.15).

If unsaturated (vinyl) groups are present in the structure, low concentrations of di-alkyl- or hydroperoxides can be used to create a crosslinked material [28, pp. 570–571]. For a saturated, unmodified PDMS, aryloxy (or acyl) peroxides can be used, resulting in a randomly cross-linked matrix with $\equiv Si - CH_2 - CH_2 - Si \equiv$ -type crosslinks [25, p. 288] [28, p. 576]. In the former case, peroxide concentration has virtually no effect on the resulting crosslinking density, whereas in the latter, the relationship is more or less linear and higher amounts of peroxide as well as higher temperatures are needed than for unsaturated systems [25, p. 288] [28, pp. 571–572]. Largely used peroxides include 2,4-dichlorobenzoyl peroxide for saturated systems and di-*t*-butyl peroxide and dicumyl peroxide for vinyl-containing systems [28, p. 577]. A post-curing cycle is commonly used with peroxide cured elastomers to enhance mechanical and thermal properties of the rubber and to remove volatile byproducts created in the crosslinking step [28, p. 576].

Room temperature vulcanization (RTV), so-called *moisture cure*, is based on condensation reactions of silanol groups in hydroxyl-terminated PDMS [25, pp. 282–284] [28, pp. 577–578]. Such a reaction can occur between the end groups of two polymer chains with no added substances, resulting in a completely inorganic backbone [28, p. 577].

However, to form a three-dimensional network, multiple hydroxyl groups would be needed. In practice, it is more feasible to have the hydroxyl end groups react with tri- or tetrafunctional silanes ($RSiX_3$ or $RSiX_4$) [25, p. 283] [28, p. 578]. This results in di- or trifunctional-terminated PDMS chains. Upon contact with moisture, these end groups undergo hydrolysis, yielding di- or trihydroxyl-terminated chains that react with each other to form a crosslinked matrix [28, p. 578]. Commonly used functional groups (X) in the multifunctional silanes include acetoxy and alkoxy (e.g. methoxy) and oxime groups [28, pp. 578–585].

Moisture cure systems are provided as either two-component or single component systems, depending on their application. In two component systems, one component contains the silanes mixed with a metal carboxylate catalyst while the other component contains the PDMS polymer [28, p. 580]. In single component systems, the components are stored as a mixture and thus must be protected from exposure to moisture before use. Titanate catalysts are often used in single component systems [28, p. 583].

Hydrosilylation cure is based on the reaction of hydridosilane (SiH) with an unsaturated carbon-carbon bond, typically a silicon vinyl group ($CH_2 = CH - Si \equiv$) [28, p. 588]. The addition reaction is catalyzed by a noble metal, typically platinum. Addition to the carbon in β-position in the silicon vinyl group is usually favored [28, p. 591]. Since vinyl groups can be incorporated in any part of the polymer chain, it is possible to design and create different types of networks by varying the substitution configuration of the polymer, resulting in property combinations unachievable with other curing methods [28, p. 601]. Drawbacks of this method include platinum-induced yellowing of the cured material, short shelf lifes at room temperature (after mixing) due to high catalyst reactivity and possible reactions of excess SiH groups with water and moisture when cured in air [28, pp. 588–601]. On the other hand, the curing process creates no byproducts and only a small amount of catalyst is needed. Therefore, this vulcanization method is of interest for food and health industries [28, p. 601].

2.2.3 Properties and Applications

Silicone polymers, such as polydimethylsiloxane, have found a variety of applications as a direct result of their excellent high temperature and oxidative stability [28, pp. 216, 230]. Silicones are also flexible at very low temperatures due to the exceptional flexibility of the polymer backbone. This makes them very useful for applications that require elasticity below ambient temperatures. Silicones have more flexible polymer chains than most organic polymers, firstly because the $Si - O$ bond is significantly longer (1.64 Å) than the $C - C$ bond (1.53 Å) and secondly because only every other atom in a siloxane chain can have side groups that sterically hinder chain movement [28, pp. 216–218].

Linear PDMS with moderate to high molecular weights show a glass transition near −123 °C and a linear dependence has been observed between T_g and molecular weight [28, pp. 218–219] [29, p. 500]. Substituent side groups can decrease T_g by increasing polymer free volume or increase T_g by decreasing chain mobility [28, p. 218]. Crosslinked networks undergo glass transition at only slightly higher temperatures than their linear precursors [28, pp. 221–223]. In contrast to several other elastomers, the use of a reinforcing filler has virtually no effect on T_g for polydimethylsiloxanes [28, p. 222]. Though hardly relevant in the case of rubbers, it is worth mentioning that melting of linear crystalline PDMS occurs in temperatures as low as −60…−40 °C [28, pp. 225–226]. Liquid crystalline silicone polymers can be prepared by side group substitution, yielding interesting property combinations [28, pp. 228–230].

The thermal stability of silicones originates from the strong $Si - O$ bonds (452 kJ/mol) that are very resistant to homolytic scission [27, p. 8]. Reported values of depolymerization onset temperature in an inert atmosphere include 343 °C for hydroxyl-terminated linear PDMS to 350 °C for trimethylsilyl-terminated linear PDMS [28, pp. 230–233]. Another reported onset value for PDMS is around 400 °C [27, p. 12]. Oxidative reactions in non-inert atmosphere will begin at lower temperatures and have been shown to start around 250 °C for PDMS [28, p. 233]. Phenylsilicones are known to remain stable at higher temperatures than methylsilicones [25, p. 257].

In general, safe temperature ranges for silicones in oxidative environments extend up to 200 °C for long-term use and even up to 450 °C for short-term use [29, p. 438]. Oxidation reactions cause degradation by attacking multiple different bonds, primarily the $Si - C$ bonds, whereas depolymerization in an inert atmosphere occurs through $Si - O$ bond scission [29, p. 495] [28, p. 230]. In contrast to depolymerization, oxidative degradation tends to increase crosslinking density, making the material harder [25, p. 297]. Depolymerization of PDMS in an inert atmosphere results in a series of cyclic oligomers, the most abundant being the cyclic trimer, followed by the tetramer and the larger oligomers in decreasing amounts [28, pp. 230–231].

Unvulcanized silicone polymers are, in general, viscoelastic fluids. When crosslinked and filled with a reinforcing filler, they become strong and elastic materials. Mechanical (and electrical) properties of silicone rubbers are less dependent on temperature than those of organic rubbers [29, pp. 497–498]. This makes them the material of choice for applications with large temperature variations, even though many of their mechanical properties (strength, elongation at break, compression set, etc.) are surpassed by several organic rubbers at room temperature.

Molecular weights of silicone elastomers (gums) used as rubber precursors are in the range of 300 000 – 700 000 g/mol for heat-vulcanizing elastomers and 10 000 – 100 000 g/mol for RTV types [29, p. 388]. As a result, reported typical values (with no infor-

mation provided on filler concentration) of tensile strength and elongation at break at room temperature include 10 MPa and 300–500% for heat vulcanized and 3 MPa and 100–150% for RTV silicone rubbers [29, pp. 388, 502].

Silicones are widely used as electrical insulators due to their low relative permittivity that is not affected by temperature to a large degree [25, p. 257]. In contrast to hydrocarbon polymers, if faced with temperatures that result in oxidative degradation, the main degradation product, silica, is an excellent insulator by itself [25, p. 257].

Silicones are generally very unreactive, except in highly acidic or basic environments [28, p. 315]. Silicone rubbers are highly resistant to oil and weathering (ozone, oxygen and UV radiation), but unmodified PDMS is easily swollen by solvents like gasoline and benzene [14, p. 257] [29, pp. 389–390, 502]. Silicone fluids are highly hydrophobic due to the organic side groups (e.g. methyl) that are typically pointed towards the material surface [25, p. 257] [30]. They have a low surface tension and are capable of wetting most surfaces [30].

Typical applications of silicones include wire and cable insulation, gaskets, seals, tubing, surgical implants, lubricants, coatings, molds and many household cleaning and personal care products [14, p. 372] [30]. They are used, e.g., in plastic, food, agricultural, textile, pulp and paper, automotive, aviation, construction, electronics and medical industries [30]. Hydrophobicity of silicones is exploited to create moisture barriers in fabrics, waxes, sealants and potting materials [25, p. 257]. Purely silicone-based or chemically modified low-viscosity fluids are also used as release agents, surfactants, foam stabilizers and defoamers [25, p. 257]. The wetting characteristics of silicones are also beneficial in terms of biocompatibility [30]. Large-scale healthcare applications of silicones include tubing and membranes in extracorporeal equipment, coatings on medical devices and tools (such as catheters, needles and syringes), as well as orthopedic and aesthetic implants [2, pp. 1106–1116].

2.2.4 Fillers for Silicone Rubbers

In this subsection, the most commonly used fillers for silicone rubbers and their effects on material properties are discussed. Primarily of interest is the effect of silica on the diffusion of organic molecules in a PDMS network. A typical silicone rubber formulation consists of silicone gum, fillers and curing agents [29, p. 400].

2.2.4.1 Common Fillers

Even when properly cross-linked, PDMS are relatively weak materials due to the lack of strong intermolecular forces [28, p. 570]. Therefore, reinforcing fillers are used in practically all applications that require mechanical strength. Silicas form clearly the most

common class of fillers used in silicone rubbers [29, p. 402]. Silica, silicon dioxide (SiO_2), consists of a network of oxygen and silicon atoms, shown in Figure 10.

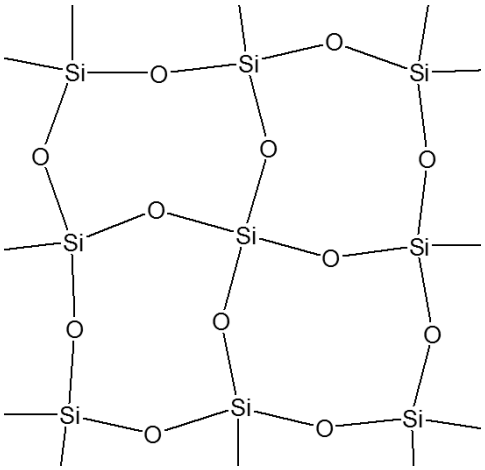

Figure 10: Solid silicone dioxide is a three-dimensional network of atoms, where each silicon atom is bonded to four oxygen atoms.

Silica exists in both amorphous and crystalline forms. Only amorphous silica is used as a filler in silicone elastomers [25, p. 462]. Though silica is chemically inert, crystalline silica particles with particle sizes ca. 1–5 µm pose health concerns as they can cause severe damage to the respiratory system if inhaled for prolonged periods of time [25, p. 462].

Two main types of synthetic, amorphous silica are used commercially: pyrogenic silica and precipitated silica. *Pyrogenic (fumed) silica* has a greater reinforcing effect of the two due to its smaller particle size and larger surface area (ca. 100–400 m^2/g) [29, p. 401] [31, p. 32]. A large surface area results in a large degree of intermolecular physical interactions. Consequently, fumed silica also causes the uncured elastomer to harden significantly during storage. It is produced by open flame combustion of chlorosilanes with a controlled amount of water [25, p. 311]. In this high temperature process, primary particles with sizes as small as 5–50 nm can be prepared [25, p. 311]. These particles coalesce to form (irreversible) aggregates and (reversible) agglomerates [31, p. 32].

Precipitated silica has a somewhat lower reinforcing effect on the material, but it improves high temperature stability in oxidative environments [29, p. 401]. It also causes less elastomer hardening during storage. Silica precipitation is commonly achieved by a condensation reaction that occurs when the pH of an aqueous sodium silicate solution is decreased [25, p. 311]. The final network structure and porosity of the product is determined by the choice of drying, washing and milling processes that follow [31, pp. 35–38].

To combat the elastomer hardening encountered with high filler loading, so-called structure control additives can be used [29, p. 403]. In contrast to silicone polymers, silica is

highly polar. Therefore, silicas are often treated with organosilanes or cyclic polyorganosiloxanes to change their surface chemistry, namely to increase their wettability by the polymer and consequently improve their dispersibility [29, p. 403]. In addition to silica, metal oxides and silicates as well as carbon black can be used as fillers for different purposes such as pigmentation and stability enhancement [29, p. 402].

2.2.4.2 Effect of Silica on Drug Diffusion

Silicones have been used successfully as biomaterials for decades due to their biocompatibility and exceptional physico-chemical characteristics and they have also been applied to the field of controlled drug delivery. Therefore, the diffusion of pharmaceuticals through silicones and the effect of material composition on diffusion have been extensively studied since the 1960s [24] [32–39]. Though a large number of variables will determine the overall effect of silica on drug permeation through a membrane, a general conclusion from the literature cited above is that the addition of silica into a silicone membrane decreases the permeation rate of pharmaceutical ingredients through the membrane.

As discussed earlier in this chapter, the PDMS polymer is hydrophobic in nature and silica, on the other hand, is highly polar and hydrophilic. Depending on the chemical structure of a drug, it will have different interactions with the membrane polymer molecules and filler particles. A highly polar drug will have low solubility in the polymer phase, but high affinity for the filler particles and will be distributed accordingly. After the drug (solution) comes into contact with the membrane, it will take a finite amount of time to saturate the filler aggregates with drug molecules, after which steady-state permeation is achieved [32]. The following observations support this explanation:

1) The solubility of a drug in a membrane can be enhanced by the addition of fillers [16] [32].
2) Filled systems show significantly longer “lag times”, but only a marginal decrease in steady-state diffusion rates [16] [32].
3) The lag time was shown to have a linear dependency on the maximum adsorptive capacity of filler, which is directly related to its available surface area [38].

The lag time is defined by extrapolating the steady-state portion of a cumulative drug release graph, as shown is Figure 11. Its magnitude represents the relative amount of drug sorption on the filler [19].

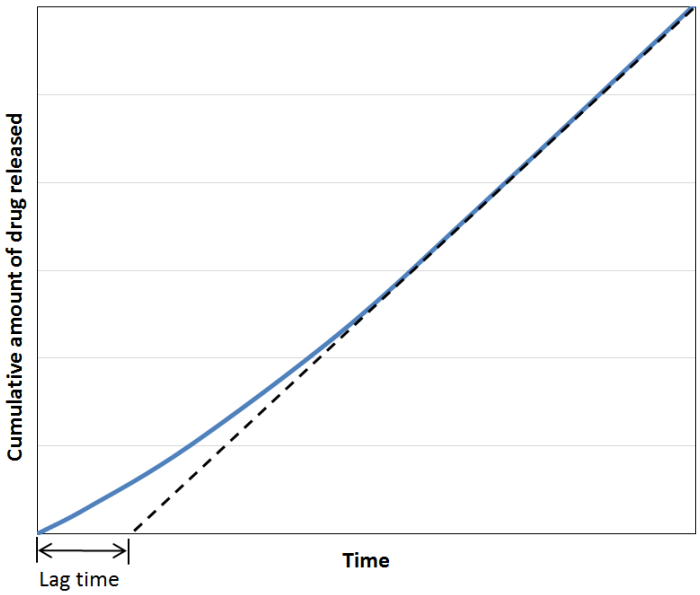

Figure 11. The determination of lag time in a permeation experiment.

Mazan and co-workers studied the dependence of progesterone steady-state diffusivity through PDMS membranes on silica content (hexamethyldisilazane-treated silica with a particle size of 10–100 nm) [33]. The dependence was relatively linear within the 0–10 weight-% SiO_2 concentration range. Measurement of a true concentration profile within the membrane at various times was accomplished with radioactively marked drug molecules. A linear dependency of *p*-aminobenzoate transmission rate and PDMS membrane fumed silica content was discovered by Most [32]. In certain studies, silica has been applied directly to the drug solution (instead of the membrane) to see how much drug it retains [34] [36].

Mazan et al. concluded that the negative effect of silica on steady-state release is caused by both silica-drug interactions and changes in the crosslink network [33]. Roseman rationalized that since all filler particles are saturated by drug molecules, the decrease in steady-state release cannot be attributed to adsorption of drug on the filler. He proposed that the small decrease can be explained simply by a decrease in polymer volume fraction and possibly increased tortuosity [16]. Flynn and coworkers elaborated on this problem and reached a similar conclusion: the influence of an inert but adsorptive, impermeable filler (such as silica in a silicone rubber) on the steady-state flux can be explained by a reduction in effective diffusional area and an increase in diffusional path length [19, p. 492]. This implies that the relationship between filler concentration and drug permeation rate is at least close to linear.

2.3 Related Concepts of Elastomer Processing

This section presents some principles and theory of elastomer processing closely related to this study: rubber compounding, mixing and mastication (or softening), extrusion and vulcanization. To limit the length of this section, the topic is covered very selectively.

2.3.1 Compounding, Mixing and Mastication

Compounding refers to the optimization of material properties by modifying a polymer material in terms of composition. A rubber compound can contain several different polymers, filler systems, stabilizers, vulcanization agents, processing aids, pigments, oils, etc. [40, p. 417]. Rubber compounding is a science on its own and compound recipes are valuable intellectual property for rubber product manufacturers. In this thesis, the terms *compound* and *formulation* are used interchangeably.

Mastication, in the rubber industry, is a process of polymer breakdown caused by mechanical work [41, p. 96]. It is performed to reduce the viscosity of a high molecular weight elastomer prior to compounding, extrusion, molding or other shape-giving steps. Mastication is absolutely necessary for viscous natural rubber and helpful for synthetic rubbers [41, p. 96]. The resulting partly degraded material is softer and stickier, making the subsequent processing easier and allowing the incorporation of large concentration of fillers and additives. For silicone rubbers, breakdown of the polymer chains is not desired. The function of this softening step for silicones is to break some of the hydrogen bonds between filler particles and polymer chains that cause the material to harden during storage. Mixing and mastication of a rubber formulation can be performed with a closed chamber mixer (also known as an internal mixer), an open-roll mill or, less commonly, a continuous mixer [42, p. 517] [41, p. 96] [43].

Internal (batch) mixers are very common in the rubber industry and can also be used for some thermoplastics and thermosets [41, p. 97]. They are advantageous in their ability to keep the mixed material at a constant temperature. Internal mixing is a more energy-intensive process than mixing with an open-roll mill, and also significantly faster [41, p. 99]. This is because mastication occurs over a much larger area than in open-roll mills. Internal mixers come in three main types: “Banbury”, “Shaw intermix” and “Baker-Perkins shear-mix” [41, p. 98]. The Banbury type is the most common one. It consists of a cylindrical chamber that contains two counter-rotating rotors revolving at different speeds [41, pp. 97–99]. The special design of rotor geometry leads to shearing and movement of the material in several directions. The mixer includes a hopper through which material is introduced and an unloading door for removal of the mixed material. Material can be forced into the mixer with a mechanical ram. The chamber walls and rotors (if hollow) are often cooled with circulating water.

Open-roll mills consist of two (or more) rollers, steel cylinders that are placed horizontally, parallel and close to one another [41, p. 97]. The rollers rotate in opposite directions and as material is fed on top of the rolls, it passes though the gap between the rolls, where mixing and mastication takes place. The front roll is usually set to revolve at a slightly slower speed than the back roll and the gap is adjusted to provide proper shearing action [41, p. 97]. A schematic presentation of the structure of a two-roll mill is presented in Figure 12. As mastication takes place and enough rubber has been added, a band of rubber is formed on the front roll and material will accumulate as a "bank" above the gap. Compounding ingredients can then be fed into the bank. Several times during the process, the elastomer band is cut with a knife from the front roll and reintroduced to the mixer so that thorough mixing occurs.

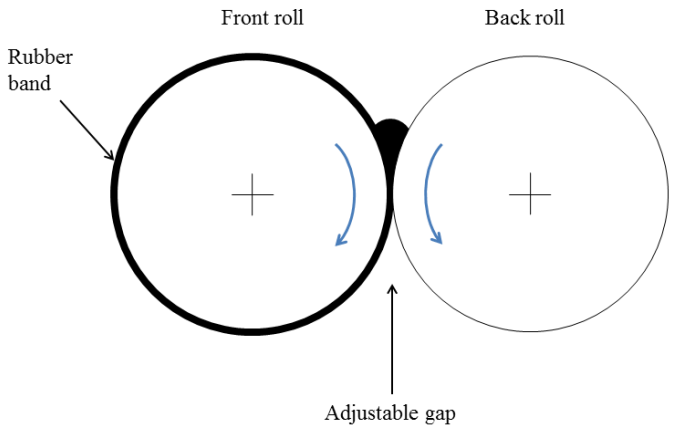

Figure 12: Schematic presentation of a two-roll mill.

Continuous mixing is achieved with modified extruders that carry out both the mixing and extrusion steps of processing [43, pp. 175–176]. The barrel and screw have been fluted (grooved) at certain position along the barrel to increase the shearing action of the extruder. Higher shear rates are needed in order to break down particle agglomerates to achieve a good dispersion of fillers and other components of the compound.

2.3.2 Elastomer Extrusion

Extrusion is the most important polymer processing method [44, p. 15]. Extrusion processes can be divided into continuous and discontinuous or batch type processes. Continuous processes involve the use of screw extruders and disk or drum extruders, whereas discontinuous (cyclic) processes are run with ram extruders or reciprocating screw extruders [44, p. 23]. Continuous screw extruders for rubber processing are of interest in this study.

Screw extruders can be classified into two groups according to the number of screws they contain: single-screw or multi-screw. Single-screw extruders form the most common class of extruders in the polymer industry. They are affordable, reliable, rugged

and simple by their design [44, p. 24]. Twin-screw extruders are also used in a very large scale, mainly for specialty polymers or heat-sensitive polymers such as polyvinyl chloride and for materials that are hard to process, as they can provide better feeding and mixing as well as more accurate temperature control [44, p. 458]. A simplified structure of a single-screw extruder is shown in Figure 13, where the blue arrows depict the direction of material flow.

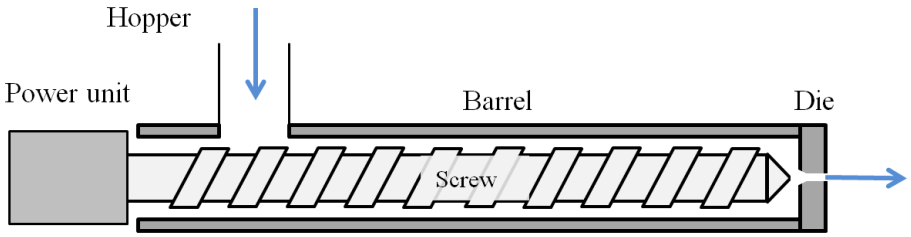

Figure 13: Simplified structure of a single-screw extruder.

Thermoplastics are usually fed into an extruder in the solid state and melted by electrical barrel heaters and the heat created within the barrel by frictional forces – the extruder has a plasticating function. Rubber extrusion differs from the extrusion of thermoplastics in the sense that the material is introduced into the extruder in a liquid, though highly viscous, state. This means that rubber extruders are essentially screw pumps that force a liquid material through a die. Both cold and hot feed extruders are used for rubbers, depending on the material [44, p. 27].

Rubber extruders differ from thermoplastic extruders by their length, heating and cooling systems, as well as by feed section and screw design [44, p. 27]. Rubber extruders are shorter than plasticating single-screw extruders [41, p. 24]. The viscosity of rubber is high compared to thermoplastics, leading to high frictional forces and excessive heat generation in long extruders. The typical L/D ratio (length/diameter of screw) is around 5 for hot feed and between 15 and 20 for cold feed rubber extruders [44, p. 27]. Rubber extruders can be either heated or cooled down, depending on the material and its rheological and curing characteristics.

The screw of a rubber extruder usually has a constant, large channel depth and a decreasing pitch, whereas a plasticating extruder usually has a constant pitch and a decreasing channel depth [44, p. 28]. These parameters are best explained by Figure 14. A deep channel results in decreased shearing and, consequently, reduced heat generation. Depending on the physical form of the material, different types of feed sections are found in rubber extruders. Rubbers are often fed into the extruder the form of strips, pellets or large lumps and sometimes also as powders [44, p. 27]. Depending on the material form, extruder feed sections can be equipped with rams or rolls to force the material into the barrel [44, p. 27].

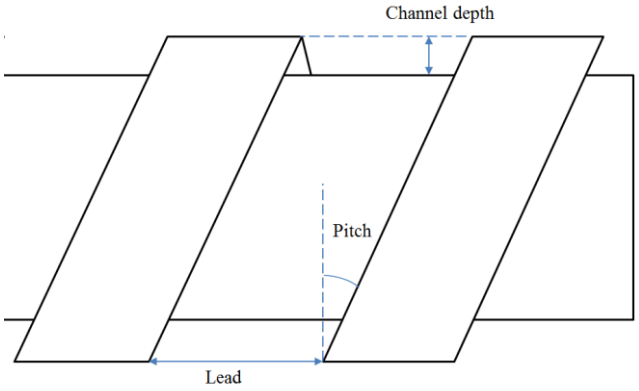

Figure 14: A simple schematic presentation of channel depth, pitch and lead – important parameters of an extruder screw.

The extruder die essentially determines the cross-sectional geometry and dimensions of an extrudate. With thermoplastics, controlled cooling of the extrudate is necessary for dimensional stability [41, p. 23]. With elastomers, some dimensional changes can occur after the die as a result of the shrinkage caused by vulcanization [45, p. 13]. Similarly to plastics extrusion, elastomer extrusion dies have to be designed to compensate for die swell. Die swell refers to the changes in geometry and dimensions of the extrudate as it exits the die caused by the viscoelastic behavior of the polymer material [45, pp. 108–109]. The design of the die obviously depends on the final shape (rod, beam, pipe, film, sheet, filament etc.) of the product. Dies that are used for tube extrusion and wire coating or jacketing applications are discussed in the next section, as they are the ones relevant to this thesis.

2.3.3 Dies for Tube Extrusion and Extrusion Coating

The extrusion of articles with hollow, circular cross-sections requires the use of a die that controls both the inner and outer diameters of the extrudate. This presents a problem: how to design the support for the inner part of a die (also known as the *mandrel*) without jeopardizing the homogeneity of the material flow? The extrusion of articles with hollow, circular cross-sections is usually accomplished with so-called mandrel support dies, screen pack dies, side-fed mandrel dies or spiral mandrel dies, the last one yielding the highest extrudate homogeneity [45, p. 153].

Typically, some kinds of *weld lines* are formed when extruding hollow products, resulting from breaking the flow of material into two or more streams and then re-introducing these streams together before they exit the die [44, p. 447]. Weld lines are regions of lower mechanical strength and a well-designed die will minimize their appearance in the extrudate. A variety of methods for improving flow homogeneity at the end of a tube or pipe extrusion die have been developed [45, pp. 153–159].

While large pipes are typically extruded with longitudinally fed (in-line) dies, crosshead dies are more commonly used for small tubing [44, p. 446] [45, p. 159]. In a crosshead die, the direction of inward flow is perpendicular to the outward flow of material [44, p. 447]. Besides tube extrusion, polymer coating of wires and cables is commonly performed with crosshead dies [46, p. 469]. The wire to be coated is pulled through the die and and the molten plastic comes in contact with its surface and covers it.

In this work, elastomeric tubing is coated with another elastomer. The process is, however, similar to the extrusion coating process of metallic wires. Wire coating extrusion processes can be divided into high pressure and low pressure extrusions (see Figure 15). In high pressure extrusion, the contact between the wire and the coating material occurs inside the die, whereas in low pressure extrusion, they come in contact after the wire has exited the die [44, p. 448]. High pressure extrusion yields better adhesion between the materials, while low pressure extrusion is a good alternative when it is important that the coating can be easily removed.

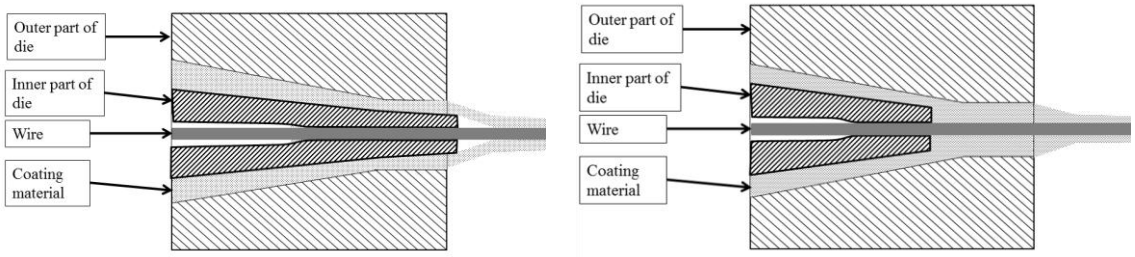

(a) (b)

Figure 15: Operating principles of wire coating dies of the low pressure (a) and high pressure (b) types.

After extrusion, the coating is hardened by passing the extrudate through a cooling medium (in the case of thermoplastics) or through a curing oven (in the case of rubbers) [41, p. 33]. Methods for continuous curing of extruded rubber products are discussed in the next subsection.

2.3.4 Continuous Vulcanization of Extruded Products

Continuous vulcanization of extruded rubber products can be achieved by various methods. Depending on the material, the continuous cure may or may not be sufficient. For heat-resistant fluorocarbon and silicone elastomers, for example, a *post-cure* cycle is needed to achieve complete cure and to eliminate peroxide residues [43, p. 191]. The continuous methods differ, for example, in attainable process speeds and in the amount of distortion to profile geometry caused by gravity and/or conveyor contact.

The most common method of continuous vulcanization in profile extrusion is to pass the extrudate through a *chamber of hot air* [43, p. 165]. As the thermal conductivity of rubber is very low, heat transfer into thick sections of a profile takes time. Additional in-

frared heaters or microwave emitters can be installed in the chamber to accelerate the heating process and to improve heat transfer. To achieve a desired degree of cure, air flow speed, extrudate movement speed, air temperatures and heater power inputs can be adjusted.

Infrared or *microwave systems* can also be used independently. Infrared systems are used in the application of surface finishes to profiles and in the extrusion of certain silicone rubber profiles and microwave systems are used with complex profile geometries when heat transfer becomes a problem and are best suitable for polar rubbers [43, p. 166]. Even *gamma irradiation cure* can be used for some rubber compounds [43, p. 167].

One alternative method is the *liquid medium cure*, where the extrudate is passed typically through a steel tank containing molten salt and a conveyor to guide the extrudate through it [43, p. 166]. After passing through the bath, the extrudate is washed to remove salt residues. The used salts are often toxic so this method may raise health and environmental concerns. Another alternative is the *fluid bed system* (or *fluidized bed*) that consists of a bed of particles, typically glass beads, fluidized by blowing hot air through it [43, pp. 166–167]. The extrudate is passed through this bed of particles and subsequently cleaned.

Quite similar methods have been used for continuous vulcanization of elastomer coated cables and wires. The vulcanization of cable coatings has been performed by passing the extrudate either through a hot steam tube, a hot air tube with the option of additional infrared heaters, a fluidized bed of glass beads, or a molten salt bath [43, p. 162].

2.4 Experimental Design and Statistical Analysis

This section discusses two concepts: designing experiments and statistically analyzing experimental data. In subsection 2.4.1 some basic principles of Design of Experiments (DoE) are discussed. The calculation, use and interpretation use of some relatively simple statistical parameters and tools relevant to this thesis are discussed in subsection 2.4.2. These include correlation coefficient and the evaluation of statistical significance with p-values as well as theory behind linear regression models.

2.4.1 Design of Experiments

2.4.1.1 Introduction

The scientific method involves the testing and refinement of hypotheses and theories through the acquisition of empirical evidence. This is achieved by conducting scientific studies. Scientific studies can be classified into *observational studies* and *experiments*

[47, p. 9]. In an observational study, a researcher passively observes a set of properties from a number of subjects, without purposefully altering their states in any way, whereas in an experiment, a set of *factors* or *independent variables* are chosen, their levels are varied and controlled, and the resulting changes in a *response* or *dependent variable* are recorded [48, p. 15] [49, p. 1].

An observational study can be prospective or retrospective, the retrospective type being the more common one [47, p. 10]. In a prospective study, a certain number of study subjects are chosen, their initial conditions are recorded and they are observed for a given amount of time. A retrospective study tries to find explanations to the present states of a group of subjects by studying their histories. An example of a retrospective observational study would be finding risk factors for a disease by taking a random sample of citizens and studying their lifestyle habits, obesity and health history and assessing if the factors correlate with morbidity. Results from an experiment can provide more information on causality and the data is easier to analyze since factors can be controlled and so-called confounding effects are less likely to occur [47, p. 10].

Design of Experiments (DoE), pioneered by R.A. Fischer in the 1920s, is a systematic method for designing efficient experiments when the effects of multiple factors on a response must be assessed. Central to DoE are the principles of randomization, replication and the control of variation, e.g., through blocking [47, p. 5] [49, p. 12]. How an experiment is designed will affect the way the data from it can be statistically analyzed [47, p. 9] [49, p. 12].

When planning a series of experiments, the first step is to recognize the problem that is to be studied and to explicitly state the questions to be answered by the study [49, p. 14]. In this planning phase, a primary experimental plan is made. Before starting the experiment, it may be helpful to perform trial or practice runs to practice the experimental technique, to ensure that measurement systems are working properly and test materials are consistent and to get an estimate of the experimental error [49, p. 20].

Experimental study of a process often occurs in consecutive, iterative steps, namely *screening, optimization* and *verification* or *confirmation* studies [49, pp. 14–15]. The screening phase of a study involves a large range and variety of process parameters. Its goal is to experiment with the process to find important parameters and possibly discover the nature (linear/curved) of their effects on the response and to give a primary idea about proper parameter values. In the optimization phase, the optimal parameter values are determined and statistical models, such as regression models and response surfaces are generated. The verification or confirmation step involves a re-run of the process with the optimal settings to create a reliable process [48, p. 15]. They serve to validate the conclusions of the study [49, p. 20].

2.4.1.2 Terminology

The term *controlled experiment* refers to the ability to control the variables that affect a studied response. Obviously not all variables can be controlled, but nevertheless their effect on the response must be accounted for. The variables that cannot be controlled are called *noise factors* [48, p. 2]. Some noise factors cannot even be recognized or observed – they are called *lurking variables* [48, p. 2]. Variables that are not controlled may *confound* the outcome of the study, leading to false conclusions about cause-effect relationships [48, p. 2]. The effect of uncontrollable variables can be managed by *blocking* and *randomization*.

Applied combinations of factors are called *treatments*. When assigning *experimental units* to different treatments, it is advisable to use randomization. Randomization is used to reduce bias [48, p. 10]. By assigning the units randomly, systematic effects caused by all uncontrolled variables become part of the variance within each treatment group and are less likely to exhibit confounding effects [47, pp. 6, 10]. Furthermore, introducing a probabilistic element makes the statistical analyses valid [47, pp. 6, 10].

Blocking is another way to deal with the effects of noise factors. When a variable is recognized and its values are known, but cannot be controlled, its effects can be cancelled out by blocking [48, p. 10]. This means dividing the experimental units into blocks (i.e., groups) so that within each block, the variable is constant and then assigning the treatments randomly within each block and analyzing the data from each block independently – for example, when studying the effect of a quenching temperature on the hardness of steel slabs with steel from three different production batches, it may be wise to create an individual block for each batch, if the batch-to-batch differences are not of primary interest [48, pp. 10, 13]. If a noise factor cannot be used for blocking, but its values can be measured, it is called a *covariate* [48, p. 11].

Replication can be used to increase the precision of an experiment [47, p. 5]. Basically *replicates* are independent experimental runs performed with identical factor levels on different experimental units. A simple, illustrative example is presented by Tamhane [48, p. 6]: in a study where the effect of dough recipe on the taste of cookies is studied, replicates would be two batches of dough made independently according to the same recipe. Replicates are not the same thing as *repeated measurements* on a single experimental unit, such as tasting of multiple cookies made from a single batch of dough. The latter is also referred to as pseudoreplication [47, p. 6].

Balance of a design means that all treatments are assigned to an equal amount of experimental units. The statistical analysis of a *balanced design* is straightforward, since each treatment is estimated with the same precision [47, p. 7]. The total error of an experiment consists of *systematic error* and *experimental error* [48, p. 10]. Experimental error consists of replication error (caused by uncontrolled variables) and measurement error

(caused by inaccurate instruments and inspectors). Replication error is typically significantly larger than measurement error [48, p. 10].

2.4.1.3 Experimental Designs

Different experimental designs are chosen depending on the phase of a study, the amount of variables and their nature and simply the amount of time and workforce available for the study. Four common designs are briefly discussed in this subsection. Design-specific methods of statistical analysis are not discussed here. Typically the analysis involves ANOVA (analysis of variance) and ANCOVA (analysis of covariance) techniques. The latter is used, if covariates are introduced as new data at the analysis stage [48, p. 70].

Completely Randomized Designs

In a completely randomized design, all experimental units are assigned to treatments at random, without restrictions. Any heterogeneity among the units is controlled by randomization [48, p. 70]. The simplest form of this design can be used to study the effects of a single factor on a response [48, p. 70]. It is often used when assigning, for example, human subjects to treatments in a comparative drug study. If two treatments are compared, subjects can be assigned simply by flipping a coin. The experiment does not have to be balanced when randomization is used, i.e., unequal amounts of units may be assigned to different treatments without complicating the statistical analysis.

Randomized Block Designs

In a randomized block design, experimental units are divided into blocks and treatments are assigned at random within units in each block [48, p. 168]. The advantages of blocking are that the effects of selected noise factors can be cancelled out and the precision of the experiment can be enhanced, as previously discussed. Blocking also exposes the effects of these subgroups or categories on the response [48, p. 168]. In the steel quenching example presented earlier, even though blocking helps to remove the confounding effects of batch-to-batch differences, it also helps the experimenter to evaluate these differences.

Factorial Designs

If one is interested in the effects of multiple different factors on a response, *factorial designs* provide a systematic and statistically valid method for their evaluation [48, p. 224]. In factorial designs, the factors are varied together, in a systematic way [49, p. 5]. Full factorial experiments study all factor level combinations, providing information not only on the independent effects (termed *main effects*) of these variables, but also on their combined effects, *interactions* [48, p. 224].

Factorial designs can be classified by the number of factors, f, and the number of different factor levels. For example, a 2^3 factorial experiment contains three factors, each having two different levels. Two-level factorial designs, 2^f, are commonly used in the screening phase of a study, when the effects of multiple factors are studied [48, p. 256]. When only a few factors are studied and the precise nature of the relationships (linear or curved) is of interest, three-level factorial designs are useful [48, p. 351]. An illustration of a 2^3 factorial design with an added center point is shown in Figure 16.

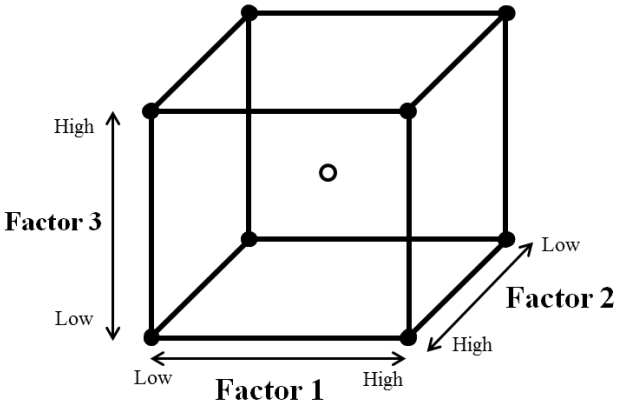

Figure 16: Geometrical presentation of a 2^3 factorial design with a center point.

To estimate response variance, replicate measurements are needed. However, replicating an entire design doubles the amount of experimental units and replicating only a fraction of the design will lead to design imbalance. Replicate measurements at the center point can provide an estimate of the replication error without a large increase in the amount of experimental units or compromising the balance of the design [48, p. 279]. Center points can be added to a factorial design only if the studied factors are quantitative [48, p. 279].

As the amount of factors is increased, the total amount of treatments grows very large. While a 2^3 factorial design has only eight treatment combinations, for a 2^{10} design, the total amount is 1024. Since it is often practically impossible to study so many combinations, and many of the combinations are not likely to provide any useful information, *fractional factorial designs*, in contrast to *full factorial designs*, are typically used for experiments with a large number of factors [48, p. 300]. In fractional factorial designs, only a selected set of factor combinations are studied [49, p. 7].

Response Surface Methods

When factors are not constrained and can be varied independently of each other, response surface methodology (RSM) can be used to optimize a response [48, p. 395]. The objective in RSM is to find the optimum response quickly by studying the response surface sequentially [49, p. 480]. For example, when trying to maximize the response,

the data from one experiment can show the direction for future experiments: the response maximum is likely to be in the direction of steepest ascent [49, p. 480].

The idea of RSM is to present the expected value of a response as a surface, which is a function of the factors [48, p. 396]. For three- or two-factor experiments, this also allows an intelligible visual presentation for the model. Sometimes the factors cannot be varied independently, for example, when optimizing a material composition by changing the relative amounts of ingredients – the relative amount of one ingredient will unavoidably affect the relative amounts of others. In this case, the standard RSM designs have to be modified accordingly [48, p. 414].

To minimize the amount of treatment combinations that need to be studied, without sacrificing useful information, special variations of RSM designs have been designed. These include the *central composite design* and *Box-Behnken design*. So-called *Taguchi designs* are used to minimize response variation around a nominal target value [48, pp. 419–422] [49, p. 22]. They are used for quality improvement, and are based on the idea of designing quality into products.

2.4.2 Statistical Analysis

2.4.2.1 Statistical Significance and Correlation

When interpreting the results from an experiment with large amounts of multivariate data, it can be hard to make out what kinds of relationships actually exist between the variables without the use of statistical methods. Calculation of test statistics such as correlation coefficients and the related p-values provides a clear-cut way to draw conclusions about the relationships. Even though these statistics are usually calculated with computers, it is useful to take a brief look at their properties and formulas.

Hypothesis testing is an important part of statistical inference. It involves presenting two contradictory claims about a variable and its effect on a response: a null hypothesis and an alternate hypothesis [50, p. 301]. The null hypothesis supports an "a priori" belief about the variables, such as the inexistence of a relationship between them, in which case an alternate hypothesis would suggest that a certain relationship exists between the two variables. For example, when conducting a study of the effects of a dietary habit on a disease, the null hypothesis might be that the habit is not correlated with the likelihood of catching the disease, in which case the alternate hypothesis would be that they are correlated. If the null hypothesis is to be rejected, a substantial amount of evidence against it must be found [50, pp. 301–302].

Correlation coefficients are useful statistics in determining, whether a relationship exists between two variables. The commonly used one is the *Pearson product-moment corre-*

lation coefficient. For two variables X and Y of a sample, Pearson product-moment correlation coefficient, R, can be calculated with the equation

$$R = \frac{\sum_{i=1}^{n}(X_i-\bar{X})(Y_i-\bar{Y})}{\sqrt{\sum_{i=1}^{n}(X_i-\bar{X})^2}\sqrt{\sum_{i=1}^{n}(Y_i-\bar{Y})^2}} \qquad -1 \leq R \leq 1 \qquad (2.16)$$

where n is the sample size, X_i and Y_i are the individual observed values and $\bar{X}$ and $\bar{Y}$ are the calculated sample means for these variables [50, pp. 508–510] [51]. The magnitude and sign of the coefficient show the strength and direction of *linear correlation* between the variables. This coefficient cannot detect a curvilinear relationship [50, p. 510] [51]. It is worth mentioning that strong apparent correlations can be obtained even for data with relatively high variance and small sample sizes and so the strength of evidence should be estimated by other parameters.

A useful parameter in deciding whether the evidence is strong enough to reject a hypothesis is the *p-value*. As expressed by Devore, the p-value is ”*the probability, calculated assuming that the null hypothesis is true, of obtaining a value of the test statistic at least as contradictory to the null hypothesis as the value calculated from the available sample*” [50, p. 329]. In other words, it indicates the likelihood that the null hypothesis falsely rejected. This is called Type I error in statistical inference. Type II error, on the other hand, occurs if the null hypothesis is not rejected when it is false [50, p. 304].

To give a numerical value to the strength of evidence that is required from an experiment, *significance levels* are used. Significance level, α, is the maximum probability of type I error allowed. If the *p-value* of a statistic, such as a correlation coefficient, calculated from the data is larger than the required significance level, rejection of the null hypothesis cannot be justified [50, p. 330]. If the p-value is smaller than the required significance level, the result is called *statistically significant* and the null hypothesis can be rejected [6, pp. 285–287]. Commonly used values of α include 0.01, 0.05 and 0.10, depending on the seriousness of the possible type I error [50, pp. 307–308].

2.4.2.2 Linear Regression Models

Regression analysis is used to estimate relationships among variables. *Simple linear regression* can be used to model a linear relationship between a single predictor variable x and a single response variable y. The regression equation is of the form

$$y = \beta_0 + \beta_1 x + \epsilon\ , \qquad (2.17)$$

where β_0 and β_1 are called regression coefficients and ϵ a random error term [50, p. 472]. The coefficients β_0 and β_1 have constant values, while ϵ is an independent, normally distributed random variable with an expected value of zero. [50, pp. 472, 477].

The coefficient β_1 is the slope of the regression line and β_0 is the intercept of the regression line with the y-axis. For a given value of x, all variance in y is caused by the error term and so y is also normally distributed.

The regression coefficients are commonly estimated from the observed data with the *least squares method*. The principle of the least squares method is to find a regression line to which the average distance of all observed data points is minimal. For a set of data with n pairs (x_i, y_i) of observed data, this is achieved by minimizing the sum of squared vertical deviations from the regression line,

$$\sum_{i=1}^{n}\left[y - \left(\hat{\beta}_0 - \hat{\beta}_1 x\right)\right]^2 , \tag{2.18}$$

where $\hat{\beta}_0$ and $\hat{\beta}_1$ are the least square estimates of the regression coefficients [50, p. 478]. Resulting formulas for the least square estimates are

$$\hat{\beta}_1 = \frac{\sum_{i=1}^{n}(x_i - \bar{x})(y_i - \bar{y})}{\sum_{i=1}^{n}(x_i - \bar{x})^2} \tag{2.19}$$

$$\hat{\beta}_0 = \bar{y} - \hat{\beta}_1 \bar{x} , \tag{2.20}$$

where x_i and y_i are individual values and $\bar{x}$ and $\bar{y}$ the sample means of the two variables [50, p. 479]. Using these estimates, an *estimated regression line*,

$$y = \hat{\beta}_0 + \hat{\beta}_1 x , \tag{2.21}$$

can be created.

Predicted values of the response are obtained by substituting values of x into the estimated regression equation (2.21). Deviations of the actual observed response from the predicted values are called model *residuals* [50, p. 481]. It is assumed that the residuals are statistically independent and normally distributed [47, p. 22]. The *sum of squared errors* (or the sum of squared residuals),

$$\begin{aligned} SSE &= \sum_{i=1}^{n}\left[y - \left(\hat{\beta}_0 + \hat{\beta}_1 x_i\right)\right]^2 \\ &= \sum_{i=1}^{n} y_i^2 - \hat{\beta}_0 \sum_{i=1}^{n} y_i - \hat{\beta}_1 \sum_{i=1}^{n} x_i y_i , \end{aligned} \tag{2.22}$$

gives an estimate to the total amount of variance of y that the model is unable to explain [50, pp. 483–485]. Similarly, the *total sum of squares*,

$$SST = \sum_{i=1}^{n}(y_i - \bar{y})^2 , \tag{2.23}$$

shows how much overall variance of y is present in the data [50, p. 485]. Intuitively, the ratio of the two sums (SSE/SST) gives an estimate to the relative amount of variance in y that the model *is not* able to explain.

To quantify the predictive capability of a regression model, a parameter called *coefficient of determination*, R^2, is typically used. It shows the relative amount of variance in y that the model *is* able to explain and is calculated as [48, p. 45] [50, p. 485]

$$R^2 = 1 - \frac{SSE}{SST}\,. \tag{2.24}$$

It shows how much of the total variance in y the model is able to explain. Values close to one imply that the model has a high predictive capability. For example, if $R^2 = 0.90$, the model can explain 90% of the observed variance of the response variable. For simple linear regression, using the least squares method, R^2 is simply the square of the correlation coefficient R between the predicted and observed values of the response [50, p. 510].

When several predictor variables are present, but their relationships can be approximated as linear, the data can be analyzed with *multiple linear regression* (MLR). The general additive MLR equation [50, p. 553],

$$y = \beta_0 + \beta_1 x_1 + \beta_2 x_2 + \cdots + \beta_k x_k + \epsilon\,, \tag{2.25}$$

with k predictor variables is essentially an extension of equation (2.17).

Even though the predictor variables in equation (2.25) have to be independent, it is possible to study non-linear relationships with a regression model by substituting the x_is with, for example, quadratic or cubic terms and *interaction terms* [49, p. 19] [50, pp. 553–555]. Let us consider a set of data with two predictor variables, x_1 and x_2. If it seems that x_2 has a quadratic relationship with the response and the effect of x_1 on the response seems to depend on the value of x_2, a regression model in the form of

$$y = \beta_0 + \beta_1 x_1 + \beta_2 x_2 + \beta_3 x_2^2 + \beta_4 x_1 x_2 \tag{2.26}$$

(with substitutions $x_3 = x_2^2$ and $x_4 = x_1 x_2$) is likely to explain the response variance to a greater extent than a strictly linear model.

The calculation of R^2 follows essentially the same principles as for a simple linear regression model, but the process is more complicated. As can be seen from equations (2.22) to (2.24), the value of R^2 cannot decrease and usually will increase when new

predictor variables are added to the model. For multiple regression, a parameter called *adjusted* R^2 is often used. It is better suited for the evaluation of an MLR model, because it will decrease if an introduced predictor does not significantly improve the model [50, p. 578]. This keeps the amount of predictors relatively low so that the model is easy to interpret while still giving good estimates for the response. The importance of choosing proper predictor variables was already discussed in subsection 2.4.1. A model with a reasonable amount of predictor variables that make practical sense is likely to be informative and easy to use.

Adjusted R^2 is calculated as

$$R_{adj}^2 = 1 - \frac{MSE}{MST}, \tag{2.27}$$

where MSE is the mean square error of the model and MST is the mean square total variance of the predictor [50, p. 578]. These are defined for a model with k predictors as [50, p. 578]

$$MSE = \frac{SSE}{n-k-1} \quad \text{and} \tag{2.28}$$

$$MST = \frac{SST}{n-1}. \tag{2.29}$$

The calculation of SSE and SST for MLR is similar to that done for simple linear regression (see equations (2.22) and (2.23)), but, a larger number of terms will obviously be included in the SST equation.

3 MATERIALS AND METHODS

3.1 Products

A short description of the two products under study is given in this section. From a drug release perspective, they can be both viewed as cylindrical, diffusion controlled CDD devices. Product A releases a single active substance, whereas Product B releases two. Both products have a circular cross-section and they are structured in the following manner. The products feature drug cores, reservoirs, consisting of a drug substance bound to an elastomer material. The core is saturated with drug and the viscosity of the core elastomer is relatively low compared to that of the membrane that surrounds the core. Product B is of purely of the reservoir type as the drug core is fully surrounded by the membrane, whereas Product A features open ends that exhibit monolithic-type release.

The structure of Product A is presented in Figure 17. The cylindrical drug-elastomer core is coated with an elastomer membrane and the resulting rod-like structure is mounted on a polyethylene body. The surface area of the open ends is small compared to the dimensions of the product. During use, the portion of release that occurs through the ends decreases, as the ends become depleted of drug and the average diffusional path increases in length.

***Figure 17**: A rough schematic presentation of Product A geometry. The innermost part is the polyethylene body, the central part (drawn in dark blue) is the drug core and the outermost part is the elastomer membrane.*

The structure of Product B is slightly more complex, as it features two different drug-elastomer core sections and additional "dummy" sections that do not contain an API. Nevertheless, it behaves somewhat similarly to Product A from a drug release perspective. In terms of cross-sectional diameter, Product B is roughly twice as large as Product A, but its membrane thickness is similar to that of Product A.

3.2 Materials and Specimen Preparation

The rate-controlling outer membranes of both products are made of silica-filled polydimethylsiloxane (PDMS) elastomers. Previous studies have shown that increasing the amount of fumed silica in the membrane material results in decreased API release rate from the product. This study seeks to further quantify the effect within a defined range of manufacturing parameters and product dimensions in order to optimize the material composition.

For the purposes of this study, specimens of both products were manufactured using five different membrane materials. Two of these materials were from established providers (Providers 1 and 2), and three were from a new provider (Provider 3). The new materials have all slightly different silica contents. The materials are presented in greater detail in the following sections. In contrast to normal product manufacturing, the specimens were not sterilized. This should be taken into account when comparing the results to ones obtained for sterilized units.

3.2.1 Experimental Design

In this experiment, **drug release rate** is the *response variable* and **membrane thickness** and membrane **material silica content** are the two *factors* that are varied. Other process factors are either controlled by keeping them constant (or within certain tolerances) or assumed to have no direct or confounded effects to the response, based on earlier experience and research on the process. A schematic presentation of the *experimental design* for the materials from the new provider along with the number of specimens in each combination is shown in Figure 18.

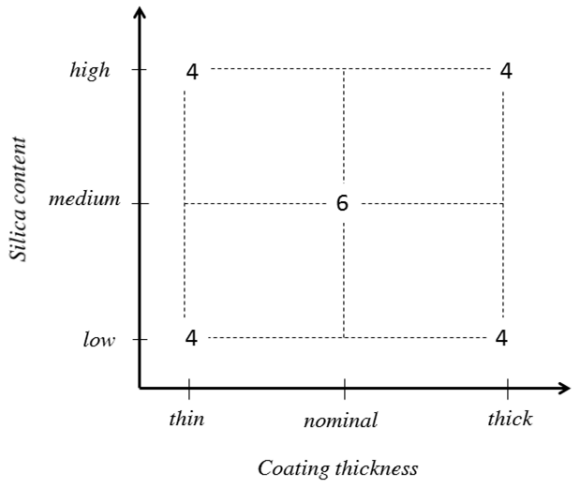

***Figure 18**: A graph presenting the amount of release rate specimens prepared for each factor level combination with Provider 3 membrane materials.*

This is essentially a simple 2^2 full factorial design with an additional centerpoint at the nominal membrane thickness and medium silica content. Having a centerpoint, this design can also give information about possible higher-order (curved) interactions and the

high amount of replicates at the centerpoint allows a good estimation of replication error. A similar design is applied for the study of both products. For the materials from providers 1 and 2, only two parallel runs were made for each membrane thickness. The principle of randomization was not applied in this work. It was assumed, according to earlier experience, that the analysis order of specimens could not have any significant effect on the results and it would have been highly impractical to apply randomization to the specimen manufacturing process.

It was estimated, based on earlier research on the process, that because the ranges of the two factors are narrow, the resulting differences in the response would be small. Therefore, it was important to have several parallel experimental points for each material-dimension combination in order to achieve statistically significant results. It was also known that slightly different results are obtained, systematically, with different shaking water baths in the release rate analysis (see subsection 3.3.6). Therefore, it was equally important that all specimens within a test series could be fit into a single water bath.

Control of bath-to-bath variation by blocking was also considered, but eventually the single-bath option was chosen to save analytical resources. This limited the total specimen amounts to 32 for Product A and 34 for Product B. To reduce the specimen count by two, it was decided that the materials from Provider 1 would not be analyzed for Product A at nominal membrane thickness, since such specimens had already been analyzed in previous studies. The small response variation caused by using a different water bath is hardly significant in terms of general evaluation of product performance, but since very small changes to the response are expected in this study, it is important to exclude all unwanted confounding effects.

3.2.2 Product A Specimen Preparation

The preparation process of Product A specimens consisted of several steps: preparation of a drug-elastomer mixture, extrusion of drug core, coating extrusion of drug core, post-curing, cutting and product assembly. Specimens with varying coating membrane thicknesses and coating materials were prepared. Only the release rate specimens required product assembly. In addition, membrane tubes were extruded for material characterization.

Temperatures were maintained at moderate levels during the extrusion and post-curing processes to ensure that no significant degradation of the API would occur. Safe temperature ranges were chosen according to earlier research within the company. Sufficient curing was confirmed by comparing the chosen process temperatures to the results of rheological tests (see subsection 3.3.1), by determining the amounts of low molecular weight species in the membrane tubes (see subsection 3.3.3) and by mechanical tests (see subsection 3.3.4).

3.2.2.1 Preparation of Drug-Elastomer Mixture

The specimen preparation process began with mixing of the drug core ingredients: unfilled, heat-vulcanizing silicone elastomer and micronized API-1 powder. The target API concentration was 65 percent by weight. The ingredients were weighed with a precision balance (PG4002-S Delta-Range®, Mettler Toledo, Switzerland). The mixing was performed with an internal mixer with two intermeshing rotors (Poly-Lab System: Rheocord/Rheomix 300p, Thermo Fischer Scientific, Karlsruhe, Germany). The ingredients were mixed in two batches due to small chamber size of the mixer.

The mixing began with feeding of the unfilled elastomer into the mixing chamber. Then, the API powder was slowly added (manually, using a steel spoon) and forced into the chamber with a mechanical ram. When all the ingredients had been added, the mixing was continued for 10 to 15 minutes. Since the batch size was very small and used mixing speeds rather low, no heat build-up was expected and thus no cooling device was used with the mixer. Higher mixing speeds (20 to 40 rpm) were used for the second than the first batch (roughly 20 rpm), but since the two batches would be later combined, no overall specimen-to-specimen variation can result from differences in mixing parameters.

After removal from the mixer chamber, both mixtures still contained some visible pockets of API in powder form. A two-roll mill (Polymix 110 P, Schwabenthan Maschinen, Berlin, Germany) was used to combine and to further homogenize the drug-elastomer mixtures. When the combined mixture seemed completely homogeneous, ten representative samples, each weighing approximately 0.3 g, were taken from the mixture for homogeneity analysis (see subsection 3.3.2) . The remaining mixture was placed in a sealable polyethylene bag and stored in a refrigerator until its extrusion.

3.2.2.2 Extrusion of Drug Core

Extrusion of the drug core was performed using a laboratory-scale single-screw extruder (LAB extruder, Mantechno Oy, Raisio, Finland) and a conveyor oven (Insrumentti Mattila Oy, Nousiainen, Finland). The extruder screw temperature was maintained at room temperature using a circulating water cooler (UWK 45, Haake, Karlsruhe, Germany). Prior to extrusion, the drug-elastomer mixture was softened using a two-roll mill (Polymix 110 P, Schwabenthan Maschinen, Berlin, Germany).

A simple longitudinally fed mandrel-support die was used for the extrusion of the hollow drug core tube. Proper conveyor oven temperature and conveying speeds were chosen according to earlier research within the company to allow sufficient cross-linking without API degradation and the extruder screw speeds were adjusted accordingly.

During extrusion, the outer diameter (OD) of the extrudate was continuously monitored with an in-line dimension measurement device, an optical micrometer (Lasermike 182-

11, Lasermike Inc., Dayton, Ohio, USA). The inner diameter (ID) was checked manually with plug gauges at the beginning of the extrusion process and at the end of each extruded drug core coil. In addition, a weight control sample was taken from each extruded coil to verify that the membrane thickness was within normal core extrusion specification limits. The coils were stored at room temperature in a polyethylene bag separated with sheets of baking release paper.

3.2.2.3 Coating and Membrane Extrusion and Post-Curing

In contrast to other phases of the specimen preparation process, in this phase variation was intentionally induced to the specimens. Five different coating materials were used and three different coating thicknesses were applied according to the experimental design shown in the beginning of this chapter.

Materials

Compositions of the Provider 3 elastomer base batches are shown in Table 2. PA-fluid (PA = Prosessing Aide) is a low molecular weight siloxane fluid that reduces the viscosity of the material and it is used to coat the fumed silica during the compounding process.

Table 2: Compositions of the Provider 3 materials elastomer bases used in this study.

Batch	***Silicone gum (weight-%)***	***PA-fluid (weight-%)***	***Silica (weight-%)***
Low silica	53.0	12.5	34.5
Medium silica	52.4	12.5	35.1
High silica	51.8	12.5	35.7

All membrane materials were known to contain significant amounts of amorphous silica filler. The silica used in the Provider 3 batches was fumed silica with a known surface area and no surface treatment prior to treatment with PA-fluid. No specific information on the type of silica was available for Provider 1 and 2 materials.

Provider 1 and 2 materials already contained a crosslinking agent, while the materials from Provider 3 did not, so the first step was the addition of peroxide to the three new materials. The used peroxide paste was a mixture of 50 w-% silicone oil and 50 w-% 2,4-dichlorobenzoyl peroxide (Azko Nobel Chemicals, Amsterdam, Netherlands). The materials were weighed with a precision balance (PG5002-S DeltaRange®, Mettler Toledo, Switzerland) and mixed with a two-roll mill (Polymix 110 P, Schwabenthan Maschinen, Berlin, Germany). The weighed amounts and calculated peroxide contents are presented in Table 3.

Table 3: Weighed amounts of Provider 3 elastomer base and peroxide paste and the resulting peroxide contents for the elastomers.

Elastomer batch	*Amount of elastomer base (g)*	*Amount of peroxide paste (g)*	*Resulting peroxide content (w-%)*
Low silica	603.73	6.64	0.544
Medium silica	605.91	6.65	0.543
High silica	599.31	6.59	0.544

The mixing procedure consisted of softening the elastomer base and turning it into a form of a sheet, weighing the elastomer sheet, weighing the peroxide paste, applying the peroxide paste on the elastomer sheet, folding the sheet and finally feeding the folded sheet to the two-roll mill and mixing the constituents. The mixed elastomers were stored in a refrigerator in polyethylene bags. All coating materials were softened with the two-roll mill before the rheological analyses and the start of the extrusion.

Extrusion process

Coating extrusion and membrane tube extrusion were accomplished with a laboratory scale single-screw extruder, consisting of a measurement and control unit (Rheocord 9000, Haake, Karlsruhe, Germany) and an extrusion unit (Rheomex 102, Haake, Karlsruhe, Germany). A circulating water cooler (UWK 45, Haake, Karlsruhe, Germany) was used to maintain the extruder screw at room temperature. A crosshead die was used so the drug core could be fed inside the extruded coating membrane (see subsection 2.3.3). After leaving the die, the extrudate passed through a shock oven and a conveyor oven (Instrumentti Mattila Oy, Nousiainen, Finland). The outer diameter (OD) of the extrudate was continuously measured with an optical micrometer (Lasermike 182-11, Lasermike Inc., Dayton, Ohio, USA), as it exited the conveyor oven. An overhead view scheme of the process is shown in Figure 19.

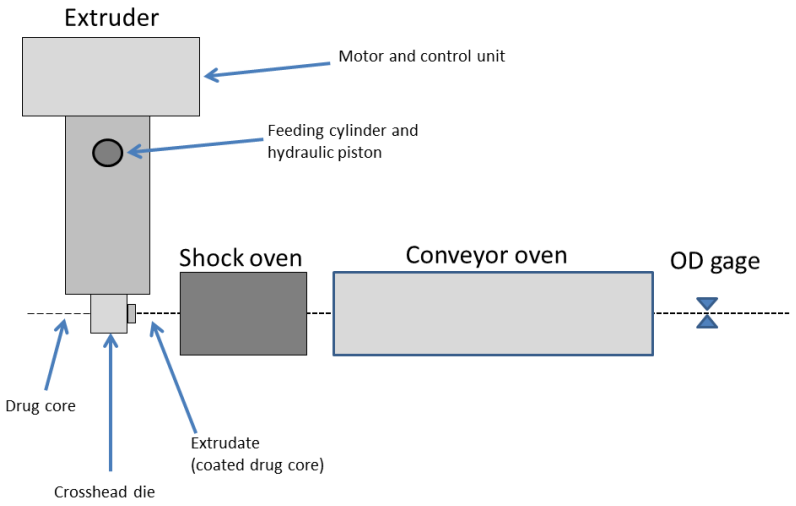

Figure 19: Schematic presentation of the coating extrusion process for Product A (an overhead view).

A shock oven was used in the process to cure the surface of the extrudate so it would not stick to the belt of the conveyor oven. The extrudate would hang freely after leaving the die until it reached the conveyor oven. According to practical experience, it was crucial not to apply any significant axial tensile stress to the uncured extrudate, as it might lead to unwanted dimensional changes of both the coating and the drug core. Care was taken to keep the length of this extrudate loop, the "tightness" of the extrudate, relatively constant to minimize any resulting specimen-to-specimen variation.

For each coated drug core batch, a batch of membrane tube was extruded with identical parameters. Oven temperatures, conveyor speeds, pressures at the die as well as screw speeds and screw temperatures were measured and monitored during the process. Variations in screw speeds between runs were necessary to achieve the desired OD values since perfect die combinations for achieving the target dimensions were not available. Luckily, the resulting variations in the pressure values at the die were small, with pressure values between 100 and 120 bars, so large variations in extrudate properties are not expected.

The extruded coils were post-cured in a convection furnace (ULE 500, Memmert GmbH & Co. KG, Germany). The post-curing temperatures and times were identical for all extruded batches, both the membrane tubes and the coated drug cores. The color of the coated drug cores changed from clear white to pale yellow during the post-curing process. The post-cured extrudates were stored in room temperature in polyethylene bags and separated with sheets of baking release paper.

3.2.2.4 Assembly, Final Inspection and Dimension Measurements

Before assembly could be performed, the coated drug cores had to be cut into cylinders of a specific length. The cutting was performed manually, with a scalpel. The specimens were cut as perpendicularly to the longitudinal axis as possible, trying to avoid any curvature. Before assembly, the cylinders were examined and their lengths verified with an optical microscope (Quadra-Chek 300, Metronics, Bedford, New Hampshire, USA). Additionally, their cross-sectional diameters and membrane thicknesses were measured and recorded.

By examining the cylinder cross-sections, it was noted that in some coated cores, the coating membrane was not of uniform thickness as the thickest spot of the membrane was up to 40% thicker than the thinnest spot. As a consequence, several cylinders were cut from different parts of the extrudates and the ones that exhibited the highest concentricities were chosen for the assembly.

To make the manual assembly of specimens possible, each cylinder was swollen in cyclohexane (analytical grade, Merck KGaA, Darmstadt, Germany) for 38–48 seconds. The cylinders with thick membranes were swollen for a slightly longer time than the

ones with thin membranes. Instantly after swelling, the cylinders were pushed onto solid polyethylene bodies that had a diameter close to the inner diameter of the drug core. The solvent was allowed to evaporate for a minimum of 2.5 hours, after which the specimens were once again examined with the microscope to see if any significant deformation had happened to the cylinder and to which extent the lengths of the cylinders differed from the ones measured before the assembly. The results are discussed in section 4.7.

3.2.3 Product B Specimen Preparation

As Product B contains two different drug core segments, the specimen preparation process differs from the one used for Product A. Instead of using coating extrusion, the membrane tubes and different core sections were manufactured separately and assembled later into complete specimens. Membrane materials used for Product B were the same as for Product A. Materials from Providers 1 and 2 were from different batches in products A and B, but materials from Provider 3 were from the same batches in both products.

3.2.3.1 Preparation of Drug Cores

Product B drug cores were prepared somewhat similarly to Product A drug cores. Both cores consisted of silicone polymer and micronized API powder. Target API concentration for API-1 core was 50 weight-percent and for API-2 core, ten weight-percent. Mixing was performed with internal batch mixers. Representative samples were taken from the API-1 mixture for API Content and Homogeneity analysis (see section 3.3.2). Homogeneity of the API-2 mixture was evaluated visually. Processing temperatures were once again chosen according to earlier research and experience within the company, to ensure that no significant degradation of the API would occur.

3.2.3.2 Extrusion of Elastomer Core

Extrusion of Product B elastomer core, “dummy core”, was performed with the same equipment as the extrusion of Product A membrane tubes and coated cores (see section 3.2.2.3 and Figure 19). Rotating speed of the extruder screw was between 25 and 32 rpm and the measured pressure at the die was approximately 5 bars. Shock oven temperature was 250 ± 5 °C and conveyor oven temperature was 200 ± 5 °C. Only Provider 2 elastomer was used for the elastomer core. The extrudate was post-cured at 200 ± 5 °C for 3 hours and stored in a polyethylene bag after it had cooled to room temperature.

3.2.3.3 Extrusion of Membrane Tubing

Prior to membrane extrusion, peroxide was mixed to two Provider 3 batches. Weighing and mixing was performed with the same devices and in the same way as in the Product A process. There was no need to mix peroxide to the medium silica elastomer base batch, since enough mixture was left over from the Product A process. Weighed

amounts and resulting peroxide contents are shown in Table 4, including the medium silica batch mixed previously. The mixed batches were studied with the rheometer, as was done in the Product A process. The mixed (and analyzed) materials were stored in a refrigerator in polyethylene bags until extrusion.

Table 4: Addition of peroxide to Provider 3 elastomer batches used in Product B membrane extrusion. Weighed amounts and resulting peroxide contents.

Elastomer Batch	*Amount of Elastomer Base (g)*	*Amount of peroxide paste (g)*	*Resulting peroxide content (w-%)*
Low silica	623.65	6.87	0.545
High silica	607.49	6.68	0.544
Med. silica	605.91	6.65	0.543

Product B membrane tubing was extruded using the same equipment as with the elastomer core, with the exception of using two different extruders. This was due to an unexpected malfunction of the Haake extruder. As a result, some variation occurred in process parameters, even though the extruders were similar in size and screw design. Shock oven temperatures and conveyor oven temperatures were varied between batches, to compensate for differences in conveyor oven speeds. Five different materials were used and three membrane thicknesses were sought, according to the experimental design shown in the beginning of this chapter.

3.2.3.4 Assembly, Inspection and Dimension Measurements

Product B specimens were assembled with a product-specific assembly process that consisted of inserting the drug and elastomer cores of specific lengths within the membrane tube and closing the ends of the tube using a silicone adhesive. Once the adhesive had cured, the integrity of the membrane and the adhesive seals was verified visually and with a microscope. Small voids were observed in some of the API-2 sections and their approximate sizes and positions were recorded. The outer diameters at different specimen sections were measured with an optical microscope (Quadra-Chek 300, Metronics, Bedford, New Hampshire, USA) and recorded.

3.3 Methods of Analysis

Several different analyses were performed for the purposes of this study. Rheological and mechanical analyses were conducted to ensure that the materials from different providers would not differ markedly from each other in terms of mechanical strength of processability and to see if small variations in material silica content would results in any noticeable changes in these properties. The drug content and homogeneity of the reservoir was evaluated by analyzing the prepared drug-elastomer mixtures. The amounts of oligomers in cured elastomer membranes were analyzed to take into account the effect of oligomers on drug diffusion through the membrane. In addition, filler concentrations of the elastomers were evaluated by thermogravimetry. Finally, the main

response variable of the present study, the drug release rate, was analyzed for both products.

3.3.1 Rheometry

To ensure material quality, rheological properties and curing characteristics of all the used coating membrane materials were analyzed with a dynamic mechanical rheological tester (RPA 2000, Alpha Technologies, Akron, Ohio, USA). The device is essentially a *rotating die rheometer* designed for analyzing elastomers and mixed rubbers. In controlled conditions, it exhibits an oscillating deformation to a specimen and records the required torque. Using the recorded data, specimen dimensions and geometry, it calculates rheological quantities such as the material's *storage and loss moduli* and *complex viscosity*. The test parameters are shown in Table 5.

Table 5: Parameters of the rheological analyses conducted for membrane materials.

Parameter	***Viscosity measurement***	***Curing analysis***
Temperature	30 °C	115 °C
Oscillation frequencies	0.1 Hz; 2.0 Hz; 20 Hz	1.7 Hz
Oscillation amplitude	0.5 °	0.5 °
Die	Biconical	Biconical
Sample volume	4.5 cm^3	4.5 cm^3
Test duration	(irrelevant) 5 measurements per frequency	5 minutes
No. of parallel samples	1	1

The tests were conducted prior to starting the coating extrusion process, when the materials already contained a curing agent and had been softened and homogenized with a two-roll mill (see subsection 3.2.2.3*)*. For each test, a minimum of 4.5 cm^3 of the material to be tested was placed between two polyester sheets and inserted between the rheometer heads and the test was started.

Figure 20: Photograph of a curing test specimen after the test.

Figure 20 shows a curing specimen that has been tested and illustrates the complex die geometry. It can also be seen that the uncured excess material at the perimeter remains opaque while the cured material has become more transparent. The obtained results are discussed in Section 4.1.

3.3.2 API Content and Homogeneity

A homogeneity analysis of the drug-elastomer mixture was conducted prior to drug core extrusion using high performance liquid chromatography (HPLC). This analysis helps to rule out any response variation caused by differences in the API content between specimens. As discussed in Sections 3.2.2.1 and 3.2.3.1, several samples were taken from the API-1 drug-elastomer mixtures after mixing. The analysis was performed according to an internal guide of Bayer.

The test begins with quantitative extraction of the API from the drug-elastomer mixture with a suitable solvent and preparation of API reference solutions. The solutions are further diluted with the mobile phase (acetonitrile/water) to predetermined volumes. Prior to analysis, system accuracy is ensured by performing multiple HPLC runs with reference solutions and evaluating the relative standard deviation of the test series. The sample and the reference are injected and the areas of the resulting chromatogram peaks are used to calculate the API content of the drug-elastomer mixture, taking into account the purity of the reference substance. The analysis was performed using an *Agilent Technologies 1200 series* HPLC apparatus with a reversed-phase column, UV-detector and automatic sample injection. The results of this analysis are discussed in section 4.2.

3.3.3 Extractable Oligomers

Literature and previous research within the company showed that low molecular weight fractions in the polymer material affect its permeability to drug molecules. This is why the amounts of PDMS oligomers were analyzed from the membrane tubes. The analysis began by weighing a glass vial and a sample of membrane tubing with an analytical balance. Then, n-hexane was added to the vial and the vial was shaken in room temperature with a planar shaker for 16–20 hours, closed with a cap that had a Teflon coating (septum) at the inner surface. After shaking, the extraction solution was removed and the vial, containing the sample, was rinsed with n-hexane. The solvent was removed and the vial and sample were dried in a vacuum in 40 °C for one hour and cooled at ambient temperature and pressure for one hour. Finally, the vial, containing the sample, was weighed and the change in sample mass was calculated.

3.3.4 Mechanical Tests

For reasons related to product use and the manufacturing process, certain mechanical properties are required from the membrane material. Silica was known to influence the

mechanical properties of the materials studied, so simple tensile tests were conducted to see if the small variations in filler content would have any discernible effect.

In the case of Product A, tests were performed on both the membrane tubes and the coated drug cores, whereas for Product B, only the membrane tubes were tested. Five specimens, each 12 cm in length, were cut from each batch and their diameters and membrane thicknesses measured from the ends of the specimens with an optical microscope (Metronics, Quarda-Chek 300, Bedford, New Hampshire, USA) in the case of Product B and with a video coordinate measurement device (Nexiv VMR-3020, Nikon Corporation, Tokyo, Japan) in the case of Product A. To ensure data comparability, the influence of measurement device on the results was evaluated by performing an identical series of dimension measurements with both devices. No significant systematic error was found.

The tests were conducted with a universal mechanical testing machine (5565, Instron Ltd., Buckinghamshire, England) and a long-travel extensometer (2603-080, Instron Ltd., Buckinghamshire, England) with a gage length of 25 mm. Pneumatic grips with rubber-coated faces were used to fasten the specimens into the machine. A testing speed of 500 mm/min was used and the tensile test was run until specimen failure. Test results are discussed in section 4.4.

3.3.5 Thermogravimetry

As no accurate information was available on silica concentrations of the elastomers from Providers 1 and 2, the concentrations had to be evaluated experimentally. In addition, analyzing all materials with the same method and device ensured data comparability. The measurements were performed with a thermogravimeter (TGA/SDTA851^e, Mettler Toledo, Greifensee, Switzerland) and a microbalance (XP6, Mettler Toledo, Greifensee, Switzerland). The thermogravimetric (TGA) analysis was performed for extruded, post-cured membrane tubes in open alumina crucibles in an inert (nitrogen) atmosphere, with a constant heating rate of 20 °C/min from 25 to 950 °C and an isothermal hold at 950 °C for 15 minutes.

Three parallel specimens were analyzed for each material. The ratios between residue weights and original specimen weights were calculated in percentages. Because the analysis was performed for extruded, post-cured tubes, the obtained weight percentages were expected to be higher than the added values of filler to the uncured elastomer. This is because mass loss occurs both during the compounding process (the addition of silica) and during the high temperature curing process as volatile byproducts and oligomers escape the material.

3.3.6 Release Rate in vitro

In vitro drug release rates from the two products were determined with a release analysis mimicking physiological conditions. The analyses were conducted according to internal guides of Bayer. Specimens were mounted in special holders inside glass bottles containing an aqueous dissolution medium. The bottles were closed and placed in a temperature-controlled shaking water bath. The temperature of the bath was maintained at 37 ± 0.5 °C and the shaking frequency and amplitude were kept constant. At predetermined intervals, the solutions were analyzed with HPLC, using a reversed-phase column and external calibration and a fresh dissolution medium was changed to the bottles. The release rate values were calculated by dividing the amount of API in the dissolution medium with the time that had passed since the previous sampling point.

To draw meaningful conclusions from the data, specimen dimensions had to be measured. In the case of Product A, cross-sectional diameters and membrane thicknesses were measured from the ends of the reservoir-membrane cylinders *before* the cylinders were mounted on polyethylene bodies. For Product B, the dimension measurements were conducted, for practical reasons, *after* the release rate analysis, when the specimens had dried. Both measurements were conducted with the same optical microscope (Quadra-Chek 300, Metronics, Bedford, New Hampshire, USA). The results are discussed in Sections 4.6 and 4.7.

4 RESULTS AND DISCUSSION

In this chapter, the results of the study are first presented and discussed in individual sections for each analysis and then statistically analyzed in section 4.7. Regression models are created and possible sources of error are discussed at the end of this chapter.

4.1 Rheometry

Results from the rheological analyses are presented in Tables 6 and 7. As foreseen, all materials were very similar in terms of viscosity and curing characteristics. The small variations in silica concentration do seem to have an effect on the viscosity but it is very small. The mixing of peroxide (see subsection 3.2.2.3) to the new materials seems to have been successful.

Table 6: Results of the individual complex viscosity ($\boldsymbol{\eta^*}$) measurements at different angular frequencies ($\boldsymbol{\omega}$) for all membrane material batches used in this study.

Provider	Batch	Reported silica content (w-%)	$\boldsymbol{\eta^*}$ $(\boldsymbol{kPa \cdot s})$		
			$\boldsymbol{\omega = 0.1}$ **Hz**	$\boldsymbol{\omega = 2.0}$ **Hz**	$\boldsymbol{\omega = 20}$ **Hz**
1	For Product A	ca. 35	104.4	12.1	1.88
1	For Product B	ca. 35	108.6	12.7	1.95
2	For Product A	37	121.2	12.5	1.89
2	For Product B	38	123.8	12.6	1.92
3	Low silica	34.5	107.3	11.8	1.84
3	Medium silica	35.1	117.2	12.6	1.92
3	High silica	35.7	117.2	12.5	1.89

*Table 7: Results of the individual curing measurements for different membrane materials. 90% cure corresponds to the point, where the storage modulus **S'** equals 90 % of its predicted maximum (as calculated by the device).*

Provider	*Batch*	*Reported silica content (w-%)*	*Time at 90 % cure (s)*	**S'** *at 90 % cure (dNm)*	*Maximum* **S'** *(dNm)*
1	For Product A	ca. 35	98	11.3	12.4
1	For Product B	ca. 35	78	11.7	12.8
2	For Product A	37	93	11.5	12.6
2	For Product B	38	79	11.6	12.8
3	Low silica	34.5	90	12.0	13.2
3	Medium silica	35.1	76	11.8	13.0
3	High silica	35.7	88	12.4	13.6

All measured viscosities at 2.0 Hz angular frequency were between 11.8 and 12.7 kPa·s and all materials achieved 90% cure in a maximum of 98 seconds and showed a maximum storage modulus between 12.4 and 13.6 dNm at the end of the 5 minute curing test. The curing test curves are shown in Appendix 1. Due to the lack of parallel experimental points, no statistical conclusions can be drawn from the data. Nevertheless, sufficient curing of extruded membrane tubes can be safely assumed, as much higher oven temperatures and longer post-curing times were used in the specimen preparation process than in this curing analysis.

4.2 API Content and Homogeneity

Results of the API content analyses by HPLC are shown in Table 8. It can be seen that the mixture was homogeneous for both products. Some variations do exist between specimens, but since the concentrations are far above the solubility of the drug, no differences in the short-term release rate should occur.

Table 8: Statistics of the API Content and Homogeneity analysis for the API-1 mixtures of both products.

Statistics	*Reservoir API-1 content in Product A [weight-%] (n=10)*	*Reservoir API-1 content in Product B [weight-%] (n=12)*
Mean	64.7	50.7
Minimum value	64.2	50.4
Maximum value	65.2	51.1
Relative standard deviation (RSD) [%]	0.4	0.4

Drug concentration of the API-2 mixture in Product B was not analyzed chromatographically. According to earlier experience and visual examination of the mixture, it was concluded that the API-2 concentration was clearly above the solubility of the drug and that the mixture was homogeneous.

4.3 Extractable Oligomers

A summary of the results of the gravimetric analysis for membrane tubes used in Product A and Product B is shown in Table 9. Tubes made from Provider 1 and 2 elastomers were analyzed only at the nominal thickness. Tubes made from Provider 3 materials were analyzed from all batches used in the final release rate specimens, with the exception of the point of high silica content and thin membrane for Product A, because no such membrane tube remained for the analysis.

Table 9: Amounts of hexane extracted oligomers in extruded membrane tubes.

Provider	***Amount of extracted oligomers (weight-%)***	
	Product A	**Product B**
1	3.26	2.39
2	3.40	3.63
3	3.17–3.28	2.18–2.84

No notable batch-to-batch differences can be found apart from the high value for Provider 2 Product B membrane. No obvious cause for this possible outlier could be found. It is possible that experimental error was involved. The test was not re-run due to lack of time and specimens.

4.4 Mechanical Tests

Results of the tensile tests are shown in Figures 21–26. Sample error bars shown in the graphs have a height of two standard deviations (±1 SD). The sample identification codes below the pillars are constructed in the following manner: the first digit refers to the material provider, the last digit refers to the thickness of the membrane (– refers to thin, + to thick and N to nominal) and the middle digit that is only seen with Provider 3 batches refers to the silica concentration (L = low, M = medium, H = high).

When conducting the tests for Product A membrane tubes, it was noticed that the extensometer caused the specimens to be strained unevenly. This was clearly visible during the test. Even though the supporting structures of the extensometer are designed so that a minimal amount of unwanted stresses are induced to a specimen, these small stresses were significant for the membrane tube specimens. The specimens were stretched to a larger extent above the extensometer than in other parts of the specimen. For the coated drug cores and Product B membrane tubes, the phenomenon was not clearly visible, as they were stiffer due to their larger cross-sectional areas. Based on these observations, the Product A membrane tube results are likely to be erroneous and, as a consequence, are not included.

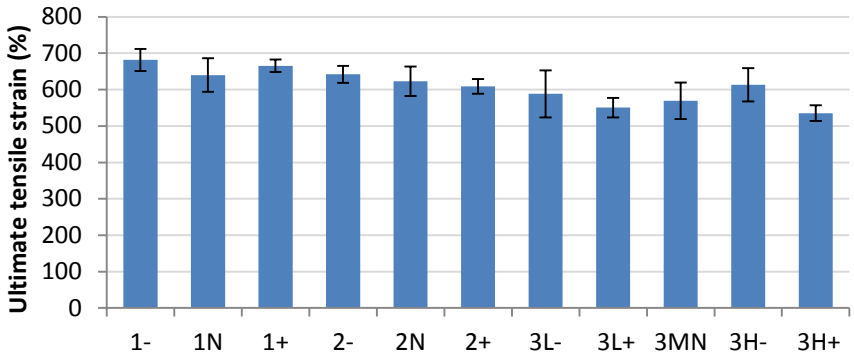

Figure 21: Average values of tensile strain at break for Product A coated drug cores. See text for key.

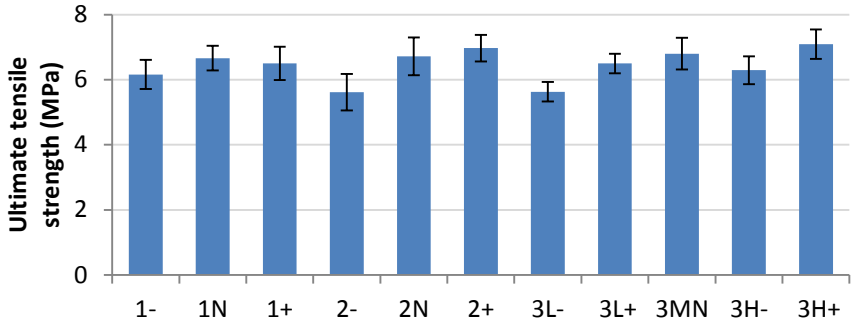

Figure 22: Average values of tensile strength for Product A coated drug cores. See text for key.

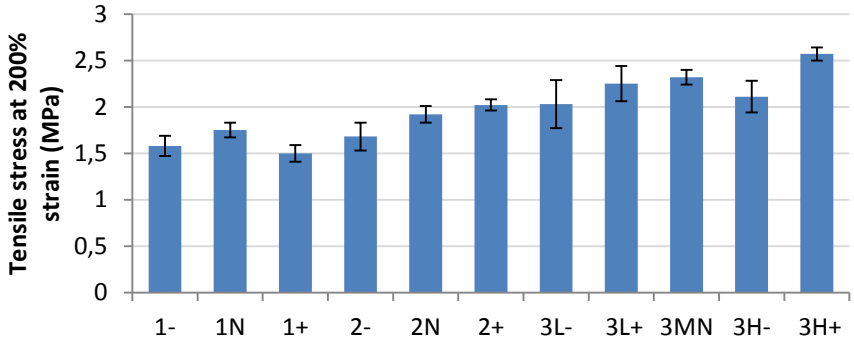

Figure 23: Average values of tensile stress at 200% tensile strain for Product A coated drug cores. See text for key.

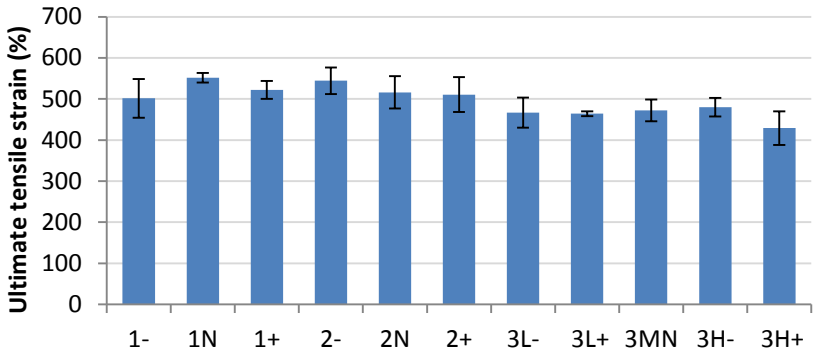

Figure 24: Average values of tensile strain at break for Product B membrane tubes. See text for key.

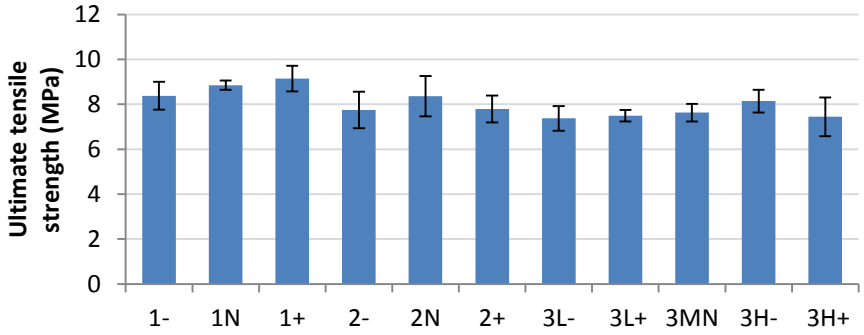

Figure 25: Average values of tensile strength for Product B membrane tubes. See text for key.

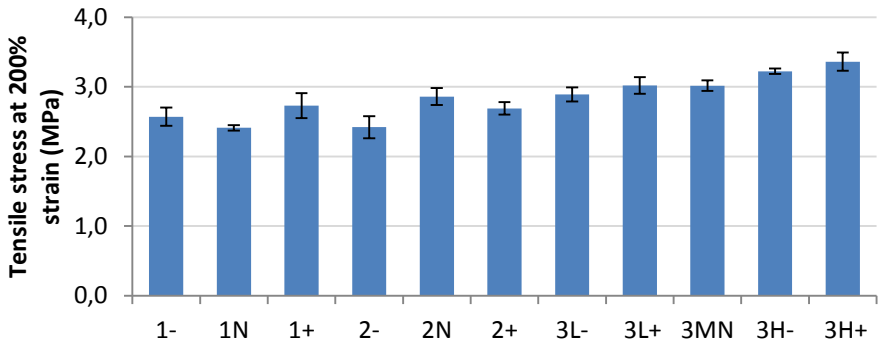

Figure 26: Average values of tensile stress at 200% tensile strain for Product B membrane tubes. See text for key.

Because the drug core material has a significantly lower stiffness and strength than the membrane materials, the stress values for Product A coated drug cores were calculated using the cross-sectional area of only the coating membrane. This means that the values of Products A and B are not entirely comparable.

It can be seen from the results that materials from Providers 1 and 2 generally show larger values of tensile strain a break but lower values of stiffness (tensile stress at 200% strain) than Provider 3 materials. For tensile strength values, no significant differences can be found between materials. Some variance in the results may be caused by

differences in extrusion parameters, such as die configuration and screw speed. Higher shear rates at the die will promote the orientation of polymer chains in the axial direction and consequently increase the tensile strength and stiffness of the extrudate. However, a clear correlation between process parameter values and the results was not found. The material silica concentration seems to have a small effect on the strength and the stiffness of the material, as would be expected. The increase in stiffness can be seen more clearly than the increase in strength. In general, variation between material batches is rather small and acceptable mechanical properties were observed for all materials.

4.5 Thermogravimetry

Results of the thermogravimetric (TGA) analysis for the extruded, post-cured membrane tubes are shown in Table 10. The individual TGA curves can be found in Appendix 2. It can be seen that for all batches, except the Provider 2 batch, the residues are markedly larger than the reported amounts of added silica. This is because volatile compounds (oligomers and water) escape the material during the compounding process and some residual oligomers can also escape later during the curing and post-curing processes. For Provider 2 materials, it seems that the reported concentration is not based on the added percentage but has been determined after the compounding via some characterization method, most likely TGA.

Table 10: Results of the thermogravimetric analysis for post-cured membrane tubes.

			Thermogravimetric residue (w-%)			
Provider	**Reported silica content (w-%)**	**Membrane thickness**	**Specimen 1**	**Specimen 2**	**Specimen 3**	**Mean**
1	ca. 35	Nominal	38.6	38.7	38.7	38.6
2	38	Nominal	38.1	38.0	38.1	38.1
3	34.5	Thick	37.6	37.6	37.6	37.6
3	35.1	Nominal	39.3	39.3	39.2	39.3
3	35.7	Thick	39.6	39.6	39.6	39.6

The residues were black in color. Since pure silica is white in color, this implies that the residues contain also some polymer degradation product besides the inert silica. It is known that the degradation process of linear PDMS in an inert atmosphere occurs through $Si - O$ bond scission and the subsequent formation of volatile cyclic oligomers. However, the polymer structure is not perfectly linear and of infinite molecular weight, and the end groups and crosslink-containing parts of the polymer may produce different degradation products than the linear parts. It is possible that reactions of these groups contribute to the black color and also, to small extent, to the residue weights.

Another, more significant observation can be drawn from the values for the Provider 3 sample: the relative magnitudes of the residues show that the reported silica concentra-

tions may be erroneous. These findings were supported by a series of tests conducted previously for uncured, compounded elastomers, showing a very similar trend to the one obtained in the present study. The percentages obtained for post-cured membrane tubes were slightly larger than the ones obtained for the uncured elastomers in the previous study, since small amounts of volatile oligomers and crosslinking byproducts will escape during the curing and post-curing processes.

4.6 Release Rate in vitro

The results of the release rate analyses will be analyzed statistically in section 4.7 in conjunction with results from TGA analyses and specimen dimension measurements, but some qualitative trends are discussed in this section. The average release rates from each specimen batch are presented as a function of time in Figures 27–29. See section 3.2 to see the true specimen amounts. The sample identification codes below the pillars are constructed in the following manner: the first digit refers to the material provider, the last digit refers to the thickness of the membrane (– refers to thin, + to thick and N to nominal) and the middle digit that is only seen with provider 3 batches refers to the silica concentration (L = low, M = medium, H = high).

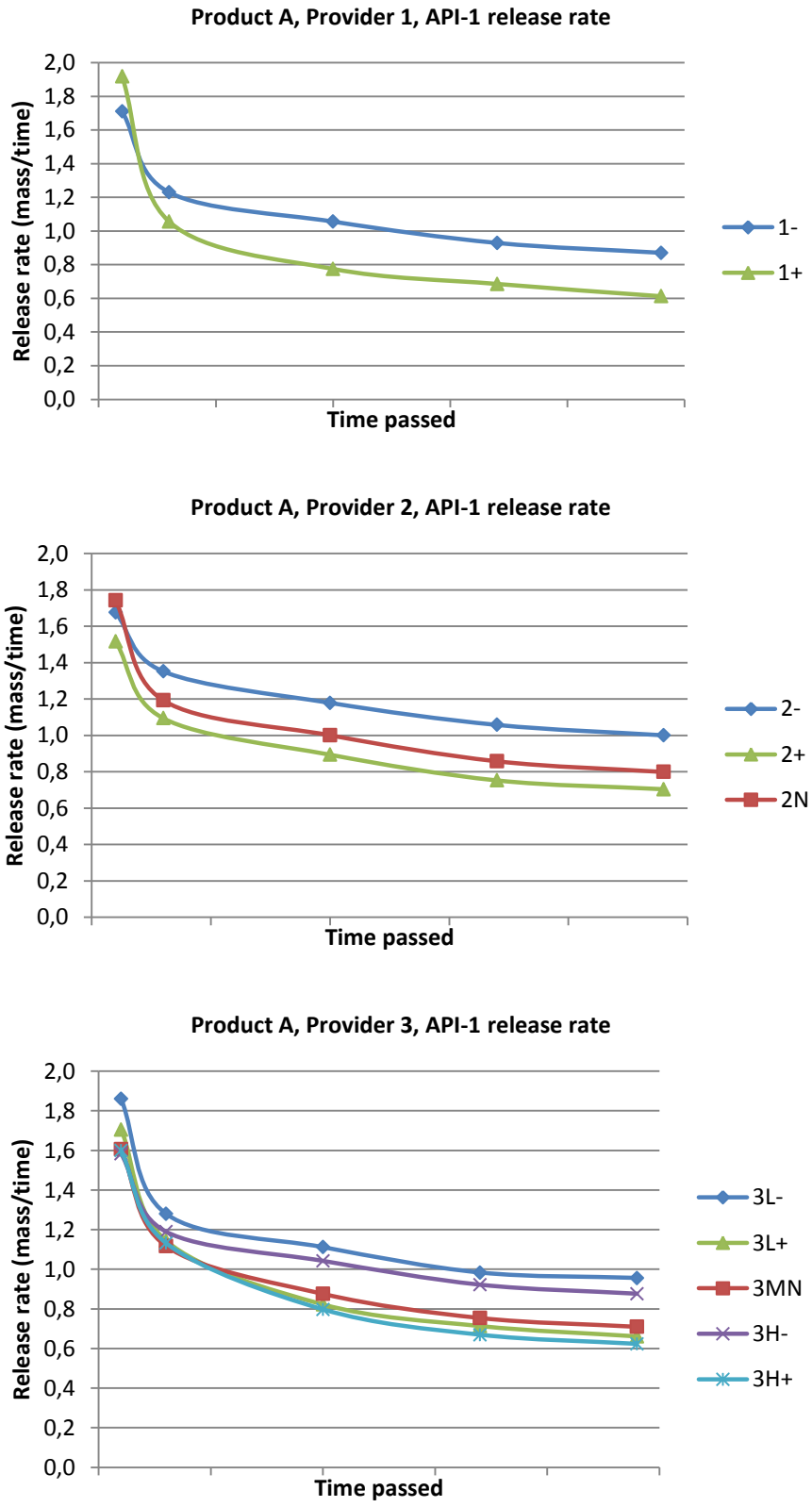

Figure 27: Averaged API-1 release rates from Product A specimens with Provider 1 (a), Provider 2 (b) and Provider 3 (c) membrane materials. See text for key.

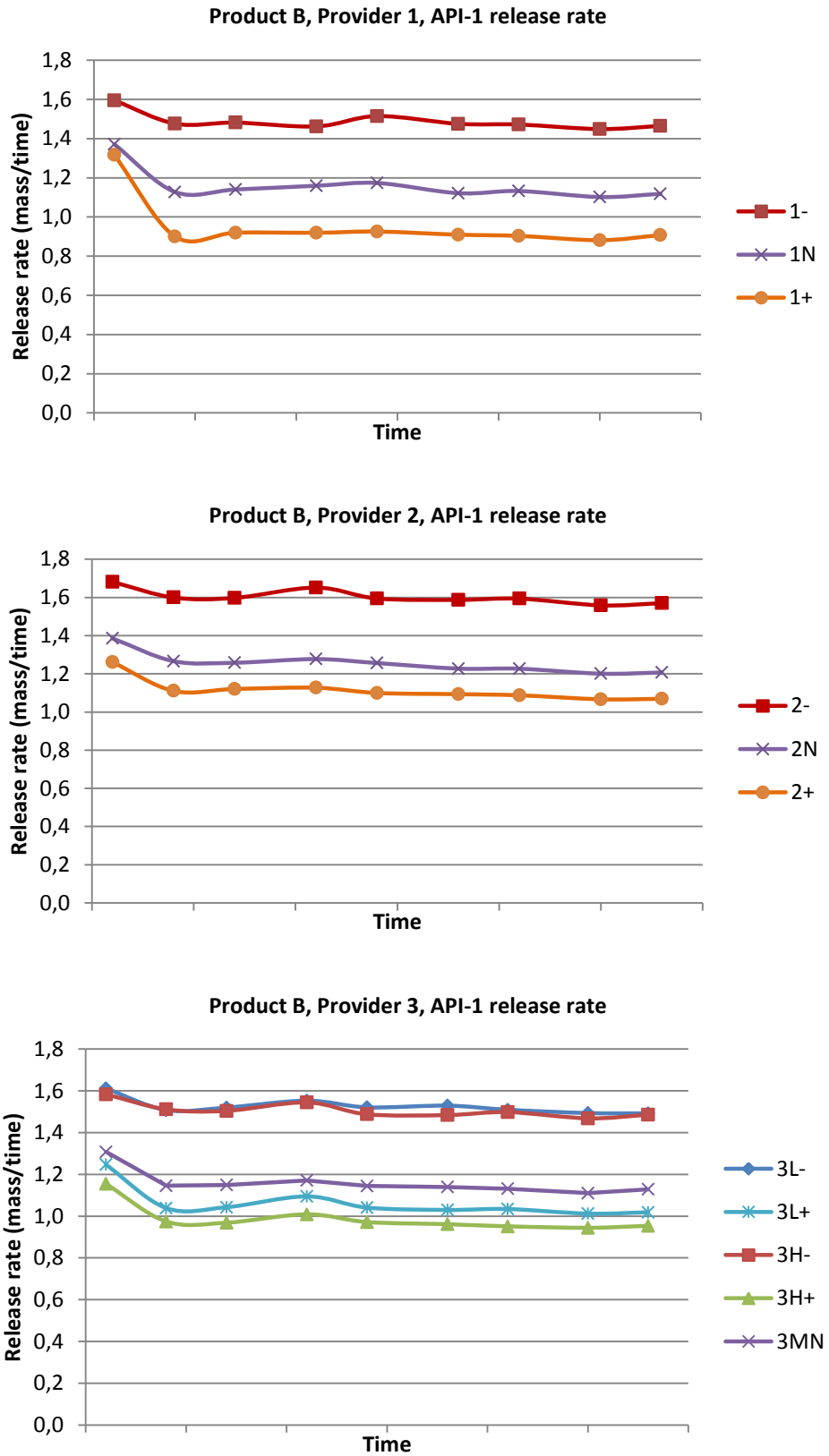

Figure 28: Averaged API-1 release rates from Product B specimens with Provider 1 (a), Provider 2 (b) and Provider 3 (c) membrane materials. See text for key.

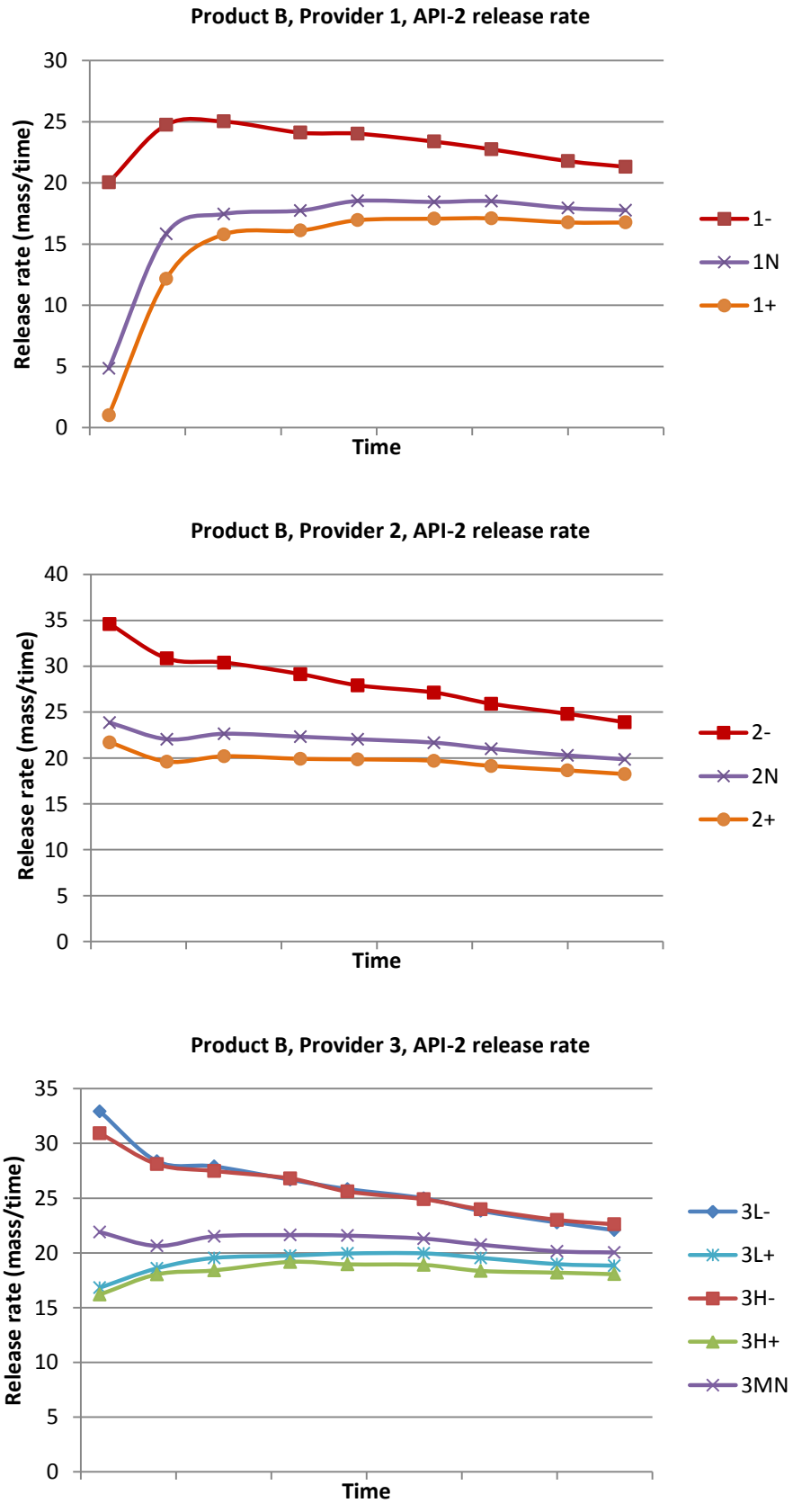

Figure 29: Averaged API-2 release rate from Product B with Provider 1 (a), Provider 2 (b) and Provider 3 (c) membrane materials. See text for key.

The observed API-1 release rates corresponded perfectly with the theoretical considerations of subsection 2.1.4.1 and specimen-to-specimen variations were small. Product A, having open ends, showed a significant burst of release in the first time points and a rapid decline of the release rate was observed with time (see Figure 27). The slope became closer to zero as time progressed, and the later time points suggested that a nearly constant rate of release would be achieved in time. All Product B specimens showed a steady API-1 release rate after the small burst at the first time point – textbook behavior for a reservoir-type device (see Figure 28). However, for API-2 release from Product B, this was not the case (Figure 29).

When the product is assembled, the drug core comes in contact with the membrane. As discussed in subsection 2.1.4.1, when this happens, the drug starts to dissolve into the membrane material and to diffuse through it. After a certain finite time of storage, a stable, location-independent concentration of drug is attained in the membrane. It can be rationalized that if this process has been completed before the product is introduced in vitro or in vivo, the product will show a burst release. If the process is far from complete, the product will show a time lag in the release.

This storage time, the time between the moment the API-2 core came in contact with the membrane and the introduction in vivo, was 6–7 days for all specimens. Thus, the differences seen in Figure 29 cannot be fully explained by differences in storage time, which means that drug solubilities and/or diffusivities in the materials must be substantially different. This suggests that Provider 1 and 2 materials differ by their composition. Provider 1 materials showed lower API-2 release rate values also at later time points, but the differences are more dramatic at early time points.

Similar variation can also be seen between Provider 3 batches, but to a smaller extent (Figure 29c). Here, however, the variations can be explained simply by differences in membrane thickness as it obviously takes a longer time for the drug to diffuse evenly into a thicker membrane. Slight variations in the storage times can also explain a part of this small variation.

It is interesting that these differences were noticeable only with API-2. This suggests that the chemical interactions of the material constituents with the two drug molecules are different. The chemical structures of the two active ingredients are, in fact, very different. The API-2 molecules are more polar than API-1 molecules, so they will have stronger interactions with highly polar silica particles. The observed differences could arise from different silica surface areas or surface treatments in the materials. A larger available silica surface area will result in increased binding sites for drug molecules and silica surface treatments can hinder (or promote) drug-silica interactions. These results show that if Provider 1 or Provider 3 materials are to be used in Product B, the storage time is a variable that must be controlled.

As mentioned in section 3.2.3.4, some voids, pockets of air, were found in the Product B API-2 sections before the release rate analysis. The pockets were also studied with a stereomicroscope (SZX12 + DP50, Olympus Optical Co. Ltd., Japan) after the analysis, when the specimen dimensions were measured. The voids were relatively small compared to the size of the drug section and they were not in direct contact with the membrane in any of the specimens. It could be seen that the amount of undissolved drug in the core mixture was smaller in the presence of a void that was close to the membrane. Nevertheless, the color suggested that there still was some crystalline drug left even in the thin sections of drug-elastomer mixture. Furthermore, the specimens with these voids did not show consistently smaller values of release rate. As a result, it was concluded that the voids did not noticeably affect the short-term release rate.

4.7 Statistical Analysis of Results

4.7.1 Statistical Correlations

The statistical correlations between the two predictor variables, the response variable, and other specimen variables were calculated. Dimension factor (DF) is a measure of specimen dimensions in the radial direction. It comes from equation (2.10) and is defined as

$$DF = \frac{1}{\ln(b/a)}\,. \tag{4.1}$$

The influence of membrane concentricity on drug release rate had been examined in earlier studies within the company. Therefore, it was also included in the analysis of this study, as cross-sectional variations in membrane thickness were observed. Membrane eccentricity is a measure of the degree of variation of membrane thickness in a specimen cross-section.

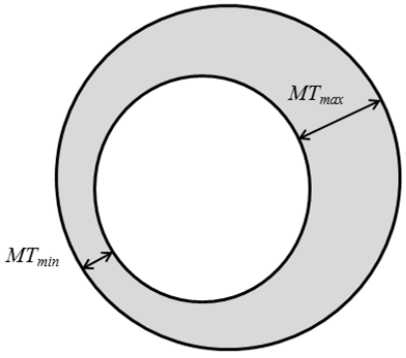

Figure 30: Measurement of maximum and minimum membrane thicknesses from the cross-section to determine membrane eccentricity.

In this study, membrane eccentricity is defined as

$$Membrane\ eccentricity = \frac{MT_{max} - MT_{min}}{\frac{1}{2}(b-a)}, \quad (4.2)$$

where MT_{max} is the highest and MT_{min} the lowest membrane thickness measured in a cross-section (see Figure 30). The correlation tables calculated with *Minitab 17* are presented in Appendix 3.

4.7.1.1 Product A

Some conclusions drawn from the correlation tables in Appendix 3 are presented here for Product A. Firstly, the correlations of release rates with TGA residue values are stronger and more statistically significant than the ones with reported silica concentrations. This supports the use of TGA residue values instead of reported concentrations in the statistical models. Secondly, correlation of release rate with the dimension factor becomes stronger and more statistically significant toward later time points, which corresponds to a decreased contribution of the open ends to the overall release rate. Thirdly, the correlations of release rate with TGA residue values decrease in strength and significance toward later time points. The correlations are not statistically significant apart from the first and perhaps the second time point ($p = 0.000$ and $p = 0.088$, respectively). The cause for this trend remains unsettled. One would expect that release rate would correlate better with TGA residue values at later time points as the release becomes more membrane-controlled.

Membrane eccentricity did not correlate significantly with drug release rates at any time point. Intuitively, no link should be present as the differences in membrane thickness average out each other in terms of diffusional path length. Length of the drug reservoir on assembled implants showed a statistically significant positive correlation with release rates at the last two time points ($p = 0.075$ and $p = 0.096$). For earlier time points, no significant correlation was found, which was expected, since the burst effect dominates the release at early time points. The length obviously has a significant effect on the release rate, but the calculated correlations remained relatively insignificant simply due to very small length variations, the effects of which were lost in random error from the analytical methods.

4.7.1.2 Product B

Slightly different conclusions can be made from the correlation tables for Product B than were made for Product A. Firstly, release rates at all time points and for both APIs correlated strongly and very significantly with the dimension factor, as would be expected for a reservoir type device ($p = 0.000$). Again, the TGA residue values correlated slightly better with release rates than the reported silica concentrations did. However,

the *correlations for neither of them were statistically significant*, as p-values varied between 0.35 and 0.89.

It is clear that a causal link exists between silica concentration and release rate. However, because the studied range of concentrations is very narrow, the correlation is not seen as statistically significant in the analysis. Nevertheless, the variable will be used in the regression models as it gives consistently a small but negative correlation with the release rate and may improve the predictive capability of the model.

Surprisingly, membrane eccentricity shows a significant correlation with release rates, but an even stronger correlation with the dimension factor. This is because systematically more eccentric membranes were obtained when manufacturing specimens with thick membranes, which means that the eccentricity is not by itself affecting the release rates. Instead, both the eccentricity and release rate are connected to the dimension factor.

4.7.2 Regression Models

As discussed in section 2.2.4.2, evidence suggests that the relationship between silica concentration and drug permeation rate through a PDMS membrane is at least close to linear for a rather wide range of concentrations. Very small concentration variations are studied in this work, so it is justifiable to study the dependence as linear. In addition, the dimension factor is linearly proportional to the release rate (see Equations (2.10) and (4.1)). This justifies the use of multiple linear regression (MLR) without higher order terms to model the drug release.

According to results from the TGA analysis and the statistical considerations presented above, the release rate variations between materials from different providers cannot be explained simply by differences in silica concentration. As a result, the predictive capability of a model that would be based on data from all materials would be poor. Consequently, only Provider 3 materials were included in the statistical models.

Since it was likely that the reported added silica concentrations of Provider 3 materials were erroneous and the release rate correlated better with the TGA residue values, the TGA residues were used as factors in the models instead of the reported silica concentrations. When using the models, it must be remembered that the cross-sectional dimensions used in the models were measured before product assembly for Product A and after product assembly and release rate analysis for Product B. Product A dimensions could not be measured after the analysis, because the duration of the release rate analysis was extended for some of the specimens (for purposes beyond this thesis). Consequently, the specimens were not available for dimension measurements.

4.7.2.1 Product A

For practical reasons, it was decided that Product A release rate should be modelled at the first, the middlemost and the last time points. Individual linear models for these time points were created, following the regression equation

$$RR = \hat{\beta}_0 + \hat{\beta}_1(DF) + \hat{\beta}_2(TGA) \ , \qquad (4.2)$$

where RR is the drug release rate (in certain units of mass/time), DF is the unitless dimension factor and TGA is the thermogravimetric residue (in w-%). The regression coefficients and model parameters calculated with *Minitab 17* software are presented in Tables 11 and 12, respectively.

Table 11: Estimated values, standard errors and p-values of the coefficients of the regression models for Product A drug release rate at three different time points.

Timepoint	*Coefficient*	*Estimated Value*	*Coefficient of standard error*	*p-value*
First	$\hat{\beta}_0$	5.289	0.786	0.000
	$\hat{\beta}_1$	0.0511	0.0284	0.088
	$\hat{\beta}_2$	–0.0975	0.0201	0.000
Middle	$\hat{\beta}_0$	1.451	0.293	0.000
	$\hat{\beta}_1$	0.1798	0.0106	0.000
	$\hat{\beta}_2$	– 0.02810	0.00747	0.001
Last	$\hat{\beta}_0$	1.475	0.206	0.000
	$\hat{\beta}_1$	0.18604	0.00746	0.000
	$\hat{\beta}_2$	– 0.03346	0.00526	0.000

Table 12: Parameters of the regression models for Product A. S is the standard distance of data points from the regression line and R^2 is the coefficient of determination.

Timepoint	*S*	*R^2 (%)*	*Adjusted R^2 (%)*
First	0.0851	59.05	54.74
Middle	0.0317	94.16	93.55
Last	0.0223	97.25	96.97

It can be seen from the R^2-values that only the middlemost and last time point models can adequately model the release rate. The last time point model can explain 97.25% of the total variance in the data, which is a very good value for a regression model. The p-values of the model coefficients show that the chosen variables give significant contributions to the model, the effect of dimension factor at the first time point being the least significant ($p = 0.088$). The dimension factor generally shows a stronger contribution than the silica concentration, as expected by the correlation coefficients presented pre-

viously. The distributions of model residuals are shown in Figure 31 and the deviations of observed values from fitted values are shown in Figure 32 with a straight line representing a perfect fit.

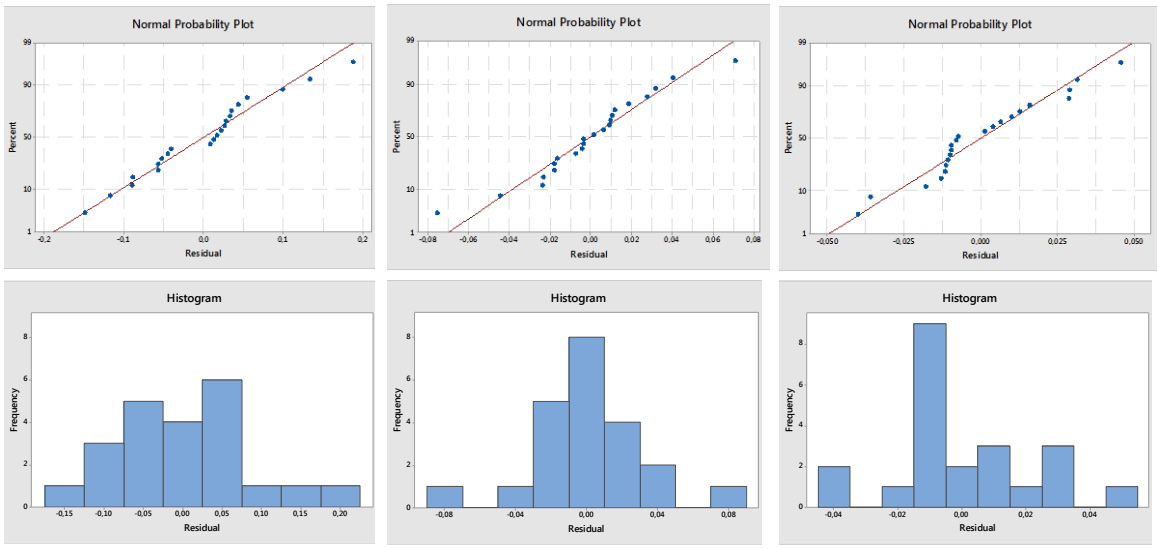

(a) (b) (c)

Figure 31: Normal probability plots and histograms of the residuals of the regression models for Product A drug release rate at the first (a), middlemost (b) and last (c) time points.

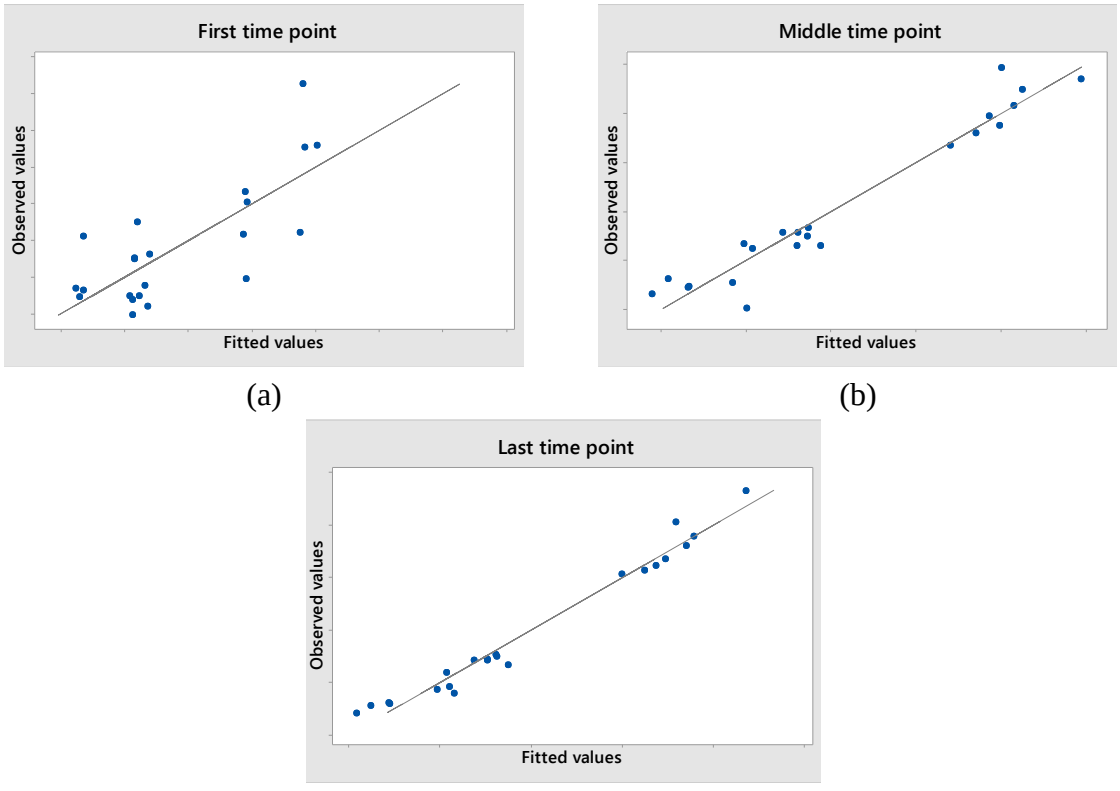

(a) (b)

(c)

Figure 32: Plots of observed vs. predicted values of Product A drug release rate at the first (a), middlemost (b) and last (c) time points. The graphs have different axis value ranges.

The model residual plots in Figure 31 show agreeable residual distributions for the first and last time point models and a highly normal distribution for the middlemost point model. A slight S-shape can be observed in all graphs. Moderate departures from normality do not seriously affect the results with large sample sizes. Figure 32 shows very clearly the differences in predictive capabilities between the models. The average distance of points from the regression line is markedly smaller with later time point models. Poor predictive capability of the first time point model was expected, because the model only includes variables related to the membrane and the release from the open ends is independent of the membrane.

4.7.2.2 Product B

The release rate of Product B was modelled somewhat differently than that of Product A. Since the API-1 release rate remained fairly constant after the initial burst at the first time point, it was decided that *all time points apart from the first one should be included in a single model*. The regression coefficients and model parameters are listed in Tables 13 and 14. No successful model could be created for the API-2 release rate as a function of membrane thickness and TGA residue. Additional studies that take the storage time dependent behavior into account will be needed if a useful model is to be created for API-2 release rate. The distribution of residuals and an observed vs. predicted values plot are shown in Figure 33.

Table 13: Estimated values, standard errors and p-values of the coefficients of the regression model for Product B API-1 release rate.

Model	***Coefficient***	***Estimated Value***	***Coefficient standard error***	***p-value***
API-1 release, Time points 2–8	$\hat{\beta}_0$	0.861	0.120	0.000
	$\hat{\beta}_1$	0.17738	0.00222	0.000
	$\hat{\beta}_2$	–0.01956	0.00304	0.000

Table 14: Parameters of the regression model for Product B. S is the standard distance of data points from the regression line and R^2 is the coefficient of determination.

Model	***S***	***R^2 (%)***	***Adjusted R^2 (%)***
API-1 release, time points 2–8	0.03636	97.42	97.39

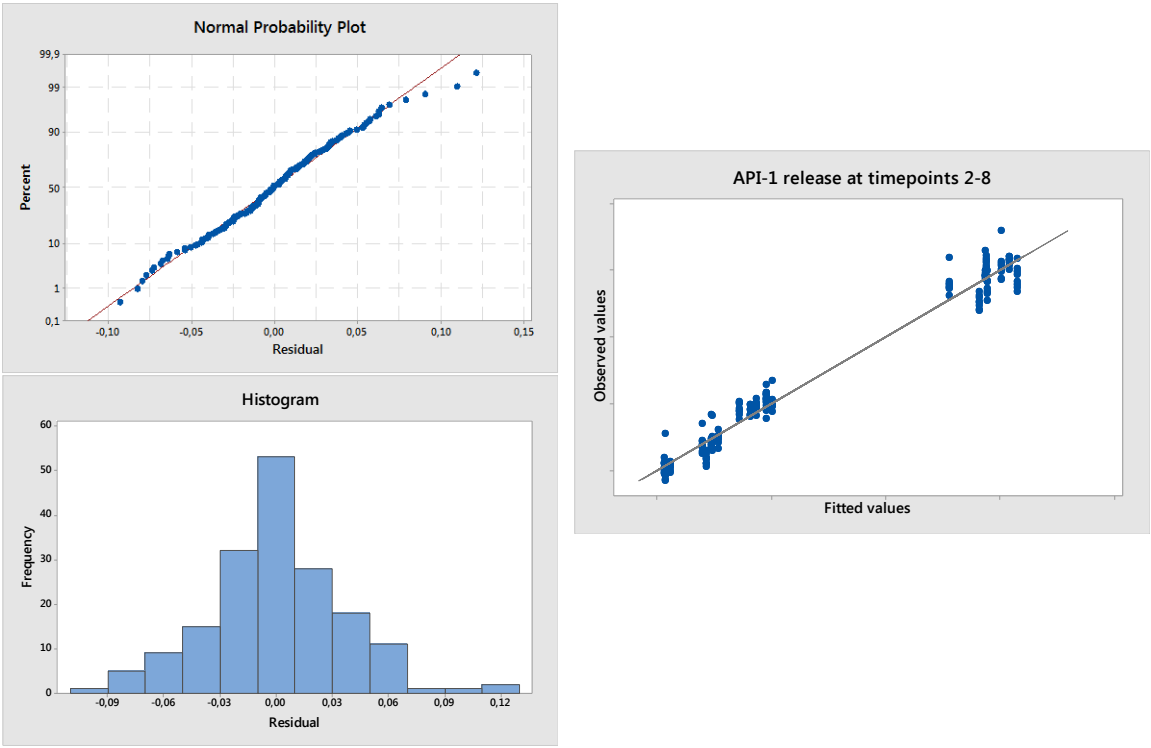

(a) (b)

Figure 33: (a) Normal probability plots and histograms of the residuals of the regression model for Product B. (b) A plot of observed vs. predicted values for the model with a line representing perfect fit.

The model shows high predictive capability as it explains 97.42% of total variance in the data (Table 14). According to Figure 33, the model residuals follow a highly normal distribution. Two possible outliers can be seen in the graphs, but these were not excluded since the values were not dramatically different and no obvious cause for the deviation was found. The grouping of points seen in Figure 33b is a result of using the same dimension factor and TGA residue values for each time point. The individual data points in the vertical "pillars" represent the values obtained at different time points for a single specimen.

4.7.3 Other Sources of Variance

A considerable amount of response variance can result from differences in drug section lengths. Based on process control limits, the length variations may be up to ± 1.6% of nominal length for Product A and up to ± 4.0% of nominal length for Product B API-1 section. This will, according to equation (2.10), result in similar variation in steady-state release rate. To improve the predictive capability of the model, it would have been possible to include the drug section length in the analysis as a covariate. However, Product B drug section lengths could not be measured accurately after the release rate analysis, because the specimens were mistakenly cut for the cross-sectional analysis before any length measurements were made.

On one hand, it would have been wise to prepare specimens that cover the whole range of drug section lengths allowed by the established process control limits, because then the models would better correspond to a real product manufacturing situation. In fact, this was the case for Product A. Product B drug section lengths were not accurately measured for reasons discussed above, so their true variance remains unknown. On the other hand, previous studies suggest that the within-tolerance length variations do not cause statistically significant differences in the release rate.

5 CONCLUSIONS

In this thesis work, the effect of fumed silica concentration of a polydimethylsiloxane elastomer membrane on the drug release rates from cylindrical, diffusion-controlled drug delivery devices was studied. The goals of the thesis were to find suitable elastomer compositions for two products so that certain predetermined release rates of two drugs, API-1 and API-2, would be achievable with materials from a new provider. In addition, the effects of silica concentration and cross-sectional dimensions of the product on drug release rates were to be modelled statistically.

Materials from three providers were studied. Materials from different providers showed somewhat different behavior in terms of mechanical, thermogravimetric and diffusional properties. Since it is known that the base polymers have similar chemical structures, the differences in properties are likely due to differences in molecular weight distribution, amount and type of peroxide initiator used, silica surface area or compounding parameters.

Even with perfectly identical material constituents, different compounding parameters could cause differences in material behavior, because the silica particles are coated with a PA-fluid during the compounding process. Poorly coated particles have more free hydroxyl groups available for drug-silica interactions and can form agglomerates more easily. Gel permeation chromatrography and peroxide quantification could have been used to rule out the effects of molecular weight and initiator concentration. The precise reason for these differences remains unsettled. The cause was not pursued further, since it was beyond the scope of this thesis.

Suitable composition ranges for the new materials were successfully determined for both products and regression models were created for API-1 release rates from the products. Additional studies should be conducted to quantify the effect of silica on steady-state API-2 release rate, since in these tests, the data was rendered partly invalid by differences in initial API concentrations in the membrane. This, however, raised an important point: the storage time between manufacturing and use or analysis of products with API-2 reservoirs must be controlled if the new materials are to be used for the product. It is likely that this will not be an issue for sterilized products, because sterilization carried out at elevated temperatures may provide sufficient heat and time to accelerate the diffusion and allow the membrane to be saturated with drug.

When comparing the results to internal product specifications, it was concluded that the use of a single elastomer composition for both products is possible, but it limits the possible ranges of product dimensions and may affect the specimen manufacturing processes. If the new materials are to be used, verification studies should be conducted near the optimal process parameters to validate the conclusions of this study and to set new process control limits. The effects of membrane thickness variations on the fluency and throughput of the assembly processes should also be evaluated.

REFERENCES

[1] J. Enderle and J. Bronzino, Introduction to biomedical engineering, 3rd ed., Academic Press, Burlington, MA, 2012, 1253 p.

[2] A. Hoffman, B. Ratner, F. Schoen and J. Lemons, Biomaterials Science: An Introduction to Materials in Medicine, 3rd ed., Academic Press, Oxford, 2012, 1519 p.

[3] Y. Ikada, "Challenges in Tissue Engineering," *Journal of the Royal Society Interface,* Vol. 3, Iss. 10, 2006, pp. 589–601

[4] ”Karolinska University Hospital. First successful transplantation of a synthetic tissue engineered windpipe", ScienceDaily, 7 July 2011. Available: http://www.sciencedaily.com/releases/2011/07/110707145620.htm [Accessed 11 September 2014].

[5] J. Siepmann, R. A. Siegel and M. J. Rathbone, Fundamentals and Applications of Controlled Release Drug Delivery, 1st ed., Springer Science+Business Media, New York, 2012, 592 p.

[6] J. P. Griffin and J. O'Grady, The Textbook of Pharmaceutical Medicine, 5th ed., Blackwell Publishing Ltd, Oxford, 2006, 870 p.

[7] L. T. Fan and S. K. Singh, Controlled Release - A Quantitative Treatment, 1st ed., Springer-Verlag, Berlin, Germany, 1989, 233 p.

[8] J. C. Wright and D. J. Burgess, Long Acting Injections and Implants, 1st ed., Springer Science+Business Media, New York, 2012, 557 p.

[9] R. Goldbart, T. Traitel, S. A. Lapidot and J. Kost, "Enzymatically Controlled Responsive Drug Delivery Systems," *Polymers for Advanced Technologies,* Vol. 13, 2002, pp. 1006–1018.

[10] D. Gourevich, O. Dogadkin, A. Volovick, L. Wang and J. Gnaim, "Ultrasound-mediated targeted drug delivery with a novel cyclodextrin-based drug carrier by mechanical and thermal mechanisms," *Journal of Controlled Release,* Vol. 170, Iss. 3, 2013 pp. 316–324.

[11] R. A. Siegel, "Stimuli sensitive polymers and self regulated drug delivery systems: A very partial review," *Journal of Controlled Release,* Vol. 190, 2014, pp. 337–351.

[12] M. H. Smolensky and F. Portaluppi, "Chronopharmacology and chronotherapy of cardiovascular medications: Relevance to prevention and treatment of coronary heart disease," *American Heart Journal,* Vol. 137, Iss. 4, 1999, pp. S15–S24,

[13] R. Schiel, "Continuous Subcutaneous Insulin Infusion in Patients with Diabetus Mellitus," *Therapeutic Apheresis and Dialysis,* Vol. 2, Iss. 7, 2003, pp. 232–237.

[14] J. R. Fried, Polymer Science and Technology, 2nd ed., Pearson Education, Inc., NJ, 2003, 582 p.

[15] J. Crank, The Mathematics of Diffusion, 2nd ed., Clarendon Press, Oxford, 1975, 414 p.

[16] T. J. Roseman, "Release of Steroids from a Silicone Polymer," *Journal of Pharmaceutical Sciences,* Vol. 61, Iss. 1, pp. 46–50, 1972.

[17] J. A. Russell, R. K. Malcolm, K. Campbell and A. D. Woolfscon, "High-performance liquid chromatographic determination of 17β-estradiol and 17β-estradiol-3-acetate solubilities and diffusion coefficients in silicone elastomeric intravaginal rings," *Journal of Chromatography B,* Vol. 744, 2000, pp. 157–163.

[18] R. Malcolm, S. McCullagh, A. Woolfson, M. Catney and P. Tallon, "A dynamical mechanical method for determining the silicone elastomer solubility of drugs and pharmaceutical excipients in silicone intravaginal drug delivery rings," *Biomaterials,* Vol. 23, 2002, pp. 3589–3594

[19] B. L. Flynn, S. H. Yalkowsky and T. J. Roseman, "Mass Transport Phenomena and Models: Theoretical Concepts," *Journal of Pharmaceutical Sciences,* Vol. 63, Iss. 4, 1974, pp. 479–510.

[20] J. Comyn, Polymer Permeability, 1st ed., Chapman & Hall, London, 1985, 383 p.

[21] L. H. Sperling, Introduction to Physical Polymer Science, 4th ed., John Wiley & Sons, Inc., NJ, 2006, 845 p.

[22] T. Higuchi, "Theoretical Analysis of Rate of Release of Solid Drugs Dispersed in Solid Matrices," *Journal of Pharmaceutical Sciences,* Vol. 52, Iss. 12, 1963, pp. 1145–1149.

[23] J. Siepmann and N. A. Peppas, "Higuchi equation: Derivation, applications, use and misuse," *International Journal of Pharmaceutics,* Vol. 418, 2011, pp. 6–12,

[24] A. D. Woolfson et al., "Design of an intravaginal ring for the controlled delivery of 17β-estradiol as its 3-acetate aster," *Journal of Controlled Release,* Vol. 61, 1999, pp. 319–328.

[25] M. A. Brook, Silicon in Organic, Organometallic and Polymer Chemistry, John Wiley & Sons Inc., New York, 2000, 680 p.

[26] W. M. Haynes, ed., "Abundance of Elements in the Earth's Crust and in the Sea", in *CRC Handbook of Chemistry and Physics, 95th edition, Internet Version*, CRC Press/Taylor and Francis, Boca Raton, FL, 2015.

[27] A. Colas, "Silicones: Preparation, Properties and Performance," Dow Corning, Life Sciences, 2005. Available: http://www.dowcorning.com/content/webabstract/ABS_01-3077.asp [Accessed: 25 March, 2015]

[28] S. J. Clarson and J. A. Semlyen, Siloxane polymers, PTR Prentice Hall, Inc., Englewood Cliffs, NJ, 1993, 673 p.

[29] W. Noll, Chemistry and Technology of Silicones, Academic Press Inc., New York, NY, 1968, 702 p.

[30] M. Andriot, S. H. Chao, A. Colas, et al. ”Silicones in Industrial Applications,”

Dow Corning Corporation, 2007. Available: http://www.dowcorning.com/content/discover/discoverchem/si-industrial-apps.aspx [Accessed: 25 March 2015].

[31] G. Wypych, Fillers, ChemTec Publishing, Toronto-Scarborough, ON, Canada, 1993, 295 p.

[32] C. F. Most, "Some Filler Effects on Diffusion in Silicone Rubber," *Journal of Applied Polymer Science*, Vol. 14, 1970, pp. 1019–1036.

[33] J. Mazan et al., "Influence of Silica and the Macromolecules on Progesterone Diffusion in a Polydimethylsiloxane Network," *European Polymer Journal*, Vol. 28, Iss. 10, 1992, pp. 1151–1154.

[34] E. G. Lovering et al., "Drug permeation through membranes IV: Effect of excipients and various additives on permeation of chlordiazepoxide through polydimethylsiloxane membranes," *Journal of Pharmaceutical Sciences*, Vol. 63, Iss. 8, 1974, pp. 1224–1227.

[35] K. Tojo et al., "In vitro apparatus for controlled release studies and intrinsic rate of permeation," *Journal of Controlled Release*, Vol. 1, Iss. 3, 1985, pp. 197–203.

[36] E. G. Lovering et al., "Drug permeation through membranes V: Interaction of diazepam with common excipients," *Journal of Pharmaceutical Sciences*, Vol. 65, Iss. 2, 1976, pp. 207–210.

[37] E. G. Lovering et al., "Diffusion layer effects on permeation of phenylbutazone through polydimethylsiloxane," *Journal of Pharmaceutical Sciences*, Vol. 63, Iss. 9, 1974, pp. 1399–1402.

[38] K. F. Finger et al., "Investigation and Development of Protective Ointments IV: The Influence of Active Fillers on the Permeability of Semisolids," *Journal of the American Pharmaceutical Association (Scientific Edition)*, Vol. 49, Iss. 9, 1960, pp. 569–573.

[39] E. R. Garrett and P. B. Chemburkar, "Evaluation, Control, and Prediction of Drug Diffusion Through Polymeric Membranes I: Methods and Reproducibility of Steady-State Diffusion Studies," *Journal of Pharmaceutical Sciences*, Vol. 57, Iss. 6, 1968, pp. 944–948.

[40] B. Rodgers and W. Waddell, "Chapter 9 - Science of rubber compounding," in *Science and Technology of Rubber*, 4th ed., Elsevier Academic Press, Burlington, MA, 2013, 764 p.

[41] M. Chanda and S. K. Roy, ”Chapter 1: Fabrication Processes,” in *Plastic Fabrication and Recycling*, CRC Press, 2009, 121 p.

[42] N. Hewitt and C. P, Compounding Precipitated Silica in Elastomers, William Andrew Publishing, Norwich, NY, 2007, 582 p.

[43] R. Simpson, "Section 5: Rubber Processing Equipment," in *Rubber Basics*, Smithers Rapra, Shrewsbury, 2002, pp. 157–198.

[44] C. Rauwendaal, Polymer Extrusion, 2nd ed., Carl Hanser Verlag, Munich,

Germany, 1990, 568 p.

[45] W. Michaeli, Extrusion Dies for Plastics and Rubber: Design and Engineering Computations, 2nd ed., Carl Hanser Verlag, Munich, 1992, 340 p.

[46] H. G. Giles, J. R. Wagner and E. M. Mount, Extrusion: The Definitive Processing Guide and Handbook, William Andrew Publishing, Norwich, NY, 2005, 542 p.

[47] G. van Belle and K. F. Kerr, Design and Analysis of Experiments in the Health Sciences, John Wiley & Sons, Inc., Hoboken, NJ, 2012, 229 p.

[48] A. C. Tamhane, Statistical Analysis of Designed Experiments - Theory and Applications, John Wiley & Sons, Hoboken, NJ, 2009, 679 p.

[49] D. C. Montgomery, Design and Analysis of Experiments, 8th ed., John Wiley & Sons Inc., Singapore, 2013, 730 p.

[50] J. L. Devore, Probability and Statistics for Engineering and the Sciences, 8th ed., Brooks/Cole, Boston, MA, 2012, 687 p.

[51] K. G. Calkins, "Correlation Coefficients (Applied Statistics – Lesson 5)," Andrews University, Berrien Springs, Michigan, 2005. Available: http://www.andrews.edu/~calkins/math/edrm611/edrm05.htm [Accessed: 25 March 2015]

APPENDICES

Appendix 1: Curing curves

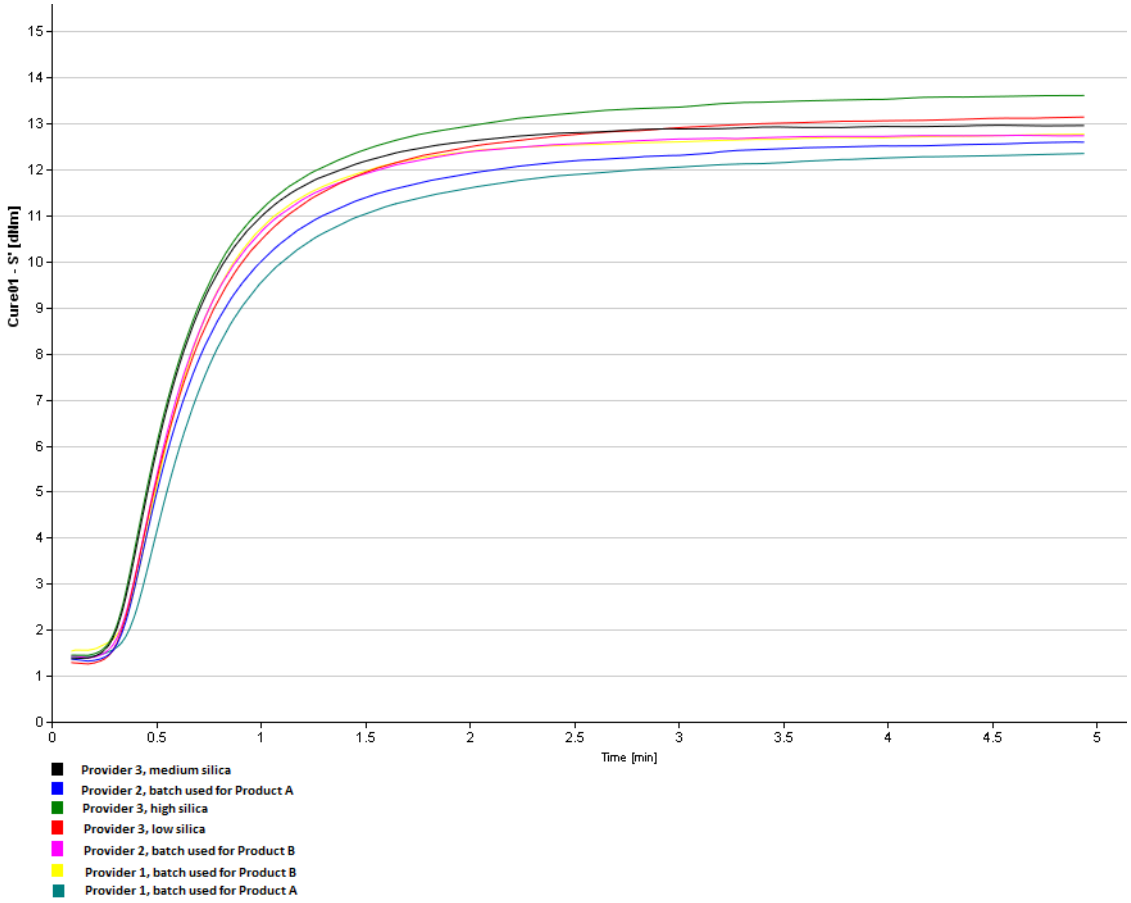

*Appendix Figure 1: Graphical presentation of results from the curing analysis for all used coating membrane material batches. **S'** is the material storage modulus. See sections 3.3.1 and 4.1 for details.*

Appendix 2: Thermogravimetric curves

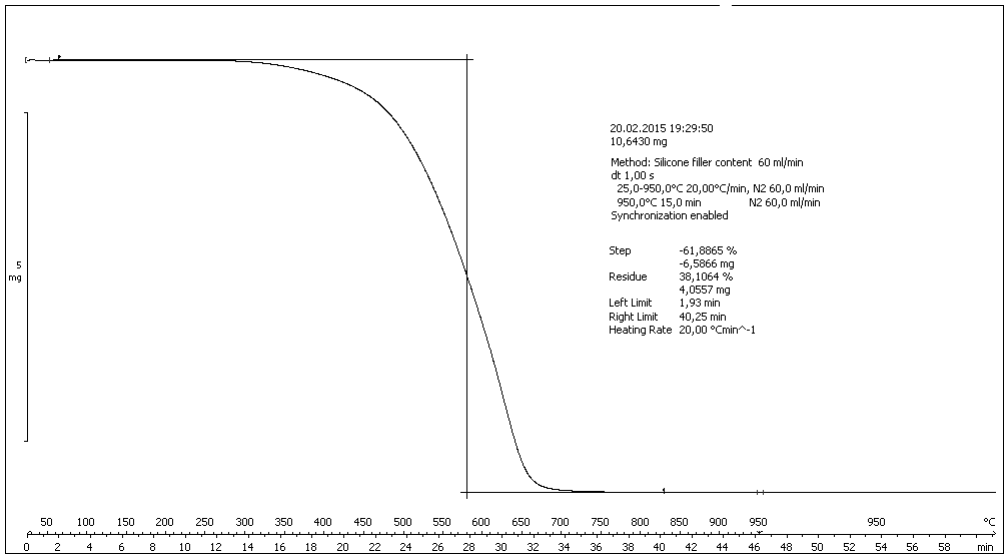

(1)

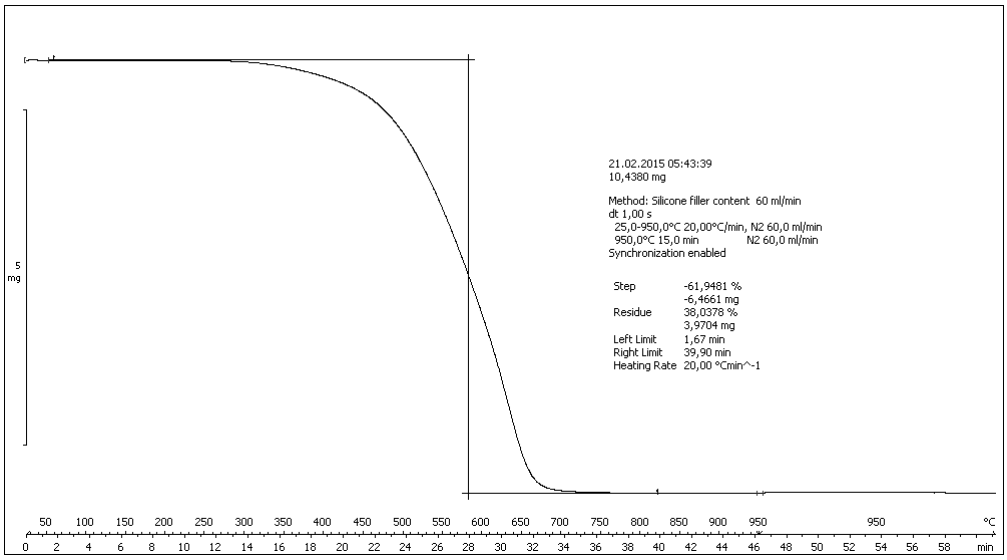

(2)

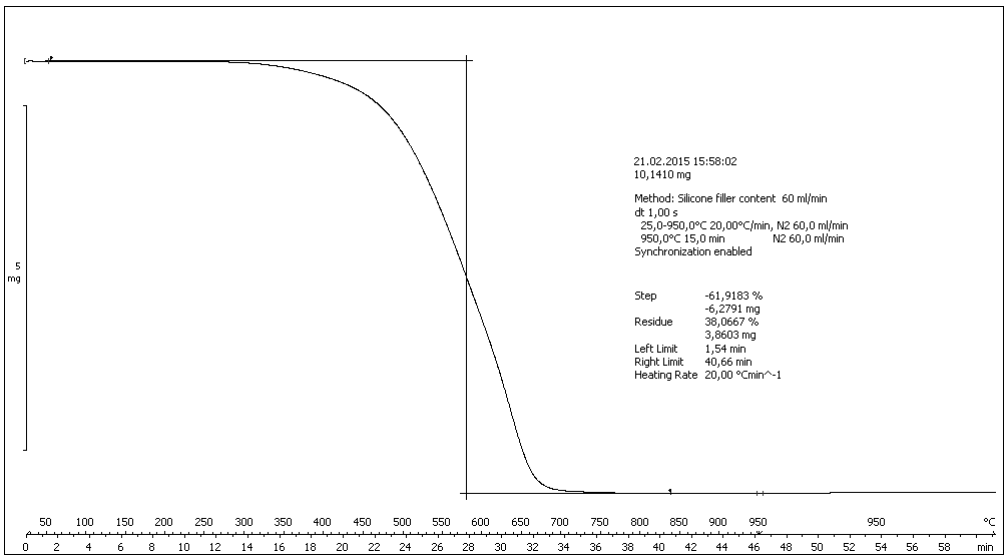

(3)

Appendix Figure 2: TGA curves for the analyzed membrane tubes: Provider 2 material, three parallel measurements (1-3).

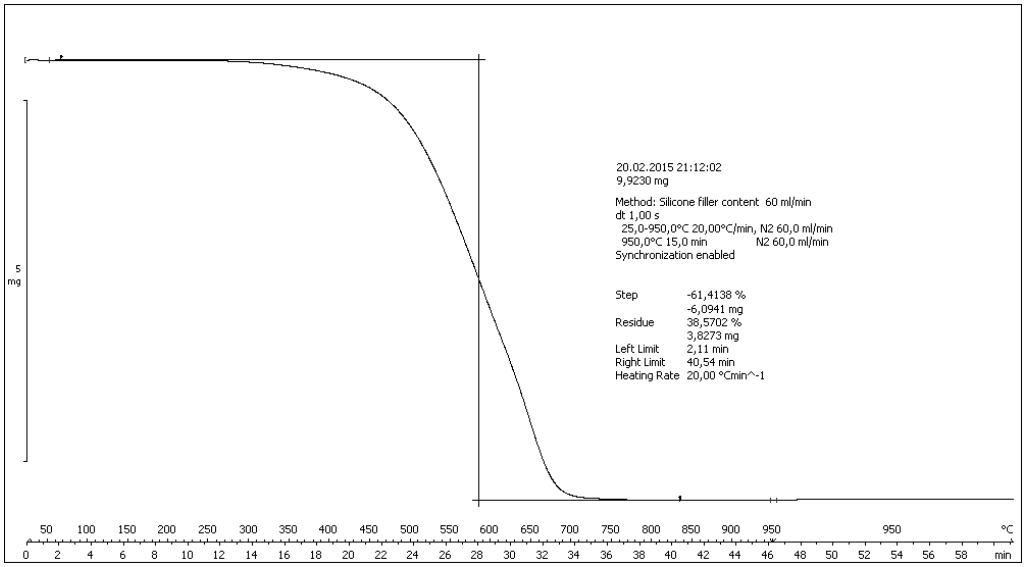

(1)

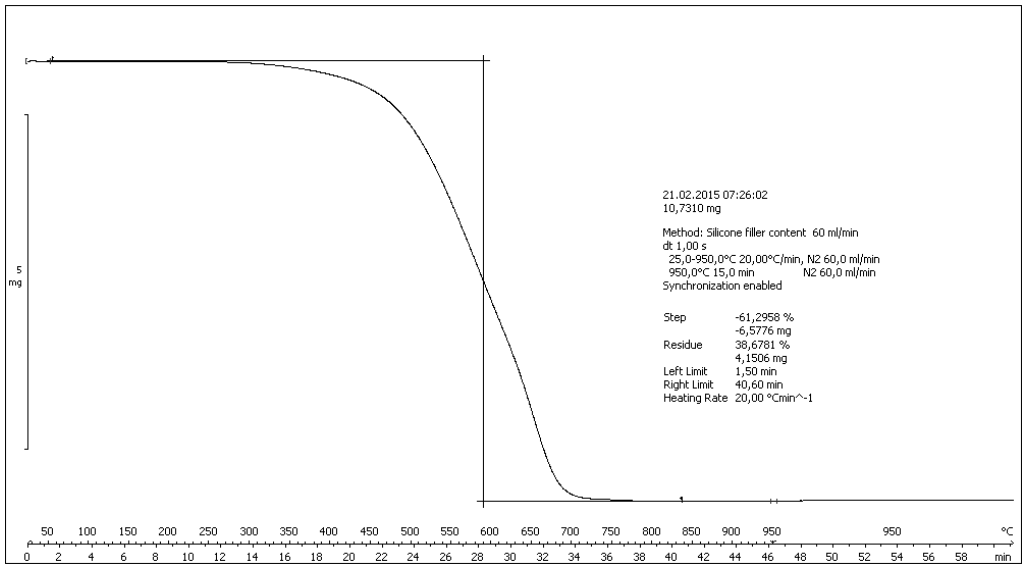

(2)

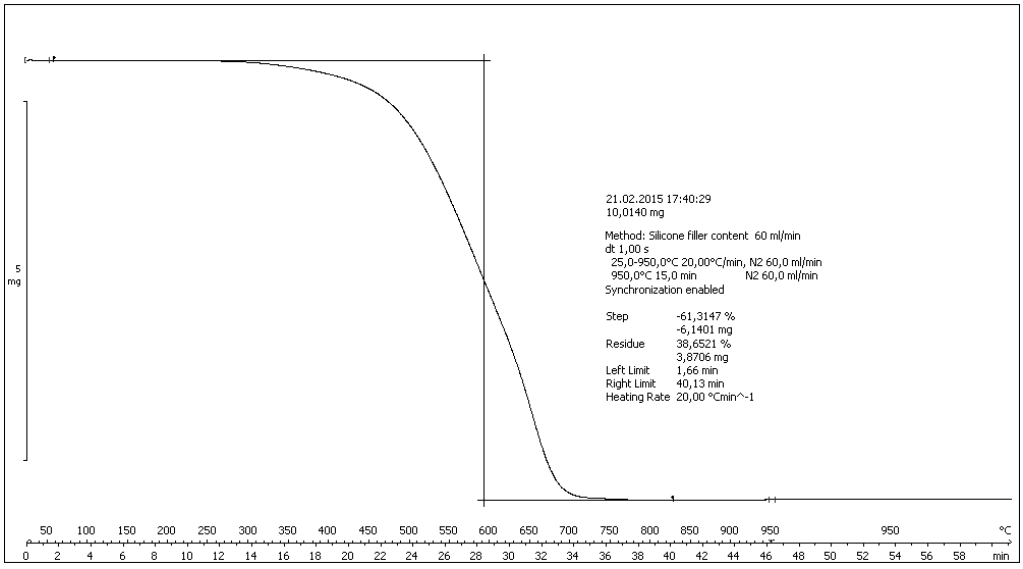

(3)

Appendix Figure 3: TGA curves for the analyzed membrane tubes: Provider 1 material, three parallel measurements (1-3).

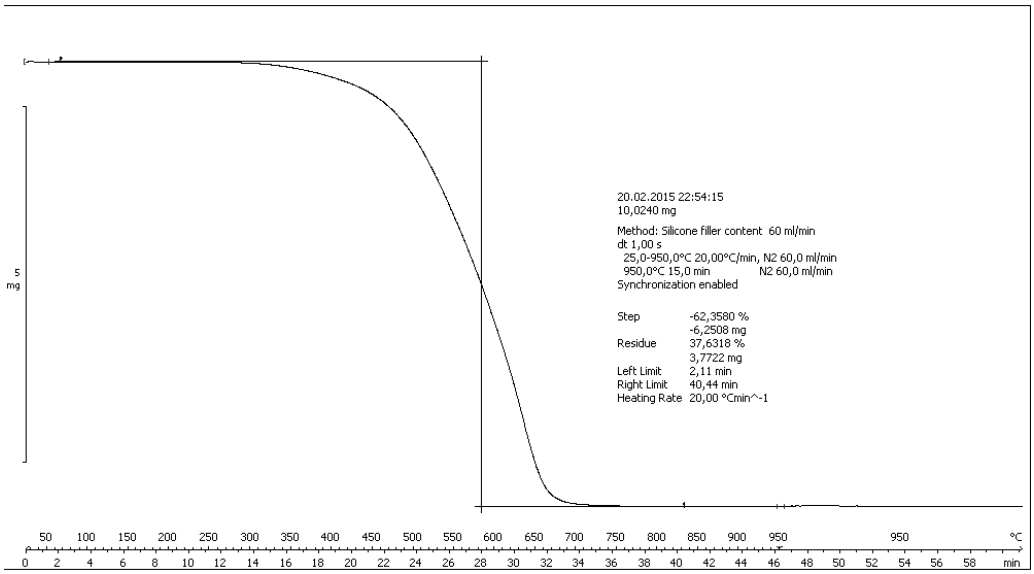

(1)

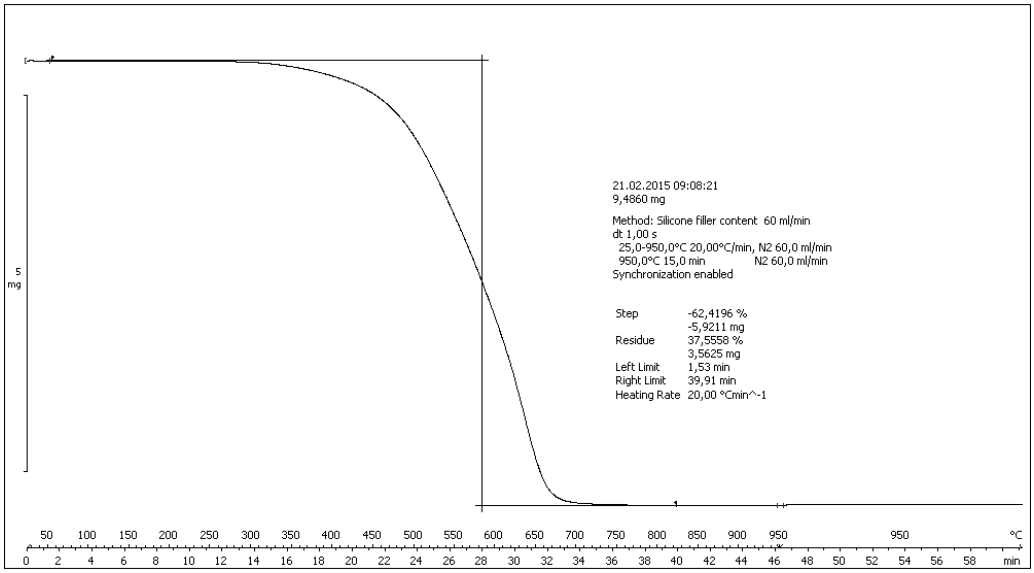

(2)

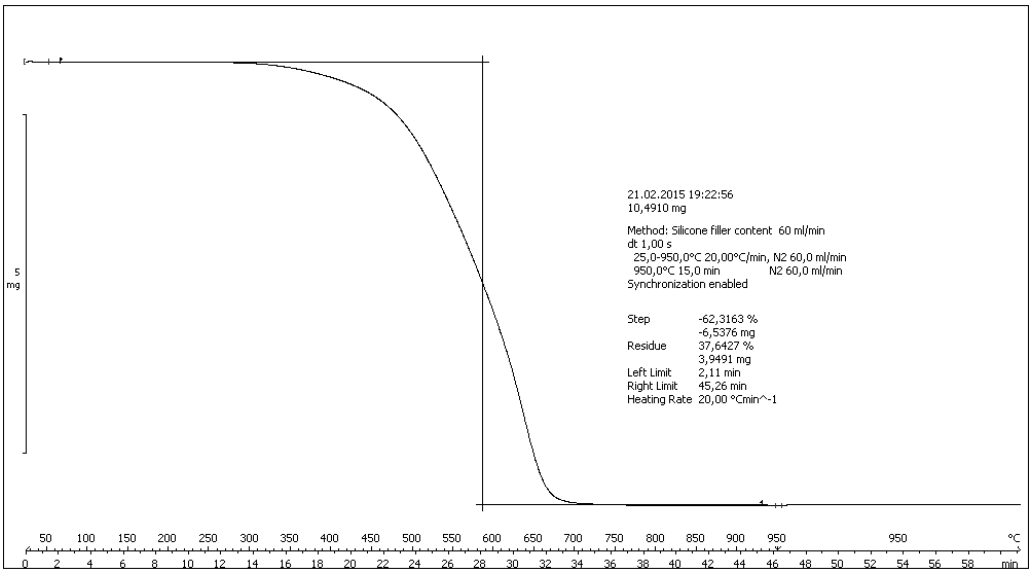

(3)

Appendix Figure 4: TGA curves for the analyzed membrane tubes: Provider 3 material with lowest silica concentration, three parallel measurements (1-3).

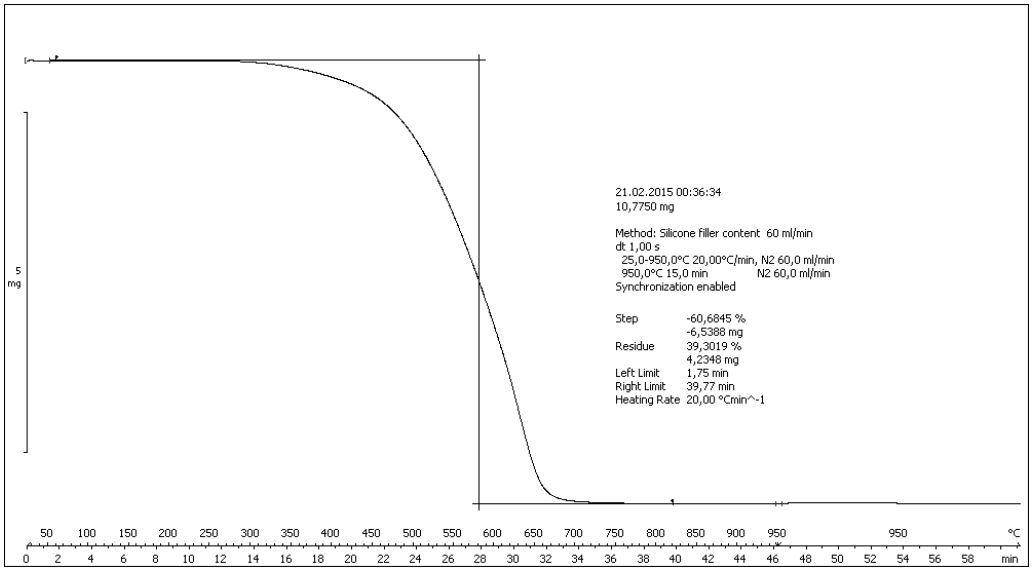

(1)

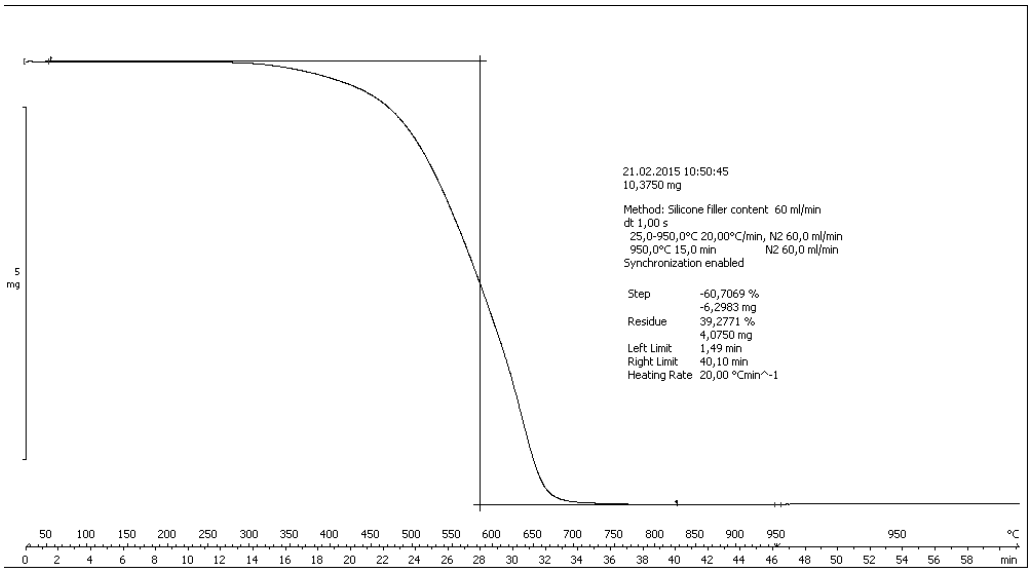

(2)

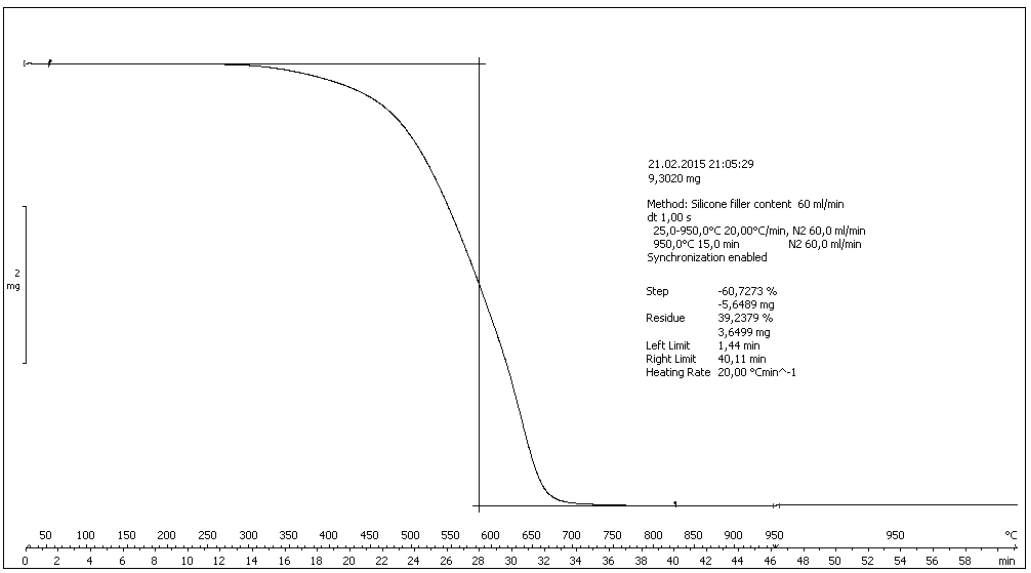

(3)

Appendix Figure 5: TGA curves for the analyzed membrane tubes: Provider 3 material with medium silica concentration, three parallel measurements (1-3).

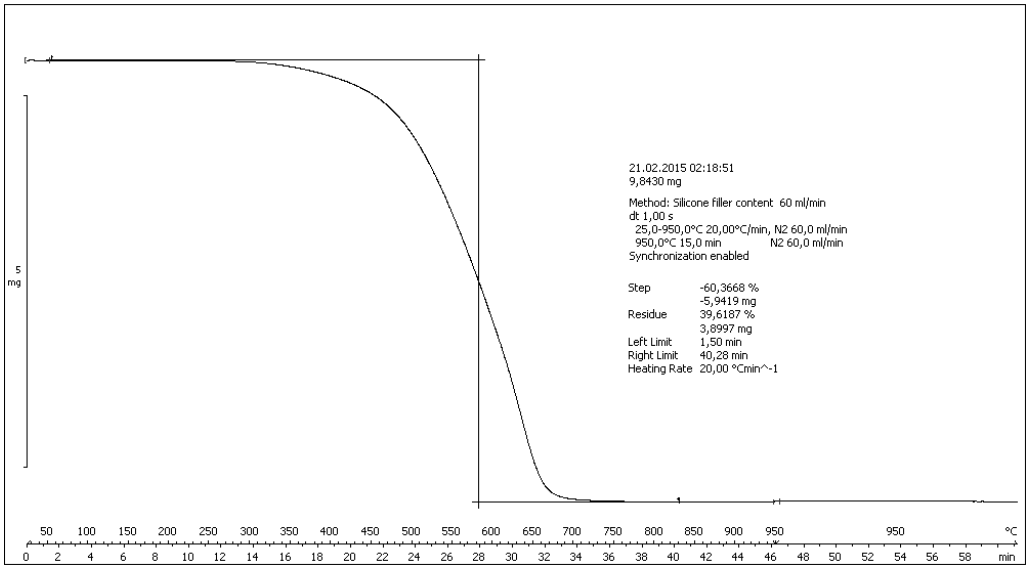

(1)

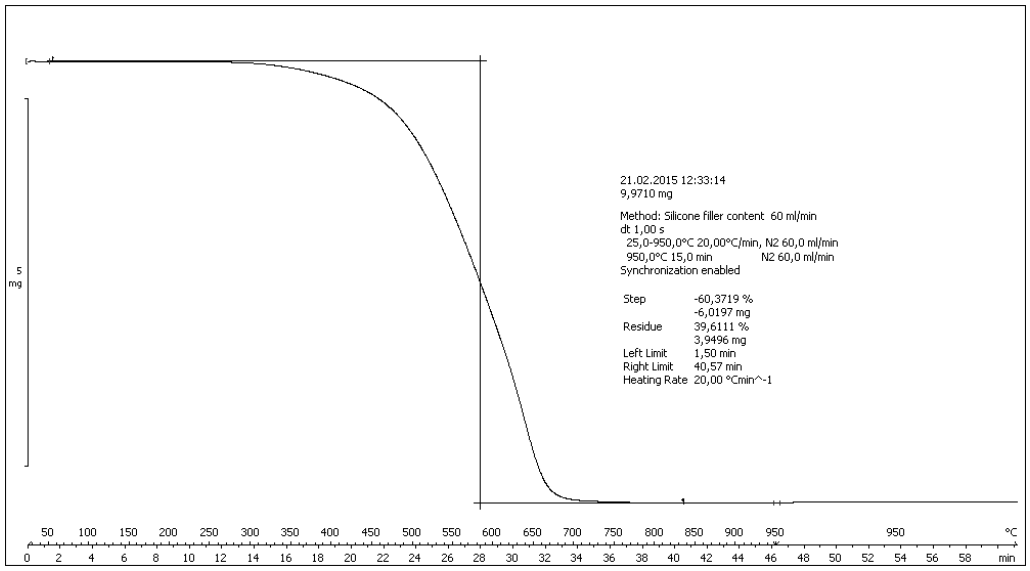

(2)

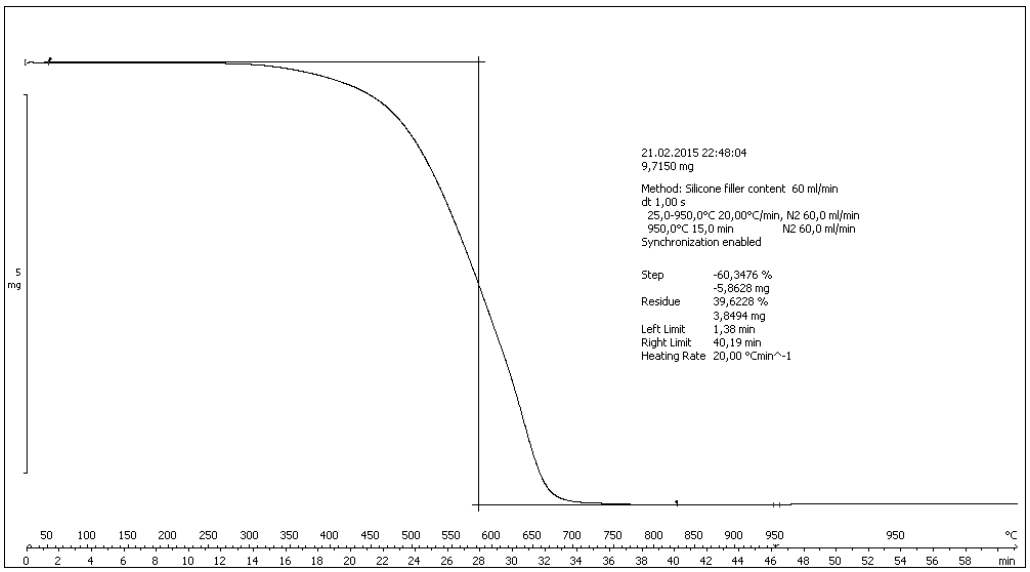

(3)

Appendix Figure 6: TGA curves for the analyzed membrane tubes: Provider 3 material with the highest silica concentration, three parallel measurements (1-3).

Appendix 3: Correlation coefficient tables

Appendix Table 1: Calculated correlation coefficients and p-values for Product A results.

			API-1 release rate at time point					*Dimension factor*	*Membrane ecc.*	*Length prior to assembly*	*Length after assembly*	*Reported silica conc.*
			1	**2**	**3**	**4**	**5**					
API-1 release rate at time point	**2**	Correlation	0.342									
		p-value	0.119									
	3	Correlation	0.435	0.627								
		p-value	0.043	0.002								
	4	Correlation	0.441	0.628	0.984							
		p-value	0.040	0.002	0.000							
	5	Correlation	0.441	0.618	0.983	0.985						
		p-value	0.040	0.002	0.000	0.000						
Dimension factor		Correlation	0.285	0.515	0.948	0.956	0.956					
		p-value	0.199	0.014	0.000	0.000	0.000					
Membrane ecc.		Correlation	–0.262	–0.151	–0.238	–0.235	–0.305	–0.229				
		p-value	0.240	0.503	0.286	0.292	0.168	0.305				
Length prior to assembly		Correlation	–0.497	–0.141	–0.227	–0.255	–0.297	–0.157	0.607			
		p-value	0.019	0.531	0.309	0.252	0.179	0.484	0.003			
Length after assembly		Correlation	–0.119	0.147	0.351	0.387	0.364	0.367	0.339	0.310		
		p-value	0.599	0.515	0.109	0.075	0.096	0.093	0.123	0.161		
Reported silica conc.		Correlation	–0.662	–0.265	–0.165	–0.189	–0.200	0.009	0.634	0.688	0.362	
		p-value	0.001	0.233	0.463	0.399	0.372	0.968	0.002	0.000	0.098	
TGA residue		Correlation	–0.722	–0.372	–0.236	–0.262	–0.270	–0.029	0.459	0.582	0.182	0.946
		p-value	0.000	0.088	0.290	0.238	0.225	0.896	0.031	0.004	0.418	0.000

Appendix Table 2: Calculated correlation coefficients and p-values for Product B API-1 results.

			API-1 Release rate at time point									*Dimensi-on factor*	*Membra-ne ecc.*	*Reported silica conc.*
			1	**2**	**3**	**4**	**5**	**6**	**7**	**8**	**9**			
API-1 release rate at time point	**2**	Correlation	0.989											
		p-value	0.000											
	3	Correlation	0.990	0.997										
		p-value	0.000	0.000										
	4	Correlation	0.980	0.982	0.988									
		p-value	0.000	0.000	0.000									
	5	Correlation	0.989	0.994	0.997	0.991								
		p-value	0.000	0.000	0.000	0.000								
	6	Correlation	0.991	0.995	0.998	0.988	0.998							
		p-value	0.000	0.000	0.000	0.000	0.000							
	7	Correlation	0.991	0.997	0.999	0.990	0.997	0.998						
		p-value	0.000	0.000	0.000	0.000	0.000	0.000						
	8	Correlation	0.988	0.995	0.998	0.989	0.996	0.998	0.999					
		p-value	0.000	0.000	0.000	0.000	0.000	0.000	0.000					
	9	Correlation	0.989	0.995	0.998	0.990	0.998	0.998	0.999	0.998				
		p-value	0.000	0.000	0.000	0.000	0.000	0.000	0.000	0.000				
Dimension factor		Correlation	0.973	0.989	0.991	0.978	0.984	0.986	0.990	0.990	0.990			
		p-value	0.000	0.000	0.000	0.000	0.000	0.000	0.000	0.000	0.000			
Membrane ecc.		Correlation	0.700	0.708	0.703	0.712	0.689	0.696	0.707	0.704	0.700	0.730		
		p-value	0.000	0.000	0.000	0.000	0.000	0.000	0.000	0.000	0.000	0.000		
Reported silica conc.		Correlation	–0.142	–0.058	–0.086	–0.090	–0.099	–0.107	–0.089	–0.089	–0.069	0.006	–0.045	
		p-value	0.529	0.797	0.705	0.691	0.661	0.635	0.695	0.694	0.761	0.979	0.842	
TGA residue		Correlation	–0.208	–0.128	–0.152	–0.168	–0.166	–0.172	–0.158	–0.161	–0.136	–0.077	–0.247	0.946
		p-value	0.353	0.571	0.500	0.454	0.460	0.443	0.483	0.474	0.548	0.732	0.268	0.000

Appendix Table 3: Calculated correlation coefficients and p-values for Product B API-2 results.

			API-2 Release rate at time point									*Dimension factor*	*Membrane ecc.*	*Reported silica conc.*
			1	**2**	**3**	**4**	**5**	**6**	**7**	**8**	**9**			
API-2 release rate at time point	**2**	Correlation	0.982											
		p-value	0.000											
	3	Correlation	0.981	0.996										
		p-value	0.000	0.000										
	4	Correlation	0.977	0.993	0.996									
		p-value	0.000	0.000	0.000									
	5	Correlation	0.976	0.984	0.994	0.994								
		p-value	0.000	0.000	0.000	0.000								
	6	Correlation	0.971	0.981	0.993	0.993	0.998							
		p-value	0.000	0.000	0.000	0.000	0.000							
	7	Correlation	0.961	0.972	0.987	0.987	0.994	0.997						
		p-value	0.000	0.000	0.000	0.000	0.000	0.000						
	8	Correlation	0.962	0.972	0.986	0.989	0.993	0.997	0.996					
		p-value	0.000	0.000	0.000	0.000	0.000	0.000	0.000					
	9	Correlation	0.953	0.961	0.976	0.981	0.986	0.990	0.994	0.996				
		p-value	0.000	0.000	0.000	0.000	0.000	0.000	0.000	0.000				
Dimension factor		Correlation	0.912	0.952	0.934	0.928	0.919	0.904	0.900	0.894	0.888			
		p-value	0.000	0.000	0.000	0.000	0.000	0.000	0.000	0.000	0.000			
Membrane ecc.		Correlation	0.565	0.646	0.601	0.600	0.570	0.552	0.552	0.539	0.530	0.731		
		p-value	0.006	0.001	0.003	0.003	0.006	0.008	0.008	0.010	0.011	0.000		
Reported silica conc.		Correlation	–0.081	–0.039	–0.086	–0.030	–0.093	–0.099	–0.102	–0.060	–0.030	0.070	0.128	
		p-value	0.719	0.861	0.704	0.894	0.680	0.662	0.653	0.791	0.893	0.756	0.571	
TGA residue		Correlation	–0.126	–0.123	–0.149	–0.095	–0.141	–0.145	–0.140	–0.101	–0.058	–0.047	–0.092	0.946
		p-value	0.578	0.585	0.508	0.675	0.533	0.519	0.533	0.654	0.797	0.834	0.683	0.000